1988

Reactions of sulfur dioxide with pentaaquoorganochromium(III) complexes and trispolypyridinechromium(II) complexes

Carol Annona Simmons
Iowa State University

Order Number 8825954

Reactions of sulfur dioxide with pentaaquoorganochromium(III) complexes and trispolypyridinechromium(II) complexes

Simmons, Carol Annona, Ph.D.

Iowa State University, 1988

U·M·I
300 N. Zeeb Rd.
Ann Arbor, MI 48106

PLEASE NOTE:

In all cases this material has been filmed in the best possible way from the available copy. Problems encountered with this document have been identified here with a check mark __✓__.

1. Glossy photographs or pages __✓__
2. Colored illustrations, paper or print __✓__
3. Photographs with dark background _____
4. Illustrations are poor copy _____
5. Pages with black marks, not original copy _____
6. Print shows through as there is text on both sides of page _____
7. Indistinct, broken or small print on several pages _____
8. Print exceeds margin requirements _____
9. Tightly bound copy with print lost in spine _____
10. Computer printout pages with indistinct print _____
11. Page(s) _____ lacking when material received, and not available from school or author.
12. Page(s) _____ seem to be missing in numbering only as text follows.
13. Two pages numbered _____. Text follows.
14. Curling and wrinkled pages _____
15. Dissertation contains pages with print at a slant, filmed as received _____
16. Other _____

_____

_____

Reactions of sulfur dioxide with pentaaquoorganochromium(III) complexes and trispolypyridinechromium(II) complexes

by

Carol Annona Simmons

A Dissertation Submitted to the
Graduate Faculty in Partial Fulfillment of the
Requirements for the Degree of
DOCTOR OF PHILOSOPHY

Department: Chemistry
Major: Inorganic Chemistry

Approved:

Signature was redacted for privacy.

In Charge of Major Work

Signature was redacted for privacy.

For the Major/Department

Signature was redacted for privacy.

For the Graduate College

Iowa State University
Ames, Iowa

1988

TABLE OF CONTENTS

LIST OF TABLES

LIST OF FIGURES

GENERAL INTRODUCTION

Chapter I describes the kinetics and mechanism of the reaction between sulfur dioxide and $(H_2O)_5CrR^{2+}$ complexes. Parallels between this reaction and other electrophilic reactions of the $(H_2O)_5CrR^{2+}$ complexes are drawn. The occurrence of two types of inorganic products is explained.

Chapter II describes the production of $^*Cr(NN)_3^{3+}$ via photochemical methods, the reductive quenching of it by $Co([14]aneN_4)^{2+}$ to form $Cr(NN)_3^{2+}$, and the electron transfer reactions of $Cr(NN)_3^{2+}$ with SO_2 and $Co([14]aneN_4)^{3+}$. The self-exchange rate constant of the SO_2/SO_2^- couple is extracted by the use of Marcus Theory.

CHAPTER I. KINETICS AND MECHANISM OF THE REACTIONS OF PENTAAQUOORGANOCHROMIUM(III) COMPLEXES WITH AQUEOUS SULFUR DIOXIDE

INTRODUCTION

Organochromium(III) complexes have been observed to react with various electrophiles and oxidants.[1] These electrophiles may be broadly divided into two categories - those which react directly with the organochromium(III) ion, and those which react with the products of its homolysis. Scheme I shows the reaction of benzylchromium(III) ion with the oxidant Fe^{3+}. As indicated in eq 1, the initial step is the homolysis of the pentaaquobenzylchromium(III) complex, and the Fe^{3+} reacts with the products of the homolysis. The oxidants O_2, Cu^{2+}, $Co(NH_3)_5Cl^{2+}$, and $Co(NH_3)_5Br^{2+}$ react similarly, although the organic products may differ.

Scheme I

$$PhCH_2Cr(H_2O)_5^{2+} + H_2O \overset{k_H}{\langle\!=\!=\!\rangle} PhCH_2^{\cdot} + Cr(H_2O)_6^{2+} \quad (1)$$

$$Cr(H_2O)_6^{2+} + Fe(H_2O)_6^{3+} \longrightarrow Cr(H_2O)_6^{3+} + Fe(H_2O)_6^{2+} \quad (2)$$

$$PhCH_2^{\cdot} + Fe(H_2O)_6^{3+} + H_2O \longrightarrow PhCH_2OH + Fe(H_2O)_6^{2+} + H^+ \quad (3)$$

Kinetic studies of these reactions show that they are first order in the concentration of benzylchromium(III) ion, but show no dependency on the concentration or identity of oxidant. The rate law obtained is

therefore:

$$\frac{-d[RCr^{2+}]}{dt} = k_H [RCr^{2+}] \quad (4)$$

The electrophiles RHg^+,[2] Hg^{2+},[2] Br_2,[3] I_2,[4] IBr,[5] and Tl^{3+} [1] have been shown to react directly with the α-carbon atom of both alkyl- and substituted benzyl- chromium complexes[6] as shown in eq 5:

$$(H_2O)_5CrR^{2+} + E^{n+} + H_2O = Cr(H_2O)_6^{3+} + E\text{-}R^{(n-1)+} \quad (5)$$

These reactions are first-order in the concentrations of both E^{n+} and organochromium(III) ion. These reactions also exhibit a small substituent effect: ρ = -1.29 (Br_2), -0.81 (I_2), -0.62 (Hg^{2+}), and -0.85 ($MeHg^+$). The negative ρ values mean that electron donating substituents stabilize the transition state, which has a partial positive charge on the α-carbon. The reactions of some $RCo^{(III)}(dmgH)_2(H_2O)$ [7] compounds with Hg^{2+} have been shown to parallel those of the alkylchromium(III) ions.[8]

For a series of substituted benzylchromium(III) complexes, p-Z-$C_6H_4CH_2Cr^{2+}$, there is a small substituent effect as Z is changed; the reaction constant ρ is -1.01. Methyl-, ethyl-, and n-propylchromium(III) complexes do not undergo homolysis, and hence show no reaction with these oxidants.

Organochromium complexes have been observed to undergo decomposition in the absence of any added oxidants or electrophiles; this reaction is called acidolysis. In general, it is described by the rate law:

$$\frac{-d[RCr^{2+}]}{dt} = (k_{1A} + k_{2A}[H_3O^+])[RCr^{2+}] \qquad (6)$$

although k_{1A}, k_{2A}, or both may be zero. The benzylchromium complexes do not undergo acidolysis; the halomethylchromium(III) complexes do so slowly ($k_{1A} \sim 10^{-5} - 10^{-9}$ s^{-1}; $k_{2A} \sim 0$); but the alkylchromium complexes do have significant acidolysis rates ($k_{1A} \sim 10^{-5} - 10^{-3}$ s^{-1}; $k_{2A} \sim 6 \times 10^{-5} - 5 \times 10^{-3}$ $M^{-1}s^{-1}$).[1]

The reaction between benzylchromium(III) ion and sulfur dioxide was first observed in 1957,[9] but no product analyses or kinetic studies were conducted. Both O_2 and SO_2 have been shown to react with other alkyl metal compounds. $RCo^{(III)}(dmgH)_2(H_2O)$ reacts with O_2 and SO_2 via an insertion mechanism to form $R\text{-}O\text{-}O\text{-}Co^{(III)}(dmgH)_2(H_2O)$ [10] or $R\text{-}(SO_2)\text{-}Co^{(III)}(dmgH)_2(H_2O)$ [11] insertion compounds, respectively. The insertion of SO_2 into various other M-R bonds - for example, $CpM(CO)(PPh_3)R$, M= Fe, Ru,[12] Me_3PhSn and Me_3PhCH_2Sn,[13] Co(salen),[14] $CpM(CO)_nR$, M = Mo, Mn, Re, Ru, W, and $CpCr(NO)_2R$,[15] and $RCu.MgX_2$[16] have also been studied. All of the above compounds yield stable $M\text{-}SO_2\text{-}R$ insertion products, with the exception of $RCu.MgX_2$, which decomposes to give the sulfinic acid.[16] None of these reactions were run in aqueous solution.

The mechanisms suggested for the $RCo^{(III)}(dmgH)_2(H_2O)$ insertions are radical reactions, for which both chain and nonchain paths have been proposed.[11] Stereochemical studies of the reaction of SO_2 with <u>threo</u>-$CpFe(CO)_2(CHD)_2C(CH_3)_3$ show that inversion occurs at the α-carbon.[17]

However, stereochemical studies of $Me_3Sn-CH=CH-C_6H_5$ [13] suggest an S_Ei mechanism.

The results of the investigation the reactions between sulfur dioxide and various pentaaquoorganochromium(III) complexes in acidic aqueous solution will be reported in this chapter. The rate law and products will be used to elucidate the mechanism of the reaction, and to compare it to other reactions of this series of chromium(III) complexes.

RESULTS

Products

The inorganic products from the reaction between SO_2 and RCr^{2+} are $Cr(H_2O)_6^{3+}$ and the previously unknown $(H_2O)_5CrSO_2R^{2+}$ complex (green). With the exception of $CrCH_2Cl^{2+}$, these are formed in about a 80%:20% yield ratio, respectively (see Table I-1).

Table I-1. Inorganic Products from the Reaction between SO_2 and Organochromium(III) Complexes in Aqueous Perchloric Acid

RCr^{2+}	% $CrSO_2R^{2+}$	% Cr^{3+}
$CH_2CH_3Cr^{2+}$	31	69
$CH(CH_3)_2Cr^{2+}$	23	77
$CH(CH_3)_2Cr^{2+}$	16	84
$PhCH_2Cr^{2+}$	8	92
$PhCH_2Cr^{2+}$	20	80
$CH_3OCH_2Cr^{2+}$	25	75
CH_2ClCr^{2+}	0	100

The organic products were identified by ^1H nuclear magnetic resonance spectroscopy and anion chromatography.

Both qualitative and quantitative HPLC analyses of the sulfonic acids produced in the reactions of the ethyl, n-propyl and iso-propyl complexes were performed (see Table I-2). For these determinations, the organochromium complexes were not ion-exchanged prior to reaction with

SO_2; their concentrations were calculated from their UV-visible spectra. In one experiment, the radical scavenger $Co(NH_3)_5Cl^{2+}$ was added to the iso-propylchromium(III) cation before the SO_2; it gave both HPLC and ^1H NMR results that were slightly different from those of the other reactions.

The HPLC trace for the i-$C_3H_7Cr^{2+}$ consisted of three peaks at 2.1, 3.5, and 4.2 minutes, whose relative peak areas were about 1:4:4 (see Figure I-1). The 4.2 minute peak is the i-propanesulfonate. The 2.1 minute peak is well separated from the 3.5 and 4.2 minute peaks, but the last two overlap. The reaction with added $Co(NH_3)_5Cl^{2+}$ gave the same peaks, but in about a 1:1:3 ratio. The area of these peaks was proportional to the concentration of the reaction mixture.

The analysis of the ethyl analogue showed two peaks (see Figure I-2). The ethanesulfonate has a retention time of 2.4 minutes. The identity of the 2.0 minute product is not known, but it is surely anionic, and is probably similar in nature to the sulfonates.

Quantitative HPLC analysis showed that approximately one-third of the alkyl groups originally present as RCr^{2+} formed a sulfonic acid, possibly by forming an alkyl sulfinic acid which disproportionated. This sequence of events is consistent with other electrophilic chemistry of SO_2 and with the known disproportionation of RSO_2H, as discussed later.

SO_2 was added to a mixture of iso-propylchromium and pentaamminechlorocobalt(III) ion in D_2O. The reaction between the SO_2 and iso-propylchromium complex proceeded as usual, after which the chromium was precipitated out of solution, and an ^1H-NMR run on the filtrate confirmed the presence of the sulfonic acid. Peaks

Table I-2. Results from HPLC Analyses of the Reaction between SO_2 and various Organochromium(III) Complexes in Aqueous $HClO_4$

R	Number of Peaks [a]	% area of sulfonic acid peak	% RSO_3H/RCr^{2+}
ethyl[b]	1		30
ethyl[b]	2	60	39 ± 1
n-propyl[b]	1		51 ± 13
i-propyl[c]	3	37	26 ± 3
i-propyl[d]	3	25	36 ± 2
i-propyl[e]	3	60	25 ± 3
i-propyl[f]	3	41	37 ± 9

[a]See text and Figures I-1 and I-2.

[b]The RCr^{2+} solution was first bubbled with O_2 for 1 minute (to remove any excess Cr^{2+}), then with N_2 for 20 minutes (to remove the O_2), then with SO_2 for 1 - 2 minutes.

[c]The RCr^{2+} was made with a 25% excess of the hydroperoxide.

[d]The RCr^{2+} was made with a 25% excess of Cr^{2+}, which was not removed by bubbling with O_2.

[e]$Co(NH_3)_5Cl^{2+}$ was added to the RCr^{2+} before reaction with SO_2. The amount of $Co(NH_3)_5Cl^{2+}$ added was 7% of the RCr^{2+} formed. The mixture was cation exchanged on a column of Dowex resin after reaction with SO_2 but before the HPLC analysis.

[f]SO_2 and O_2 were simultaneously bubbled into an Erlenmeyer flask, and from there into the RCr^{2+} solution.

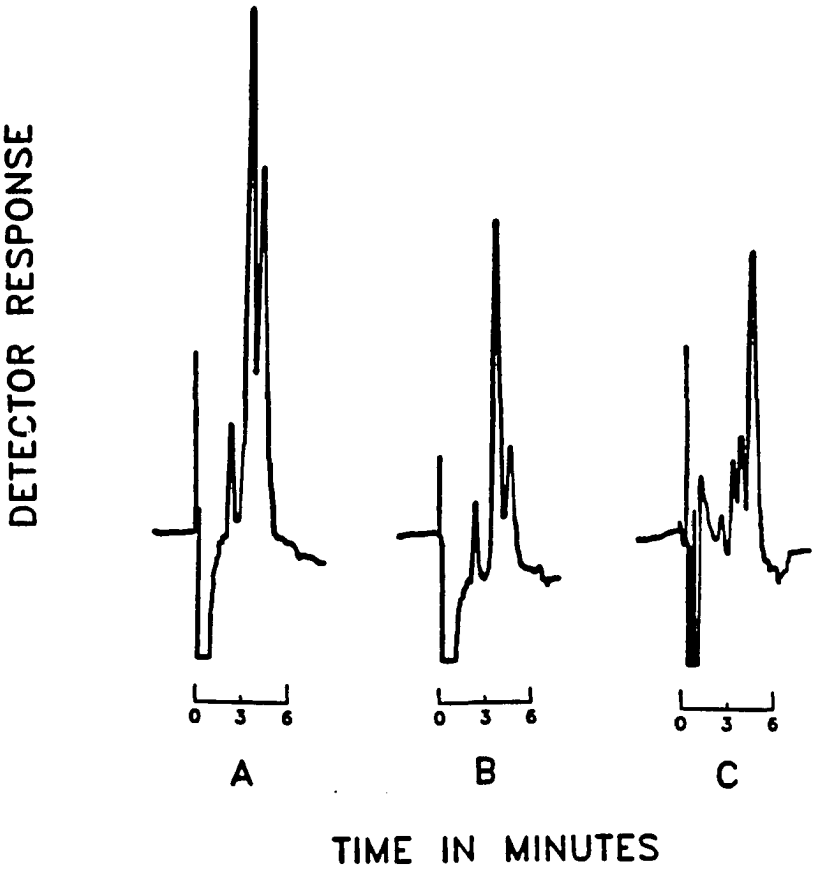

Figure I-1. HPLC separation of the products from the reaction of $\underline{i}$-$C_3H_7Cr^{2+}$ and SO_2. The first two peaks are unidentified, the last is isopropanesulfonate. a) $\underline{i}$-$C_3H_7Cr^{2+}$ made with excess hydroperoxide; [$\underline{i}$-$C_3H_7SO_3^-$] ~ 8 ppm. b) $\underline{i}$-$C_3H_7Cr^{2+}$ made with excess Cr^{2+}; [$\underline{i}$-$C_3H_7SO_3^-$] ~ 4 ppm. c) $\underline{i}$-$C_3H_7Cr^{2+}$ had $Co(NH_3)_5Cl^{2+}$ added before the SO_2, then ion-exchanged on Dowex resin; [$\underline{i}$-$C_3H_7SO_3^-$] ~ 4 ppm. Eluant: 1.5 mM succinic acid, flow rate = 2 mL/min

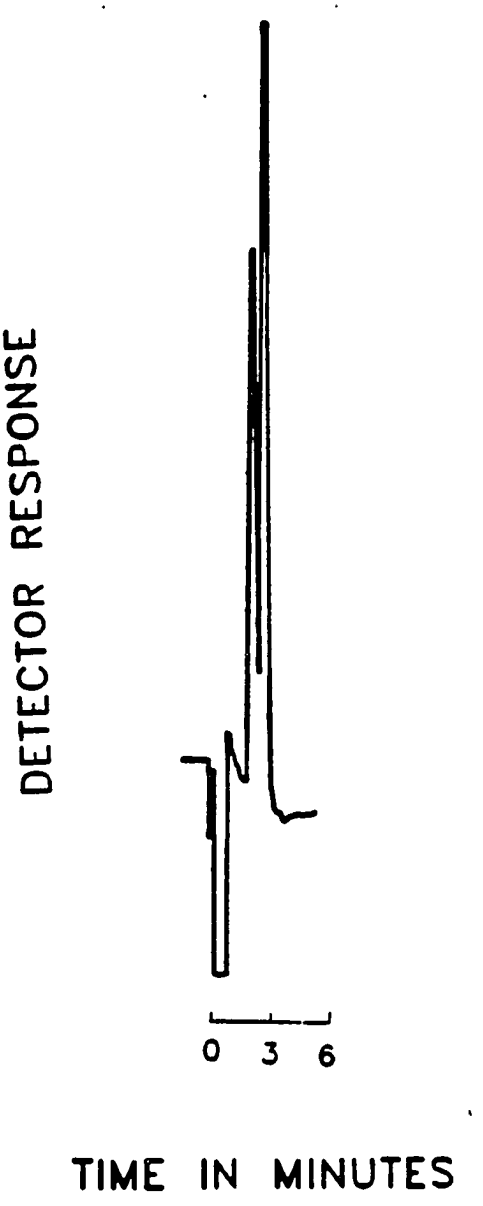

Figure I-2. HPLC separation of the products from the reaction of $C_2H_5Cr^{2+}$ and SO_2. The first peak is unidentified; the second is ethanesulfonate ($[EtSO_3^-]$ ~ 8 ppm). Eluant: 1.5 mM succinic acid, flow rate = 2 mL/min

corresponding to the sulfonic acid standard were clearly seen. Within the limits of the experiment, (there was some paramagnetic broadening due to small amounts of unprecipitated Cr^{3+}) the same result was obtained for the reaction without added pentaamminechlorocobalt(III) ion and for the reaction between ethylchromium and SO_2. No other peaks were seen.

The ^1H NMR spectra of $CDCl_3$ extractions of the aqueous reaction mixtures showed the presence of other products. These products are still unidentified, but based on the dynamic range of the NMR spectrometer they only account for about 0.5% of the total products. No peaks consistent with thiol sulfonate (RSO_2SR) were found. It is not expected that $RSSO_3H$ (another possible product) would be extracted from aqueous solution by $CDCl_3$.

Kinetics

The kinetic runs were performed by reacting an excess of aqueous sulfur dioxide with CrR^{2+} and monitoring the loss of CrR^{2+} at the absorption maximum of the particular organochromium complex between 350 and 410 nm. The reactions were conducted at 25.0 ± 0.1 °C (unless otherwise indicated). Second-order rate constants were obtained from the kinetic data as described in the experimental section.

The observed rate constants were found to increase with increasing $[SO_2]$, but were independent of both $[H^+]$ and ionic strength in the range 0.02 to 1.4 M. Each complex reacted with SO_2 at a different rate, as illustrated in Figure I-3, which shows plots of k_{obs} versus $[SO_2]$ for $MeCr^{2+}$, $EtCr^{2+}$, n-$PrCr^{2+}$, and i-$PrCr^{2+}$, and in Figure I-4, which shows plots of k_{obs} versus $[SO_2]$ for p-CH_3O-$C_6H_4CH_2Cr^{2+}$, p-CH_3-$C_6H_4CH_2Cr^{2+}$,

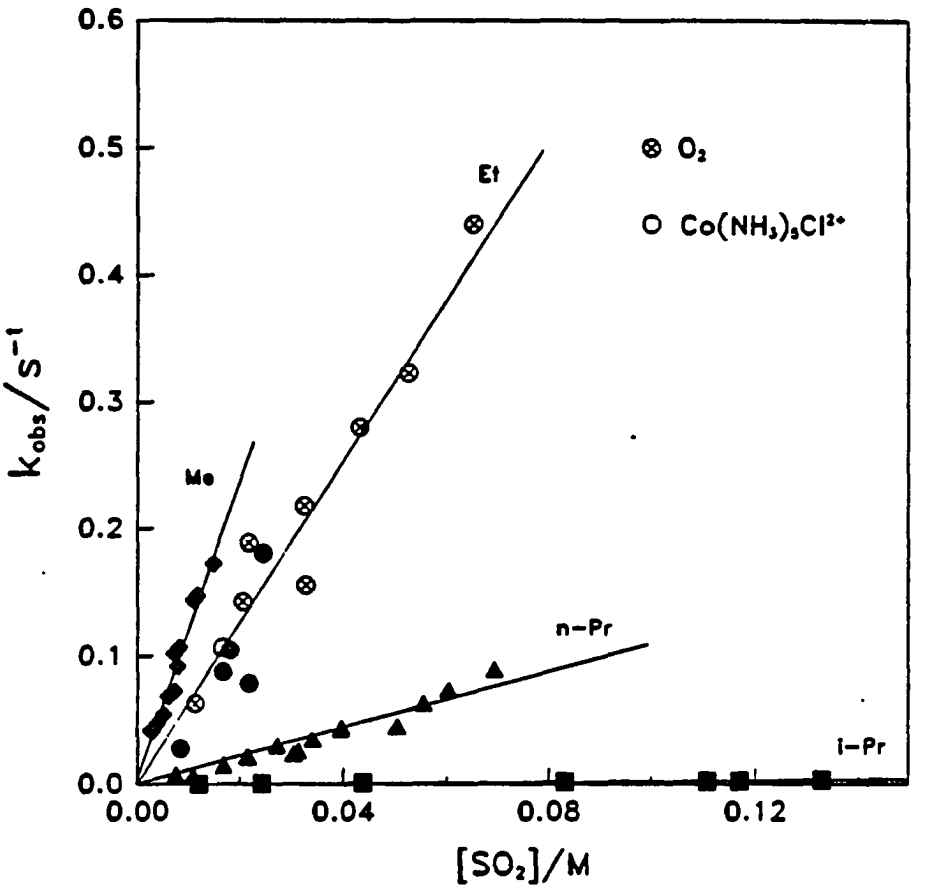

Figure I-3. Linear plots of k_{obs} versus $[SO_2]$ for the reaction of SO_2 with CH_3Cr^{2+} (◆), $C_2H_5Cr^{2+}$ (●,O,⊗), n-$C_3H_7Cr^{2+}$ (▲), and i-$C_3H_7Cr^{2+}$ (■), illustrating the first-order dependence on $[SO_2]$. The kinetics for the $C_2H_5Cr^{2+}$ complex are unaffected by the addition of O_2 (O) or $Co(NH_3)_5Cl^{2+}$ (⊗)

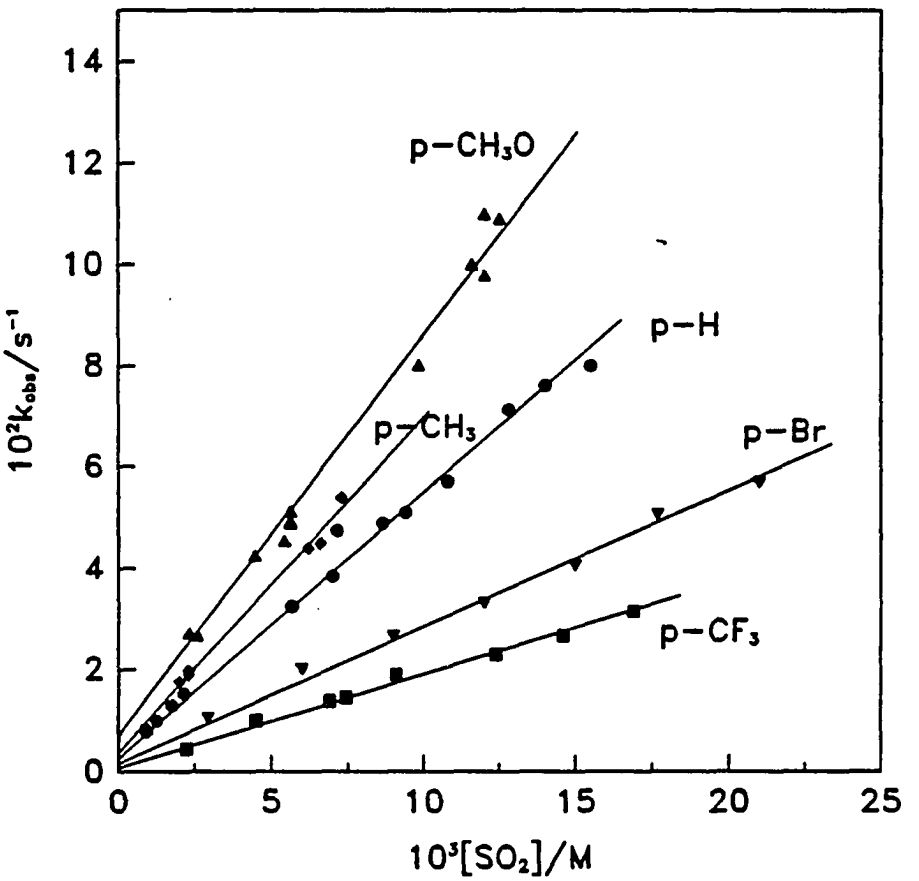

Figure I-4. Linear plots of k_{obs} versus $[SO_2]$ for the reaction of SO_2 with p-$CH_3OC_6H_4CH_2Cr^{2+}$ (▲), p-$CH_3C_6H_4CH_2Cr^{2+}$ (◆), $PhCH_2Cr^{2+}$ (●), p-$BrC_6H_4CH_2Cr^{2+}$ (▼), and p-$CF_3C_6H_4CH_2Cr^{2+}$ (■), illustrating the first-order dependence on $[SO_2]$

$PhCH_2Cr^{2+}$, p-Br-$C_6H_4CH_2Cr^{2+}$ and p-CF_3-$C_6H_4CH_2Cr^{2+}$ (data for other organochromium ions are given in Appendix I). The linearity of these plots leads to the rate law given in eq 7:

$$\frac{-d[CrR^{2+}]}{dt} = (k_A + k_H + k_S[SO_2])[CrR^{2+}]. \qquad (7)$$

The first two terms arise from the decomposition of the CrR^{2+} due to acidolysis [1,18] and homolysis;[1,19] the third is from its reaction with SO_2. A few kinetic runs were done in the presence of $Co(NH_3)_5Cl^{2+}$. Subsequent analysis showed that no Co^{2+} was produced, which means that no $Cr(H_2O)_6^{2+}$ reacted with the $Co(NH_3)_5Cl^{2+}$ in these runs.

Mixing Cr^{2+} and SO_2 results in the formation of a highly absorbing bright green solution, which over the course of two hours decomposes to a blue solution, which then becomes cloudy. The initial reaction between SO_2 and Cr^{2+} is probably on the same timescale as that between $Co(NH_3)_5Cl^{2+}$ and Cr^{2+}, which has a second-order rate constant of $\sim 10^7$ $M^{-1}s^{-1}$. The solutions from the reactions of SO_2 with the iso-propyl and cyclopentyl compounds become cloudy at the end of the reactions because the homolysis reaction (k_H), which produces Cr^{2+}, is large compared to the SO_2 reaction ($k_S[SO_2]$). The cloudiness is due to the reaction between SO_2 and Cr^{2+}. The rate constants of the SO_2 reactions do not change upon the addition of $Co(NH_3)_5Cl^{2+}$ or O_2. These results imply that $Cr(H_2O)_6^{2+}$ is not formed in the SO_2 reaction.

Tables I-3 and I-4 show that the reactivity trends of the CrR^{2+} with SO_2, Hg^{2+}, and Br_2, are similar. This will be discussed in greater detail below.

Table I-3. Rate Constants for the Reaction of Various Benzylchromium(III) Complexes with SO_2, Hg^{2+}, Br_2, and their Variations with the Hammett σ_p Parameter for the Substituent on the Benzyl Group

R	σ_p [a]	k_S [b] $M^{-1}s^{-1}$	$10^{-4}k_{Hg}$ [c] $M^{-1}s^{-1}$	$10^{-5}k_{Br}$ [d] $M^{-1}s^{-1}$
p-CH_3O-$C_6H_4CH_2$	-0.27	7.8	(7.2)[e]	(20)[e]
p-CH_3-$C_6H_4CH_2$	-0.17	6.7	5.22	(14)[e]
$C_6H_5CH_2$	0.0	5.51	4.87	8.3
p-Br-$C_6H_4CH_2$	0.23	2.8	2.98	2.32
p-CF_3-$C_6H_4CH_2$	0.54	1.82	2.1	1.55
2,4,6-$(CH_3)_3$-$C_6H_2CH_2$		5.9		
$(CH_3)_5C_6CH_2$		23		

[a]Lowry and Richardson.[20]

[b]The kinetic data on which these values are based are given in the Appendix.

[c]Ref. 4.

[d]Ref. 3.

[e]Extrapolated from the fit of the known rate constants[3,4] to the Hammett equation.

Table I-4. Rate Constants for the Reaction of Various Organochromium(III) Complexes with SO_2, Hg^{2+}, and Br_2

R	$10^3 k_S$ [a] $M^{-1}\ s^{-1}$	$10^{-2} k_{Hg}$ $M^{-1}\ s^{-1}$	$10^{-4} k_{Br}$ $M^{-1}\ s^{-1}$
CH_3	11300	100000 [b]	210 [c]
CH_2CH_3	5200	1400 [b]	49 [c]
$CH_2CH_2CH_3$	920	350 [b]	19.9 [a]
$CH(CH_3)_2$	22	0.0156 [b]	1.8 [d]
c-C_5H_9	9.75	0.0108 [d]	1.3 [d]
CH_2OH	192	2.88 [e]	8.7 [a]
CH_2OCH_3	1.25	0.905 [e]	
CH_2CH_2CN	0.79	0.81 [f]	0.0540 [a]
CH_2Cl	0.00848	0.0059 [b]	0.000106 [g]

[a]The kinetic data on which these values are based are given in the Appendix.

[b]Ref. 4.

[c]Ref. 2.

[d]Ref. 5.

[e]Espenson and Bakac.[21]

[f]Ref. 1.

[g]Ref. 17.

Activation parameters

The activation parameters were determined for the reaction of $CrCH_2C_6H_5^{2+}$ with SO_2 by performing the reaction at 1.9, 11.4, 25.0, and 39.9 °C. The data were fit to the Eyring equation, $k/T = (R/Nh)\exp(\Delta S^{\neq}/R)\exp(-\Delta H^{\neq}/RT)$, by a least-squares computation (see Figure I-5). The values of $\Delta S^{\neq}$ and $\Delta H^{\neq}$ are -39.1 ± 0.8 cal mol^{-1} K^{-1}, and 4.8 ± 0.2 kcal mol^{-1}, respectively.

Characterization of new complexes

The new complexes made were $p\text{-}CH_3OC_6H_4CH_2Cr^{2+}$, $(CH_3)_5C_6CH_2Cr^{2+}$, and $2,4,6\text{-}(CH_3)_3C_6H_2CH_2Cr^{2+}$. The UV-visible spectra of these were similar to those of the other known $Z\text{-}C_6H_4CH_2Cr^{2+}$ complexes. The new complexes also undergo homolysis and react with SO_2.

The rate constant for homolysis, k_H, of the $p\text{-}CH_3OC_6H_4CH_2Cr^{2+}$ complex was derived from its reactions with the radical scavengers Fe^{3+}, Cu^{2+}, O_2 and SO_2. Unlike the other benzylchromium(III) compounds, a second-order reaction with Fe^{3+} and Cu^{2+} was observed. The rate law follows the form:

$$\frac{-d[RCr^{2+}]}{dt} = (k_H + k_{rs}[rs])[RCr^{2+}] \qquad (8)$$

The second-order rate constant, k_{rs}, and the first-order rate constant, k_H, calculated from a plot of k_{obs} versus [agent], are shown in Table I-5 (individual runs are listed in Table AI-24). Direct reactions with Fe^{3+} and Cu^{2+} have also been observed for the α-hydroxyalkylchromium complexes,[1] in which the metal is proposed to bind to the oxygen.

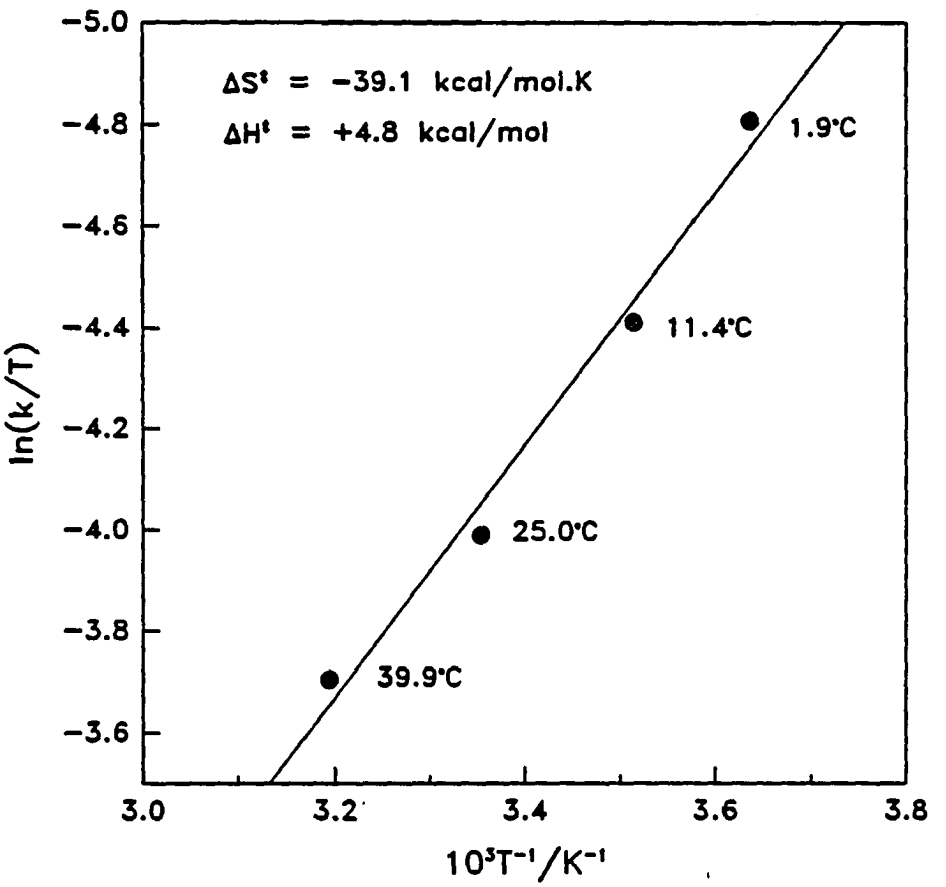

Figure I-5. An Eyring plot (ln(k/T) versus 1/T) for the reaction of SO_2 with $PhCH_2Cr^{2+}$

The reaction of $p\text{-}CH_3OC_6H_4CH_2Cr^{2+}$ with O_2 gives $k_{obs} = 0.016\ s^{-1}$, which implies that the O_2 undergoes some sort of chain or second-order reaction with the p-methoxybenzylchromium(III) ion in addition to homolysis. All of the kinetic traces were first-order. The k_H value of $7.2 \times 10^{-3}\ s^{-1}$ does agree with that calculated from Hammett correlations by Nohr and Espenson[19]. The reaction of $p\text{-}CH_3OC_6H_4CH_2Cr^{2+}$ with SO_2 is similar to the other substituted benzylchromium complexes (see Figure I-4). k_H is the intercept of the line k_{obs} versus $[SO_2]$.

Table I-5. Kinetic Data for the Reaction of Radical Scavengers with $p\text{-}CH_3OC_6H_4CH_2Cr^{2+}$

Agent	$10^3 k_H/s^{-1}$	$k_{rs}/M^{-1}\ s^{-1}$
Cu^{2+}	7.3 ± 0.3	0.011 ± 0.001
Fe^{3+}	7.4 ± 2.1	2.2 ± 0.2
SO_2	7.1 ± 1.4	7.8 ± 0.3

The $2,4,6\text{-}(CH_3)_3C_6H_2CH_2Cr^{2+}$ complex exhibits a slight acid-dependent term for homolysis:

$$k_{obs} = (0.156 + 0.025\ [H^+])\ s^{-1} \quad (9)$$

$$k_H = 0.156\ s^{-1} \quad (10)$$

$$k_{2A} = 0.025\ M^{-1}s^{-1} \quad (11)$$

No direct reaction of Cu^{2+} with the complex was noticed; tests for a direct reaction with Fe^{3+} were not performed. If one assumes that the

Hammett σ parameters are additive,[22] then the k_H for this complex can be correlated with the p-Z-$C_6H_4CH_2Cr^{2+}$ complexes. The observed k_H is much faster than calculated (in 1.0 M $HClO_4$, expect k_H = ~ 0.1 s^{-1}). This is probably because the ortho methyl groups cause steric crowding at the α-carbon which helps weaken the Cr-C bond.

The $(CH_3)_5C_6CH_2Cr^{2+}$ complex shows no acid or oxidant dependent pathways in its homolysis, as is typical for the p-Z-$C_6H_4CH_2Cr^{2+}$ series of complexes. The observed k_H is 0.25 s^{-1}; the calculated value is about 0.14 s^{-1}, assuming additivity of Hammett σ values.

The previously unknown $(H_2O)_5Cr(SO_2)R^{2+}$ complexes were obtained from the SO_2 reaction solutions by elution from Sephadex SP-C25 resin. They were identified on the basis of their their UV-visible spectra, and their decomposition products (RSO_3H, found via HPLC) after base hydrolysis. Their UV-visible spectra are shown in Table I-6 below.

Table I-6. UV-Visible Spectra of Various $(H_2O)_5CrSO_xR^{n+}$ Compounds

Compound	λ_{max} (ε) /nm ($/M^{-1}cm^{-1}$)	λ_{max} (ε) /nm ($/M^{-1}cm^{-1}$)	λ_{max} (ε) /nm ($/M^{-1}cm^{-1}$)
$CrSO_3^+$	590(20.5)	430(22.2)[a]	
$CrSO_4^+$	587(19.0)	417(18.8)[b]	
$CrSO_2CH_2CH_3^{2+}$	590(20.0)	420(23.3)[c]	
$CrSO_2CH(CH_3)_2^{2+}$	590(~20)	420(~23)	260(~940)[c,d]
$CrSO_2CH_2Ph^{2+}$	-	415(~23)	220(~7500)[c,d]
$CrSO_2CH_2OCH_3^{2+}$	590(~20)	420(~23)	260(~1100)[c,d]

[a]Carlyle and King.[23]

[b]Finholt et al.[24]

[c]This work.

[d]The extinction coefficients in the visible part of the spectrum are assumed to be the same as those measured for the ethyl complex. The extinction coefficients in the UV region are calculated based on this assumption.

DISCUSSION

Linear free energy correlations

Changing the substituent Z on p-Z-$C_6H_4CH_2Cr^{2+}$ for the reactions with SO_2 produce a change in the second-order rate constant k_S. When Z is changed, the amount of electron density which is present at the reactive α-carbon site is altered without changing any steric factors. The rate constants may be correlated by plotting $\log_{10}(k_S)$ versus $\sigma_p(Z)$, where $\sigma_p(Z)$ is the Hammett substituent constant for Z. This plot is shown in Figure I-6. The least-squares slope of the line is $\rho = -0.79 \pm 0.06$. The negative ρ values mean that electron donating substituents stabilize the transition state, which has a buildup of partial positive charge on the α-carbon. The magnitude of ρ is small, which means that bond breaking and bond making are nearly synchronous, and that electronic factors are not of great importance to the rate of this reaction.

The $(CH_3)_5C_6CH_2Cr^{2+}$ and 2,4,6-$(CH_3)_3C_6H_2CH_2Cr^{2+}$ complexes have different steric factors from the other complexes, as they have <u>ortho</u> substituents which crowd the reactive site. The 2,4,6-$(CH_3)_3C_6H_2CH_2Cr^{2+}$ complex has $k_S = 5.9\ M^{-1}s^{-1}$, compared to a calculated value of ~12 $M^{-1}s^{-1}$ based on only electronic factors. This lowering reflects the fact that the SO_2 is less able to reach the reactive α-carbon site. The $(CH_3)_5C_6CH_2Cr^{2+}$ complex has an observed rate constant of $23 \pm 2\ M^{-1}s^{-1}$, compared to the calculated value of 18 $M^{-1}s^{-1}$. These two values are within experimental error of each other; one would expect the observed value to be lower due to steric factors. It is at present unclear why the correlation should work for one complex and not the other - although

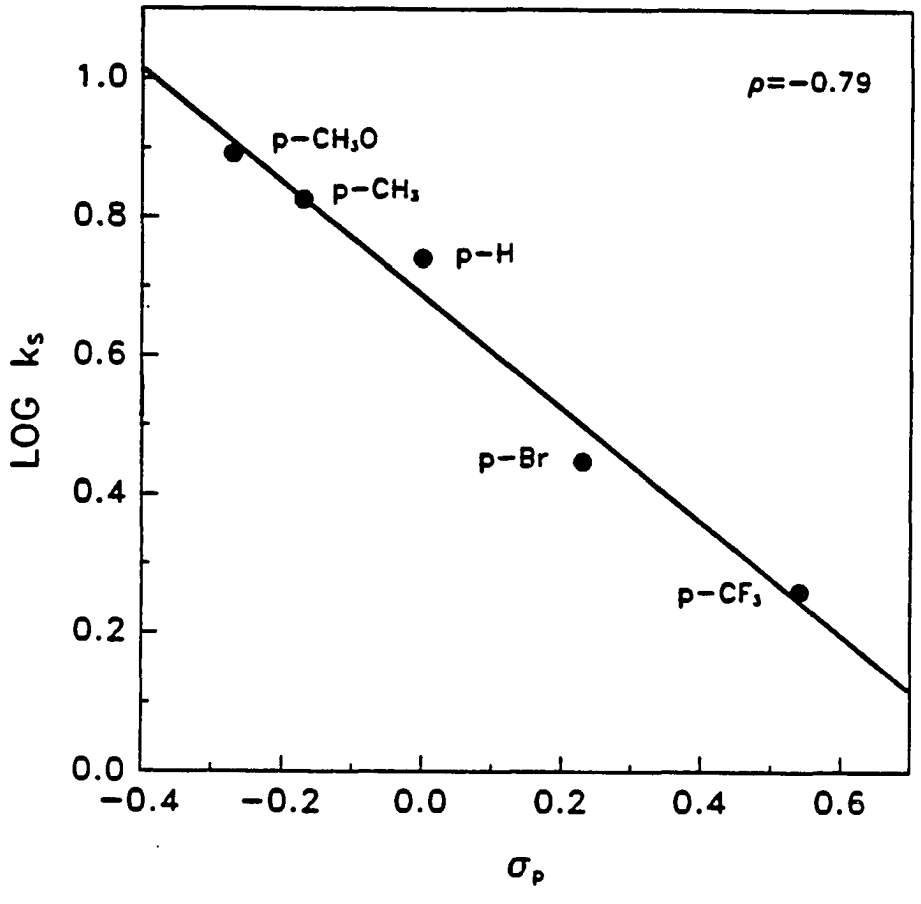

Figure I-6. Plot of $\log_{10}(k_S)$ versus the Hammett substituent constant, σ_p, for the reaction of a series of para-substituted benzylchromium compounds with SO_2

the apparent agreement may only be coincidental. Nonetheless, one may surmise that these complexes react via the same mechanism as do the other p-Z-$C_6H_4CH_2Cr^{2+}$ complexes, in spite of the different steric constraints.

The alkylchromium complexes differ from each other more in the amount of crowding at the α-carbon than they do by electronic factors. The large variation of k_S between them therefore implies that the reaction does not proceed by an electron transfer mechanism, as an electron transfer mechanism would be insensitive to the steric bulk. The order of reactivity, $1° \geq PhCH_2 > 2°$, and the fact that both compounds which do and do not undergo homolysis react, imply that the reaction is electrophilic. Indeed, the correlation of $\log_{10}(k_S)$ versus $\log_{10}(k_{Br})$ is quite good (see Figure I-7), and the bromine reaction is known to be electrophilic.[3] The analogous correlations for $\log_{10}(k_S)$ versus $\log_{10}(k_{Hg})$ and $\log_{10}(k_{Br})$ versus $\log_{10}(k_{Hg})$ (Figures I-8 and I-9) show that the iso-propyl and cyclopentyl compounds do not lie on the same line as the others do. This might suggest that they may have found an alternative reaction pathway for reacting with SO_2, but the iso-propyl compound gives the same type of reaction products as the ethyl and n-propyl compounds do (see Tables I-1 and I-2). The other suggestion is that the iso-propyl and cyclopentyl complexes have found an alternative pathway for the Hg^{2+} reaction.[2] The SO_2 and Br_2 molecules are both about the same size (r = 2.8 A°,[25] and 2.3 A° [sum of covalent atomic radii] respectively) and both have no charge. The Hg^{2+}, on the other hand, is much smaller, and dicationic. For these reasons, the SO_2 and Br_2 may be a better-matched pair of reagents than either of them with the Hg^{2+} for the comparisons which are being done here.

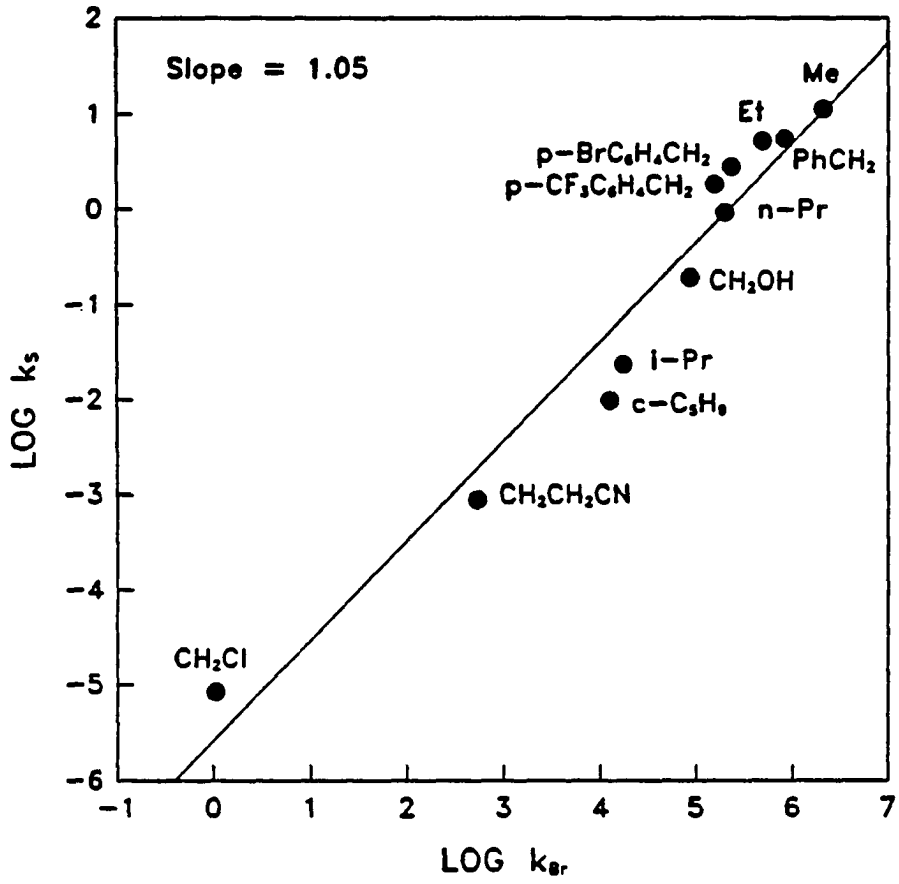

Figure I-7. Plot of $\log_{10}(k_S)$ versus $\log_{10}(k_{Br})$ for the reactions of various organochromium(III) complexes with SO_2 and Br_2

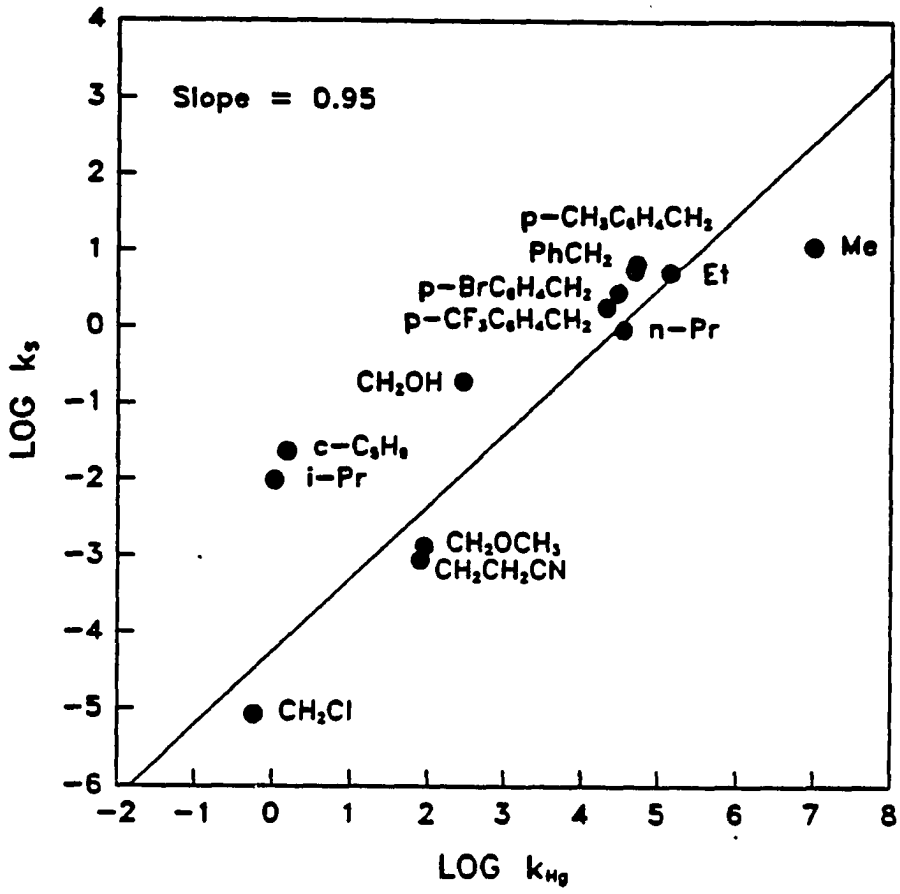

Figure I-8. Plot of $\log_{10}(k_S)$ versus $\log_{10}(k_{Hg})$ for the reactions of various organochromium(III) complexes with SO_2 and Hg^{2+}. The cyclopentyl and iso-propyl complexes are not included in the calculation of the line

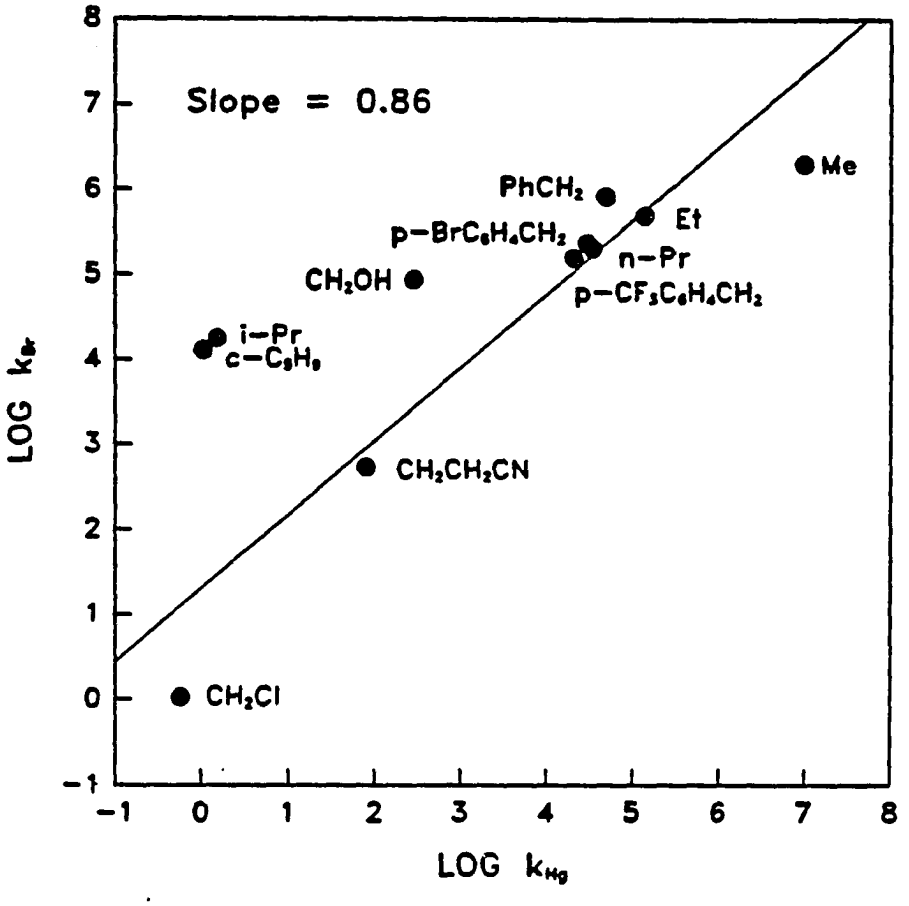

Figure I-9. Plot of $\log_{10}(k_{Br})$ versus $\log_{10}(k_{Hg})$ for the reactions of various organochromium complexes with Br_2 and Hg^{2+}. The cyclopentyl and iso-propyl complexes are not included in the calculation of the line

Energies of activation

The large, negative value of $\Delta S^{\neq}$ (-39.1 ± 0.8 cal $mol^{-1}K^{-1}$) for the reaction between $C_6H_5CH_2Cr^{2+}$ and SO_2 shows that there is a loss of freedom of the vibrational and translational modes of the reactants when forming the transition state. Indeed, similarly large, negative $\Delta S^{\neq}$ values have been observed for other SO_2 insertion reactions.[13,15] The $\Delta H^{\neq}$ for the reaction between $C_5H_5CH_2Cr^{2+}$ and SO_2 is 4.8 ± 0.2 kcal mol^{-1}. Reactions of the electrophiles Hg^{2+}, Br_2, and $MeHg_2^+$ with alkyl and substituted alkylchromium complexes yield $\Delta H^{\neq}$ values of about 7 - 10 kcal mol^{-1} and $\Delta S^{\neq}$ values of -19 to -32 cal $mol^{-1}K^{-1}$.[1] The activation parameters for this SO_2 reaction exhibit the same general trends as these other S_E2 reactions, in contrast to the homolysis reaction, which has $\Delta H^{\neq}$ = 31.8 kcal mol^{-1} and $\Delta S^{\neq}$ = 36.6 cal $mol^{-1}K^{-1}$.[19]

Mechanism for the reaction of pentaaquoorganochromium(III) complexes with SO_2

The proposed reaction scheme is:

$$(H_2O)_5CrR^{2+} + SO_2 \longrightarrow RSO_2^- + (H_2O)_6Cr^{3+} \quad (80 \pm 20)\% \quad (12)$$

$$(H_2O)_5CrR^{2+} + SO_2 \longrightarrow (H_2O)_5Cr(SO_2)R^{2+} \quad (20 \pm 10)\% \quad (13)$$

$$RSO_2^- + H^+ \rightleftharpoons RSO_2H \quad (14)$$

$$3RSO_2H + H_2O \longrightarrow RSSO_2R + RSO_3H \quad (15)$$

Adding 12, 14, and 15:

$$3RCr^{2+} + 3H^+ + 3SO_2 \longrightarrow RSO_3H + RSO_2SR + H_2O + 3Cr^{3+} \quad (16)$$

Many reactions of alkylmetal compounds and SO_2 give stable insertion products,[17] although a few are known to decompose.[16] In this case, both insertion and decomposition products were found. The decomposition products were rationalized on the basis of known chemistry. Reactions 14 and 15 are well known chemistry for arylsulfonic acids,[26] and the disproportionation is known to be acid catalyzed.[27] The situation for the lower aliphatic sulfinic acids is less clearly defined; however, they are known to be less stable than the aromatic sulfinic acids[16,28] and are more difficult to isolate in pure form. The fact that 33%, and not 67% of the product was sulfonic acid shows that the reaction did not yield $RSO_2\cdot$ at any time, as the following reaction sequence would have occurred:[27]

$$2RSO_2^{\cdot} = RSO_2SO_2R \qquad (17)$$

$$RSO_2SO_2R + H_2O = RSO_2H + RSO_3H \qquad (50\%\ RSO_3H) \qquad (18)$$

$$3RSO_2H = RSO_2SR + RSO_3H \qquad (17\%\ RSO_3H) \qquad (19)$$

There were also unidentified peaks in the HPLC trace, one of which was quite large. One suggestion for the identity of the large HPLC peak is $RSSO_3H$, produced from

$$RSO_2SR + HSO_3^{-} = RSO_2^{-} + RSSO_3H \qquad (20)$$

$$RSO_2SR + Nu^{-} = RSO_2^{-} + NuSR. \qquad (21)$$

This reaction is analogous to reaction 21, which has been studied for R = aryl and $Nu^{-} = OH^{-}$, OOH^{-}, and SO_3^{2-}.[27] At the pH of the HPLC experiments, the SO_2 would be present as HSO_3^{-}, and would therefore be

expected to attack the $RSSO_3H$. If SO_2 can also act as a nucleophile, this would explain the absence of RSO_2SR in the ^1H NMR, and would also imply that the yield of sulfonic acid should increase slightly. The calculated yields of RSO_3H:$RSSO_3H$:$(H_2O)_5Cr(SO_2)R^{2+}$ based on equations 12 - 15 are 40%:40%:20%, in agreement with the experimental results of 25% - 40% RSO_3H and 20 ± 10% $(H_2O)_5Cr(SO_2)R^{2+}$. In the presence of the radical scavenger $Co(NH_3)_5Cl^{2+}$, the $RSSO_3H$ peak is diminished relative to the RSO_3H peak (see Figure I-2). However, it is not known how $Co(NH_3)_5Cl^{2+}$ would affect reaction 20.

Nature of the transition state

The suggestion for the transition state is,[29]

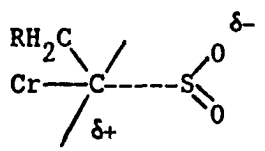

in which the electrophilic sulfur of SO_2 attacks the α-carbon. (This diagram is not intended to indicate any stereochemical configuration in the products. The transition state shown is consistent with the trends observed when the substituent Z in the p-Z-$C_6H_4CH_2Cr^{2+}$ series is changed and when the steric bulk of the alkyl group in the alkyl series changes. The reaction between organochromium(III) complexes and SO_2 also shows the same variations of rate constant with substituent as do other confirmed S_E2 mechanisms,[1] as shown by the log-log plots in Figures I-7 to I-9.

Since no pentaaquoorganochromium(III) complexes that are chiral at the chromium-carbon bond have been prepared, the question of stereochemistry in these cases cannot be given a definite answer. Since

the relative rates of the insertion of SO_2 into alkylchromium(III) complexes compare well with the Br_2, Hg^{2+}, and $MeHg^{2+}$, reactions, one may speculate that the stereospecificity is also the same - that is, inversion.

Two post-transition state rearrangements are postulated to explain the formation of two types of chromium(III) products. One postulate is the formation of a contact ion pair, $[(H_2O)_5Cr^{3+}||RSO_2H^-]$; about 80% of the time this falls apart and a solvent water molecule attacks the chromium, forming $(H_2O)_6Cr^{3+}$; the rest of the time the two ions react with each other to form the insertion product. A similar mechanism has been suggested for SO_2 insertion reactions of other alkyl metal complexes in organic solvents, in which the product is 100% S-sulfinate[17]. In the pentaaquoorganochromium(III) series, it is not known if the Cr-O or Cr-S bonded sulfinate is formed. The second postulate is that after the transition state the R_3C-SO_2 moiety undergoes geometrical changes[30] such that an O of the SO_2 may bind to the chromium, and the Cr-C bond breaks simultaneously:

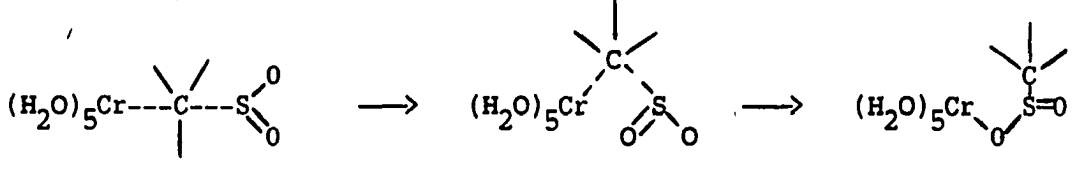

This procedure occurs in competition with the attack of an O from a solvent H_2O molecule and loss of RSO_2^-, which leads to the formation of $(H_2O)_6Cr^{3+}$. If this mechanism is correct, then the O-bonded sulfinate should be the one that is initially formed; subsequent isomerization to an S-bonded form is possible,[31] but the experiments done cannot tell if this has actually happened.

Summary

The reaction of SO_2 with a series of pentaaquoorganochromium(III) complexes has been shown to occur via an S_E2 mechanism. The rate constants of the SO_2 reaction correlate well with those of the Br_2 reaction, and also with those of the Hg^{2+} reaction, with the exception of the iso-propyl and cyclopentyl complexes. The formation of two different chromium products, $(H_2O)_6Cr^{3+}$ and $(H_2O)CrSO_2R^{2+}$ is due to the attack of either H_2O or RSO_2^- on the Cr after the transition state.

EXPERIMENTAL

Materials

The benzyl bromides were all reagent grade commercially available materials, with the exception of the p-methoxybenzyl bromide, which was made by refluxing 10 ml p-methoxybenzyl alcohol (p-anisyl alcohol, Aldrich) in 50 ml benzene with 50 ml HBr for one hour at 100°C. The reaction mixture was heterogeneous, and was stirred rapidly at all times. The p-methoxybenzyl bromide was isolated by neutralizing the benzene layer with $NaHCO_3$ solution, separating the aqueous layer, and then removing the benzene via rotary evaporation to isolate the oily product.[32] The ^1H NMR gives the following peaks: 3.79 (s, OCH_3); 4.62 (s, CH_2); 6.88, 6.91, 7.36, 7.39 (phenyl ring). The benzylchromium complexes were made from the appropriate benzyl bromide and Cr^{2+}, according to the literature.[19] They were purified by cation exchange on a Sephadex SP-C25 resin.[33] The benzylchromium complexes were identified based on their UV-visible spectra and the rate constants of their homolysis reactions (see Table I-7).

The molar absorptivities, ε, for p-$CH_3OC_6H_4CH_2Cr^{2+}$ (see Figure I-10) were determined by taking the UV-visible spectrum of the compound, and then using NaOH and H_2O_2 to oxidize a known amount of it to CrO_4^{2-}. The $[CrO_4^{2-}]$ was found from its extinction coefficient of 4830 $M^{-1}cm^{-1}$ at 372 nm, hence the concentration of the p-$CH_3OPhCH_2Cr^{2+}$ and its extinction coefficients of the could be determined.

2,4,6-$(CH_3)_3C_6H_2CH_2Cr^{2+}$ and $(CH_3)_5C_6CH_2Cr^{2+}$ were made from the appropriate benzyl chloride (Alfa). In a typical experiment, 0.3 g benzyl chloride was dissolved in 40 ml acetone, deaerated with argon, and

Table I-7. UV-Visible Spectra and Homolysis Rate Constants of Various Substituted Benzylchromium Compounds

R	λ	ε [a]	λ	ε	λ	ε	λ	ε	$10^3 k_H$ [b]
p-CH_3O	362	1290	294	2140	280	2740	225	4280	7.3[c]
p-CH_3	360	1200	300	4200	276	4800			3.74[d,e]
p-H	356	2200	295	6970	273	7670			2.63[f]
p-H							240	~7500[c]	
p-Br	360	1500	300	5700	280	5700	250		1.56[d,e]
p-Br							250	~5500[c]	
p-CF_3	354	500	298	2360	280	2400	245		0.728[d,e]
2,4,6-$(CH_3)_3$	370	530	305	1650	284	1880	235	1540	180[c,g]
$(CH_3)_5$	375	850	315	1960	287	2520			250[c,g]

[a] λ is in nm; ε is in $M^{-1}cm^{-1}$.

[b] k_H is in s^{-1}.

[c] This work.

[d] J. Chang.[34]

[e] Ref. 18.

[f] Ref. 4.

[g] The k_H of these compounds is so high that up to 50% decomposition may have occurred in the time taken to record their spectra.

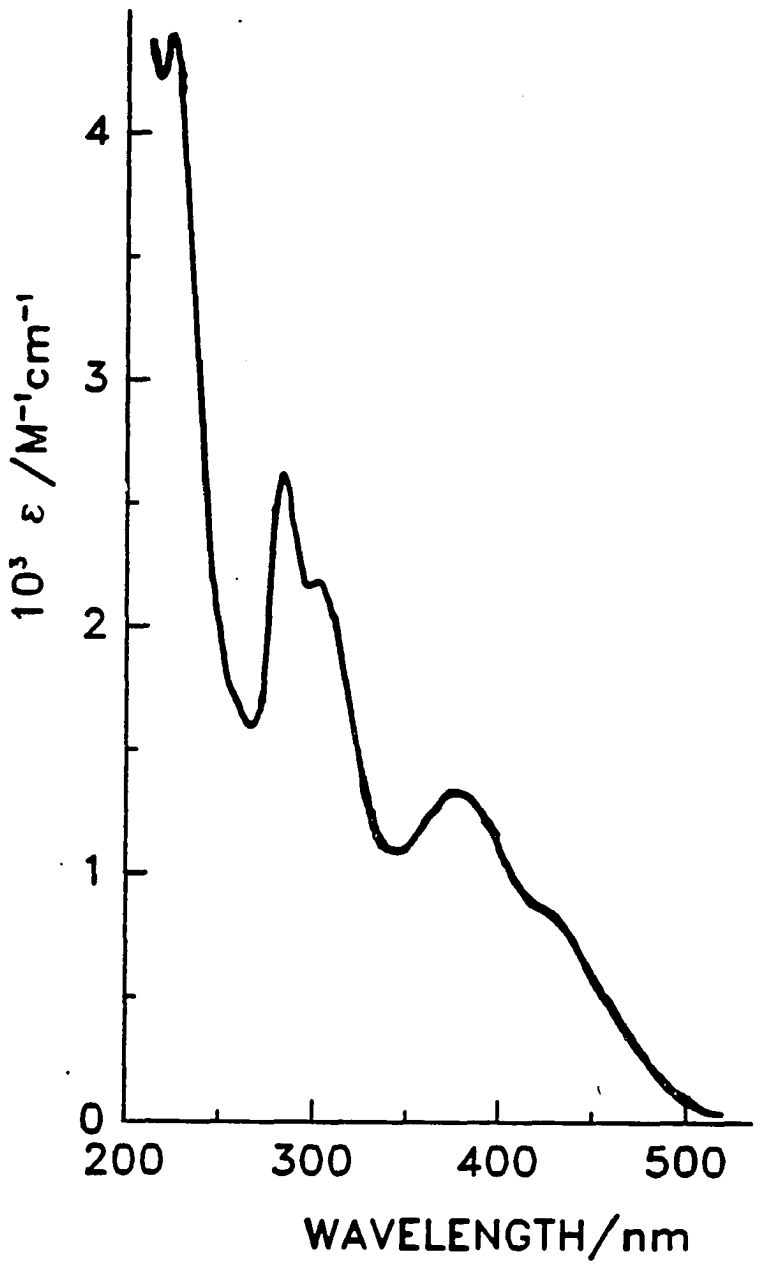

Figure I-10. The UV-visible spectrum of p-$CH_3OC_6H_4CH_2Cr^{2+}$ in 0.29 M $HClO_4$

then 5 ml 0.28 M Cr^{2+} in 0.1 M perchloric acid was added. The solution changed color from pale green to dark green to dark amber over a timescale of about one to two hours. The solution was then diluted with about 200 ml 0.05 M perchloric acid, and cation-exchanged under an argon atmosphere on a Sephadex SP-C25 resin at 0°C like the other organochromium compounds. Photographs of this procedure are shown in Figure I-11. Note the pale blue Cr^{2+} in Figure I-11B; for benzylchromium complexes made from the bromides, $(H_2O)_5CrBr^{2+}$ (bright green) elutes before the RCr^{2+}, but there is no Cr^{2+} left. The product solutions were yellow, and were characterized by their reactions with the oxidants Fe^{3+}, Cu^{2+}, and $Co(NH_3)_5Cl^{2+}$, and their UV-visible spectra (see Table I-7, Figures I-12 and AI-13).

The $CrCH_2Cl^{2+}$ was made from the bromide, similarly to the benzylchromium complexes.[4] The $CrCH_2Cl^{2+}$ was also identified on the basis of its UV-visible spectrum: λ = 517 nm, ε = 23.7 $M^{-1}cm^{-1}$; λ = 393 nm, ε = 225 $M^{-1}cm^{-1}$; λ = 260 nm, ε = 3560 $M^{-1}cm^{-1}$.[7]

The benzyl-, methyl-, ethyl-, n-propyl- and iso-propylchromium complexes were made by reacting the appropriate hydroperoxide with Cr^{2+} and identified by their UV-visible spectra (see Figure I-12, Table AI-1). The hydroperoxides were made from the appropriate alcohol, H_2O_2, and H_2SO_4, according to literature methods [2,4,7]. The hydroperoxide syntheses gave blue $Cr(H_2O)_6^{3+}$ as a by-product; this elutes after the RCr^{2+} on a Sephadex SP-C25 resin.

The c-C_5H_9, CH_2OH, CH_2OCH_3, and CH_2CH_2CN complexes were prepared by Fenton chemistry; H_2O_2 was added to a mixture of Cr^{2+} and cyclopentane,[5] methanol, dimethyl ether,[35] or propionitrile[36] in dilute perchloric

Figure I-11. Photographs of the purification of $(CH_3)_5C_6CH_2Cr^{2+}$ on Sephadex SP-C25 cation exchange resin. A. The amber solution is being loaded onto the white resin. From top to bottom one sees the solution, unused white $(CH_3)_5C_6CH_2Cl$ on the resin, and the amber solution on the resin. B. The solution has been completely loaded. From top to bottom one sees the eluant, 0.29 M $HClO_4$, amber $(CH_3)_5C_6CH_2Cr^{2+}$, pale blue Cr^{2+}, and unused white resin. Note the argon line feeding into the top of the column, and the ice water bath from which water is pumped into the jacket of the column. The resin has shrunk slightly during the elution.

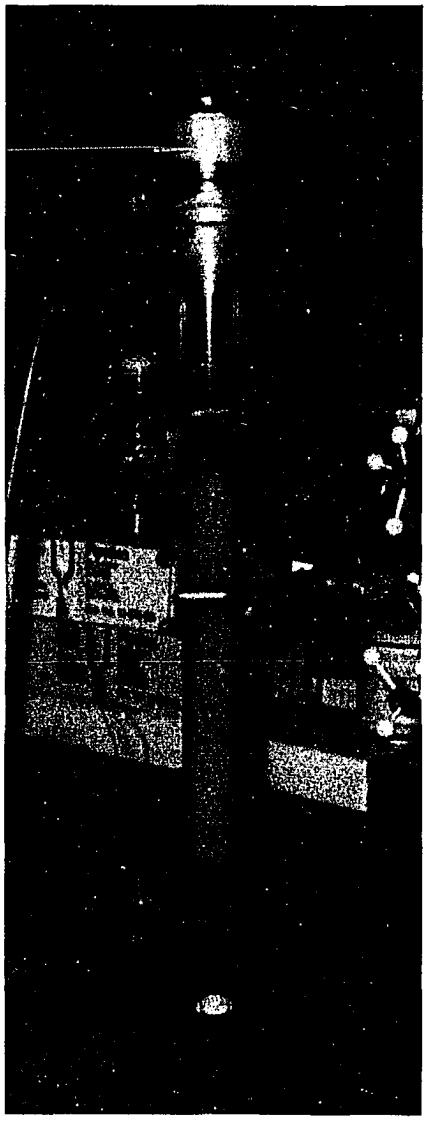

A.

B.

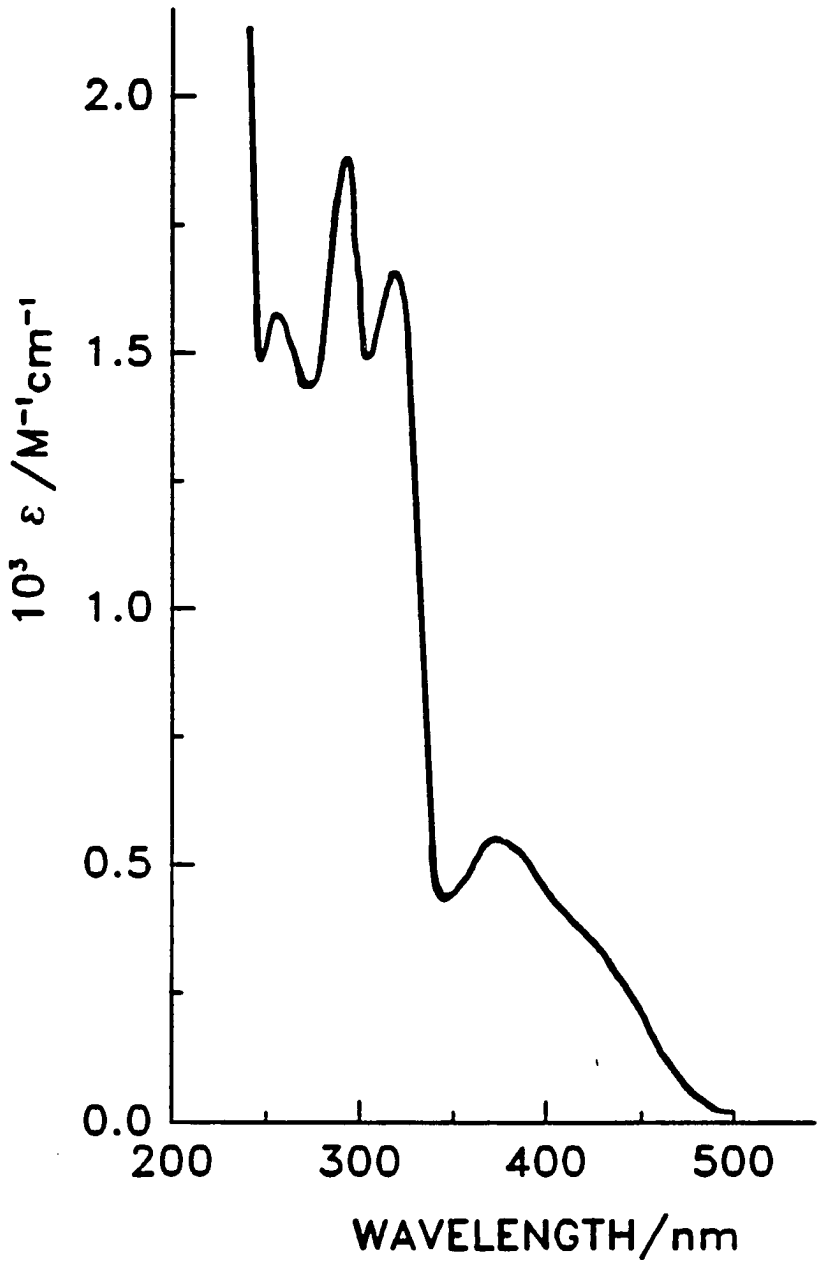

Figure I-12. The UV-visible spectrum of 2,4,6-$(CH_3)_3C_6H_2CH_2Cr^{2+}$ in 0.1 M $HClO_4$

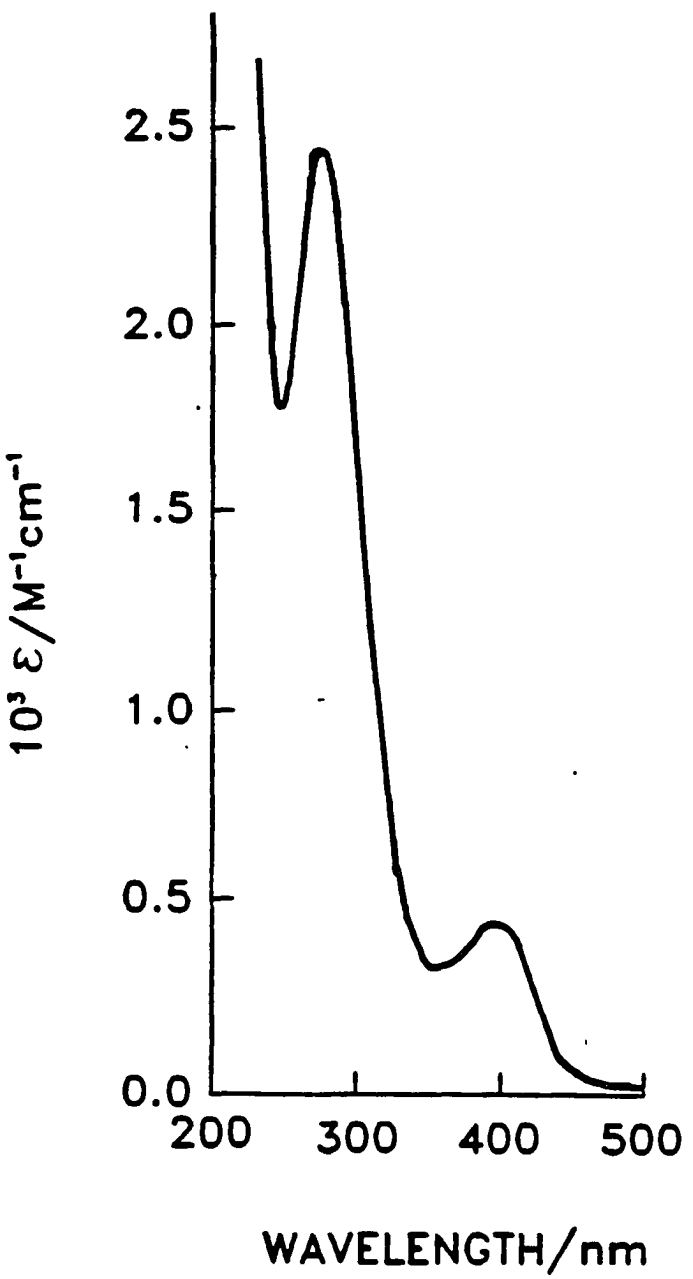

Figure I-13. The UV-visible spectrum of $CH_3CH_2Cr^{2+}$ in 0.1 M $HClO_4$

acid. The compounds were identified by their UV-visible spectra (see Table AI-1).

The CH_3Cr^{2+} and $HOCH_2Cr^{2+}$ compounds were the only ones which were not cation exchanged before the kinetic data were collected, as they decompose rapidly (half-live of about 20 minutes).[1]

Cr(III) perchlorate was made from CrO_3 and H_2O_2 in $HClO_4$, and recrystallized twice from dilute $HClO_4$. Its UV-visible spectrum is $\varepsilon(574) = 13.3\ M^{-1}cm^{-1}$, $\varepsilon(408) = 15.85\ M^{-1}cm^{-1}$, and $\varepsilon(260) = 5\ M^{-1}cm^{-1}$. Cr(II) perchlorate was prepared by the reduction of Cr(III) perchlorate over zinc amalgam. Deuterated Cr(III) perchlorate is made by recrystalization from dilute $HClO_4$ in D_2O.

These reagents were used as obtained from the supplier: anhydrous SO_2 gas (Matheson); ethane sulfonic acid (Pfaltz & Bauer); 1-propane sulfonic acid (Kodak); 2-propane sulfonic acid, sodium salt (Kodak); D_2O, NaOD (Aldrich), bromine, $HClO_4$ (Fisher); pentamethylbenzyl chloride, and 2,4,6-trimethylbenzyl chloride (Alfa).

The SO_2 solutions were made by bubbling SO_2 gas into deaerated $HClO_4$ of known concentration, and then diluting the SO_2 by transferring a small amount of the "stock" SO_2 solution into a syringe of $HClO_4$. In this way, the $[HClO_4]$ was known, and the $[SO_2]$ could be calculated from $\varepsilon(280) = 449 \pm 22\ M^{-1}cm^{-1}$ in 1.2 M $HClO_4$. The ε was found by oxidizing a known volume of saturated SO_2 solution to SO_4^{2-} with a known excess of I_2 (in I_3^-) solution, and titrating the excess I_2 with $S_2O_3^{2-}$.[37] This same SO_2 solution was then diluted from 1/5 to 1/500 fold, the UV spectra were taken for these different solutions, and a Beer's law plot was made. In general, the "stock" SO_2 solution was about 1 - 1.2 M. It was found that

SO_2 solutions of about 0.1 M could conveniently be kept in a stoppered glass syringe for about 12 hours without noticeably decreasing in concentration, but 1 M solutions do give off a lot of gas. This value of the molar absorptivity is somewhat higher than those reported in the literature; $\varepsilon(280) = 367 \pm 18$ $M^{-1}cm^{-1}$ in 5.8 M $HClO_4$ [38] and $\varepsilon(276) = 388$ $M^{-1}cm^{-1}$ in 0.1 M H_2SO_4.[39]

The bromine was dissolved in 1 M $HClO_4$ to give a 0.20 M[40] solution. Bromine solutions for the kinetics were made by appropriate dilutions of this standard solution.

Kinetics

The kinetics with SO_2 were done by the addition of a known amount (usually 0.05 to 0.5 mL, 0.02 to 0.2 M) of thermostated SO_2 solution to thermostated RCr^{2+} in a 1 cm cell, and monitoring the $[RCr^{2+}]$ at the visible peak in the region 350 to 410 nm on a Cary 219 spectophotometer. The final concentrations were typically in the following ranges: $[CrR^{2+}] = (0.1 - 5) \times 10^{-3}$ M, $[SO_2] = (0.7 - 140) \times 10^{-3}$ M, and $[HClO_4] = 1.0 \pm 0.1$ M. The kinetics were done in 1.0 M $HClO_4$ at 25.0 ± 0.1°C under N_2 or Ar unless otherwise noted. Basically, the runs followed pseudo-first-order kinetics and were analyzed by standard methods. However, it was noticed that the presence of any excess Cr^{2+} would interfere with the reaction - an intense green species would form upon the addition of the SO_2, and then, on a timescale longer than that of the reaction of interest, this species would decay to a blue solution which would then get cloudy. This made it difficult to find a D_∞ for the reaction of interest. To circumvent this problem, the organochromium complexes were

either ion-exchanged; or were quickly bubbled with O_2, (to remove any Cr^{2+}) then deoxygenated with N_2. The iso-propyl and cyclopentyl complexes, whose k_H was large compared to their k_S showed evidence for the presence of Cr^{2+} at the end of their reactions, as the solutions were cloudy.

The kinetic data for the bromine reactions were collected using a Durrum D-108 Stopped-Flow apparatus that was interfaced to a Northstar Horizon computer by On-Line Instrument Services, Inc. The reactions were monitored in the 240-290 nm region. The concentrations were typically in the following ranges: $[Br_2] = (0.1 - 20) \times 10^{-3}$ M; $[RCr^{2+}] = (1.0 - 10) \times 10^{-5}$ M. The traces all followed pseudo-first-order kinetics, and were analyzed using the data analysis routines of the OLIS computer system (see Figure I-14).

Product analysis

Inorganic The inorganic products from this reaction were found by bubbling SO_2 from a lecture bottle into solutions of column-purified $(H_2O)_5CrR^{2+}$ for two minutes. The chromium products were then separated on a column of Sephadex SP-C25 cation exchange resin (Pharmacia) by elution with 0.05, 0.11, and 0.42 M $HClO_4$, successively. This process gave a green band, of +1 or +2 charge, which is stable for days in acidic solution, and a blue band of $(H_2O)_6Cr^{3+}$ (identified by its UV-visible spectrum). To further identify the green band obtained from such treatment of the iso-propylchromium complex, KOH was added until the solution was at pH 6, and then qualitative HPLC was run. This showed that iso-propanesulfonate was present in the solution, which means that

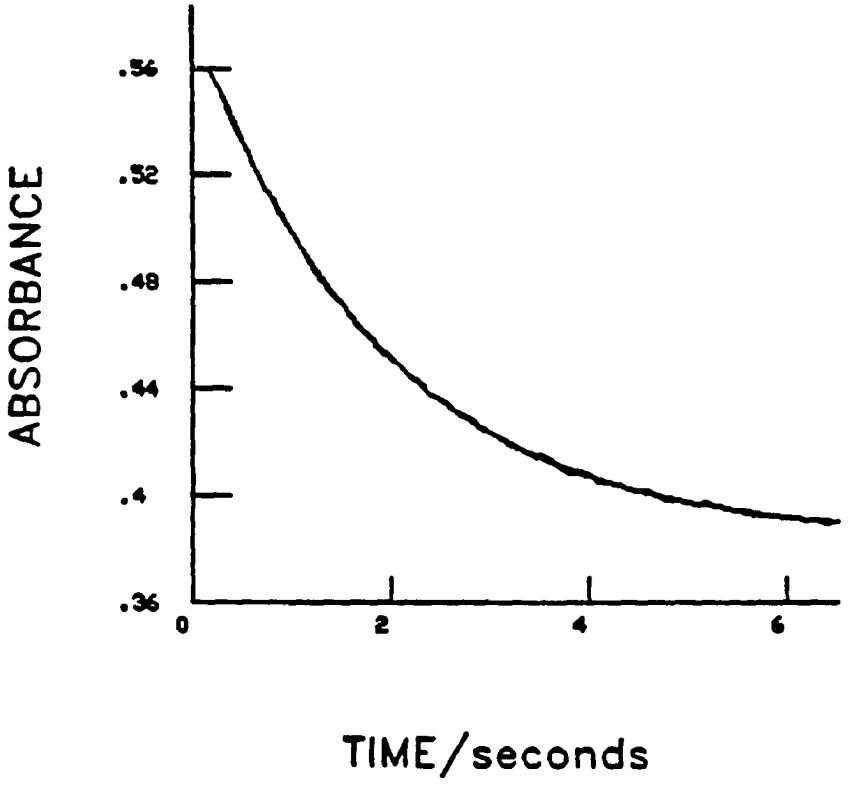

Figure I-14. Kinetic trace for the reaction of $NCCH_2CH_2Cr^{2+}$ with Br_2

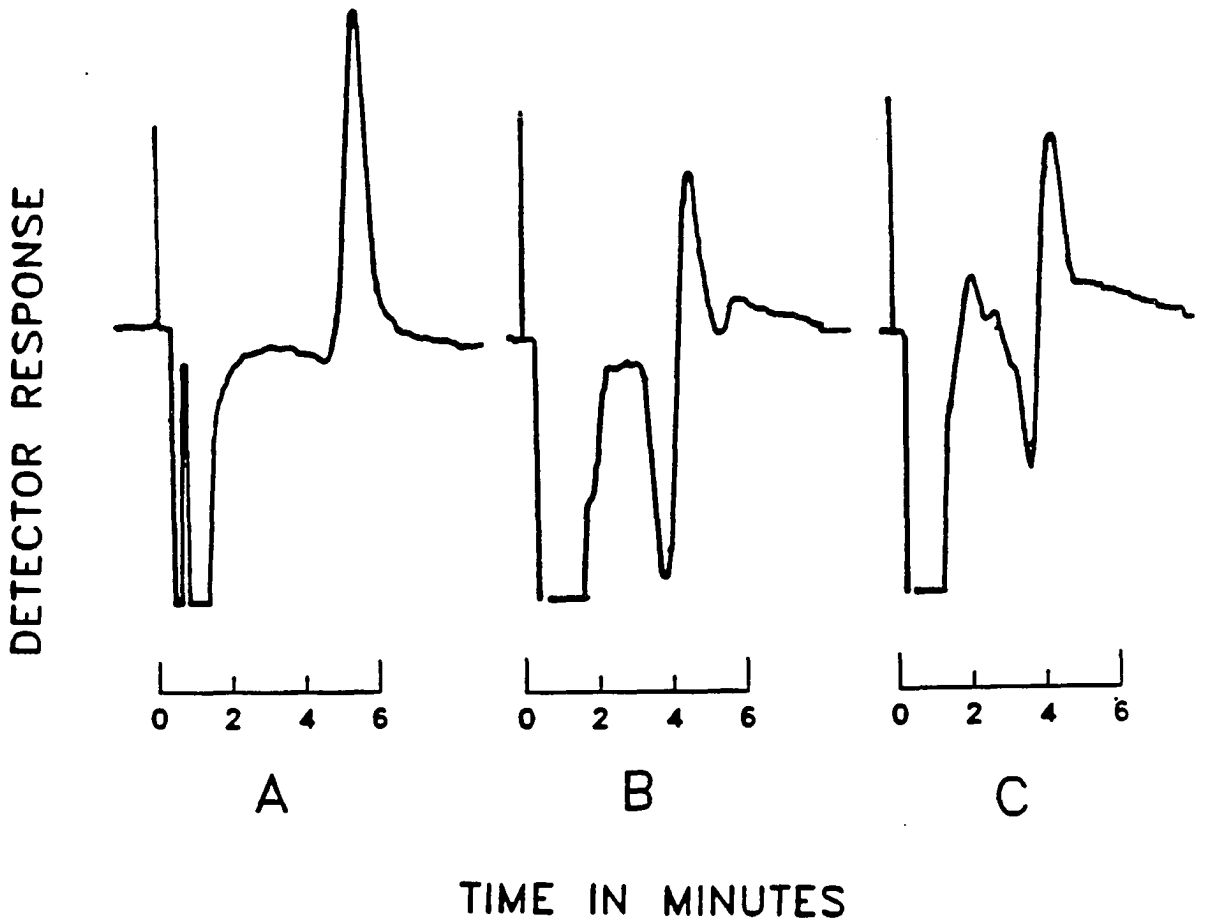

Figure I-15. HPLC separation of the green band from $\underline{i}$-$C_3H_7Cr^{2+}$ and SO_2 after addition of KOH and suction filtration. a) standard; [$\underline{i}$-$C_3H_7SO_3^-$] ~ 10 ppm. b) sample; [$\underline{i}$-$C_3H_7SO_3^-$] ~ 10 ppm. c) 1:1 mixture of standard and sample. Eluant: 1.5 mM succinic acid, flow rate = 1.5 mL/min

the green complex was $(H_2O)_5CrSO_2CH(CH_3)_2^{2+}$ (see Figure I-15).

Organic

HPLC The instruments used[41] were an Hitachi D-2000 Chromato-Integrator, a Curken chart plotter, a Wescan conductivity detector, an LKB Bromma 2150 HPLC pump, and an Eldex Laboratories column heater and temperature controller. The eluant was 1.5 millimolar succinic acid in conductivity water, and the separation was done at 25°C. Flow rates were either 1.0 or 2.0 mL/min. The column was a home-made anion exchange 20 - 26 μm XAD-1 resin [Rohm and Haas] coated with a proprietary weak base anion exchange material, in a 250 mm x 2.0 mm inner diameter glass-lined stainless steel column.[41]

The reaction solutions for the HPLC separations had a higher $[(H_2O)_5CrR^{2+}]$ and a lower $[HClO_4]$ than used in the kinetic experiments, and to achieve this the compounds were not ion-exchanged prior to reaction with SO_2. However, various slight changes in the preparations were made to show that the lack of ion exchanging would have no effect on the reaction products (see Table I-2).

^{1}H NMR The ^{1}H NMR spectra were collected on an 300 MHz Nicolet NT-300 NMR spectrometer. In some cases, this involved making the $C_2H_5Cr^{2+}$ in D_2O, bubbling SO_2 into the D_2O solution, removing the SO_2 with argon, and then adding NaOD to remove the chromium by precipitation. This latter experiment was fraught with problems, as it was difficult to precipitate out all of the chromium, and if any were left, there would be considerable paramagnetic broadening in the spectrum. Nonetheless, a

spectrum identical to that of the sulfonic acid was seen. Alternatively, ion-exchanged organochromium complex was bubbled with SO_2, and the products extracted with $CDCl_3$. The $CDCl_3$ was dried with anhydrous magnesium sulfate, and the ^1H NMR spectrum collected. These products accounted for about 0.5% of the total.

REFERENCES

1. Espenson, J. H. Adv. Inorg. Bioinorg. React. Mech., 1982, 1, 1.

2. Leslie, J. P. II; Espenson, J. H. J. Am. Chem. Soc., 1976, 98, 4839.

3. Espenson, J. H.; Williams, D. A. J. Am. Chem. Soc., 1974, 96, 1008.

4. Chang, J. C.; Espenson, J. H. J. Chem. Soc. Chem. Commun., 1974, 233.

5. Espenson, J. H.; Samuels, G. J. J. Organomet. Chem., 1976, 113, 143.

6. Espenson, J. H.; Connolly, P.; Meyerstein, D.; Cohen, H. Inorg. Chem., 1983, 22, 1009.

7. dmgH = dimethylglyoxime, $HON{:}CH(CH_3)CH(CH_3){:}NOH$.

8. Adin, A.; Espenson, J. H. J. Chem. Soc. Chem. Commun., 1971, 653.

9. Anet, F. A. L.; Leblanc, E. J. Am. Chem. Soc., 1957, 79, 2649.

10. a) Bied-Charreton, C.; Gaudemer, A. J. Organomet. Chem., 1977, 124, 299. b) Giannotti, C.; Septe, B. J. Organomet. Chem., 1973, 52, C45. c) Giannotti, C.; Gaudemer, A.; Fontaine, C. Tetrahedron Lett., 1970, 37, 3209. d) Duong, K. N. V.; Fontaine, C.; Giannotti, C.; Gaudemer, A. Tetrahedron Lett., 1971, 17, 1187. e) Jensen, F. R.; Kiskis, R. C. J. Am. Chem. Soc., 1975, 97, 5825.

11. a) Crease, A. E.; Johnson, M. D. J. Am. Chem. Soc., 1978, 100, 8013. b) Johnson, M. D.; Derenne, S. J. Organomet. Chem., 1985, 286, C47. c) Johnson, M. D.; Lewis, G. J. J. Chem. Soc. A, 1970, 2153.

12. Joseph, M. F.; Baird, M. C. Inorg. Chim. Acta, 1985, 96, 229.

13. a) Fong, C. W.; Kitching, W. J. Organomet. Chem., 1973, 59, 213. b) Moore, C. J.; Kitching, W. J. Organomet. Chem., 1973, 59, 225.

14. a) Murray, K. S.; Cozens, R. J.; Deacon, G. B.; Felder, P. W.; West, B. O. Inorg. Nucl. Chem. Lett., 1986, 4, 705-708. b) Cozens, R. J.; Deacon, G. B.; Felder, P. W.; Murray, K. S.; West, B. O. Aust. J. Chem., 1970, 23, 481.

15. Jacobson, S. E.; Wojcicki, A. J. Organomet. Chem., 1974, 72, 113.

16. Cahiez, G.; Bernard, D.; Normant, J. F.; Villieras, J. J. Organomet. Chem., 1976, 121, 123.

17. Wojcicki, A. Adv. Organomet. Chem., 1974, 12, 31.

18. Hyde, M. R.; Espenson, J. H. J. Am. Chem. Soc., 1976, 98, 4463.

19. Nohr, R. S.; Espenson, J. H. J. Am. Chem. Soc., 1975, 97, 3392.

20. Lowry, T. H.; Richardson, K. H. Mechanism and Theory in Organic Chemistry, Harper and Row: New York, 1981, 2nd Ed., 130-145.

21. Espenson, J. H.; Bakac, A. J. Am. Chem. Soc., 1981, 103, 2728.

22. Hansch, C.; Leo, A.; Unger, S. H.; Kim, K. H.; Nikaitani, D.; Lien, E. J. J. Med. Chem., 1973, 16, 1207.

23. Carlyle, D. W.; King, E. L. Inorg. Chem., 1970, 9, 2333.

24. Finholt, J. E.; Anderson, R. W.; Fyfe, J. A.; Caulton, K. G.; Inorg. Chem., 1965, 4, 43.

25. Stanbury, D. M.; Lednicky, L. A. J. Am. Chem. Soc., 1984, 106, 2847-2853.

26. Kice, J. L.; Adv. Phys. Org. Chem., 1980, 17, 65-170.

27. Oae, S.; Kunieda, N. Organic Chemistry of Sulfur, Plenum Press: New York, 1977, 603-648.

28. Marvel, C. S.; Johnson, R. S. J. Org. Chem., 1948, 13, 822.

29. Collman, J. P.; Hegedus, L. S.; Norton, J. R.; Finke, R. G. Principles and Applications of Organotransition Metal Chemistry, University Science Books: Mill Valley, California, 1987, 446.

30. Sisley, M. J.; Jordan, R. B.; Inorg. Chem., 1986, 25, 3547.

31. Moritzen, P. A.; El-Awady, A. A.: Harris, G. M. Inorg. Chem., 1985, 24, 313.

32. Fieser, M.; Feiser, L. Reagents for Organic Synthesis, Wiley-Interscience: New York, New York, 1967, Vol.1, 450.

33. Melton, J. D.; Bakac, A.; Espenson, J. H. Inorg. Chem., 1986, 25, 3360.

34. J. Chang, Ames Laboratory and Department of Chemistry, Ames, Iowa, 50011. Unpublished results.

35. Bakac, A.; Espenson, J. H. J. Am. Chem. Soc., 1981, 103, 2721.

36. Funke, L. A.; Espenson, J. H. Inorg. Chem., 1981, 20, 897.

37. Skoog, D. A.; West, D. M. Fundamentals of Analytical Chemistry, Third Edition, Holt, Rinehart, Winston: New York, 1976, 360-362.

38. Siskos, P. A.; Peterson, N. C.; Huie, R. E. Inorg. Chem., 1984, 23, 1134.

39. Seo, E. T.; Sawyer, D. T. J. Electroanal. Chem., 1964, 7, 184.

40. Bakac, A. Ames Laboratory, Ames, Iowa, 50011. Personal Communication. 1986.

41. I am indebted to Dr. James Fritz and Ms. Linda Warth for the use of their equipment, columns, and valuable advice.

APPENDIX I. CHARACTERIZATION AND KINETIC DATA FOR REACTIONS OF PENTAAQUOORGANOCHROMIUM(III) COMPLEXES

Table AI-1. UV-Visible Spectra of Various Organochromium(III) Complexes

R	λ (ε)	λ (ε)	λ (ε)	Reference
CH_3	550 (12)	392 (246)	258 (2400)	4
C_2H_5	560 (8.5)	394 (390)	275 (2400)	4
$\underline{n}$-C_3H_7	550 (8.3)	393 (380)	276 (2650)	4
$\underline{i}$-C_3H_7	557 (10.0)	399 (366)	290 (1800)	4
$\underline{c}$-C_5H_9		400 (413)	287 (2427)	5
CH_2OH		393 (570)	282 (2400)	28
CH_2OCH_3	530 (15.3)	385 (404)	270 (2590)	28
CH_2CH_2CN	524 (16)	396 (230)	264 (3530)	29

Table AI-2. Rate Constants for the Reaction between CH_3Cr^{2+} and SO_2 in $HClO_4$ at 25.0 ± 0.1 °C [a]

$[H^+]$/M	$10^3[SO_2]$/M	k_{obs}/s^{-1}
0.5	2.85	0.0423
1.0	2.86	0.0411
1.0	3.91	0.0473
1.0	5.17	0.0543
1.0	6.00	0.0682
1.0	7.23	0.0726
1.0	7.24	0.102
1.0	7.93	0.0923
1.0	8.22	0.107
1.0	11.1	0.144
1.0	11.8	0.148
1.0	14.9	0.173

[a]The second order rate constant, k_S, derived from a plot of k_{obs} versus $[SO_2]$ (see Figure I-3) is 11.3 ± 0.4 $M^{-1}s^{-1}$; the intercept, k_A, is 5.0×10^{-3} $M^{-1}s^{-1}$.[1]

Table AI-3. Rate Constants for the Reaction between $C_2H_5Cr^{2+}$ and SO_2 at 25.0 ± 0.1 °C [a]

$10^2[SO_2]$/M	$[HClO_4]$/M	OXIDIZING AGENT	PREPARATIVE METHOD	k_{obs}/s^{-1}
0.838	0.063	NONE	EtBr hν[b]	0.0277
1.13	0.89	O_2	C_2H_4 hν[c]	0.063
1.68	1.0	NONE	ROOH[d]	0.088
1.66	1.0	CoA_5Cl^{2+}	ROOH	0.107
1.82	0.133	NONE	EtBr hν	0.105
2.07	1.08	O_2	C_2H_4 hν	0.143
2.18	0.02	O_2	EtBr hν	0.189
2.18	0.02	NONE	EtBr hν	0.079
2.46	0.178	NONE	EtBr hν	0.181
3.25	1.02	O_2	C_2H_4 hν	0.218
3.28	0.02	O_2	EtBr hν	0.156
4.33	0.96	O_2	C_2H_4 hν	0.280
5.27	0.91	O_2	C_2H_4 hν	0.323
6.54	0.85	O_2	C_2H_4 hν	0.440

[a]The second-order rate constant, k_S, derived from a plot of k_{obs} versus $[SO_2]$ (see Figure I-3) is 5.2 ± 0.4 $M^{-1}s^{-1}$; the intercept, $(k_H + k_A)$ is 3.3 x 10^{-4} $M^{-1}s^{-1}$.[1]

[b]The compound was made via the photolysis of ethyl bromide.

[c]The compound was made via the photolysis of ethene.

[d]The compound was made from the hydroperoxide (see text, Chapter 1).

Table AI-4. Rate Constants for the Reaction between $\underline{n}$-$C_3H_7Cr^{2+}$ and SO_2 at 25.0 ± 0.1 °C [a]

$[SO_2]$/M	$[HClO_4]$/M	OXIDIZING AGENT	PREPARATIVE METHOD	k_{obs}/s^{-1}
0.00751	1.35	NONE	SEPHADEX[b]	0.00767
0.0109	1.06	NONE	ROOH[c]	0.00700
0.0169	0.91	O_2	PrBr hν[d]	0.0150
0.0214	1.28	NONE	SEPHADEX	0.0214
0.0217	1.08	O_2	ROOH	0.0210
0.0273	1.25	NONE	SEPHADEX	0.0303
0.0304	0.96	O_2	ROOH	0.0240
0.0313	0.84	O_2	PrBr hν	0.0264
0.0340	1.21	NONE	SEPHADEX	0.0349
0.0395	0.89	O_2	PrBr hν	0.0428
0.0397	1.19	NONE	SEPHADEX	0.0443
0.0505	1.14	NONE	SEPHADEX	0.0454
0.0556	1.11	NONE	SEPHADEX	0.0633
0.0604	1.08	NONE	SEPHADEX	0.0738
0.0695	1.04	NONE	SEPHADEX	0.0898

[a]The second order rate constant, k_S, derived from a plot of k_{obs} versus $[SO_2]$ (see Figure I-3) is 0.92 ± 0.05 $M^{-1}s^{-1}$; the intercept, $(k_A + k_H)$, is 3.6×10^{-4} $M^{-1}s^{-1}$.[1]

[b]The compound was purified using Sephadex SP-C25 cation exchange resin, as described in Chapter 1.

[c]The compound was made from the hydroperoxide (see text, Chapter 1).

[d]The compound was made via the photolysis of propyl bromide.

Table AI-5. Rate Constants for the Reaction between $\underline{i}$-$C_3H_7Cr^{2+}$ and SO_2 at 25.0 ± 0.1 °C in 1.0 M $HClO_4$ [a]

$[SO_2]$/M	$10^4 k_{obs}/s^{-1}$
0.0121	6.15
0.0244	8.99
0.0440	14.6
0.0831	23.2
0.111	26.4
0.117	27.4
0.133	35.1

[a]The second-order rate constant, k_S, derived from a plot of k_{obs} versus $[SO_2]$ (see Figure I-3) is 0.022 ± 0.001 $M^{-1}s^{-1}$; the intercept, $(k_A + k_H)$ is 2.8 x 10^{-4} s^{-1}.[1]

Table AI-6. Rate Constants for the Reaction between c-$C_5H_9Cr^{2+}$ and SO_2 at 25.0 ± 0.1 °C in 1.0 M $HClO_4$ [a]

$[SO_2]$/M	$10^3 k_{obs}/s^{-1}$
0.0243	1.023
0.0487	1.188
0.0609	1.241
0.0730	1.149
0.0974	1.621
0.0974	1.455
0.122	1.695

[a]The second-order rate constant, k_S, derived from a plot of k_{obs} versus $[SO_2]$ (see Figure AI-1) is (9.8 ± 0.8) x 10^3 $M^{-1}s^{-1}$; the intercept, $(k_A + k_H)$, is 5.8 x 10^{-4} s^{-1}.[5]

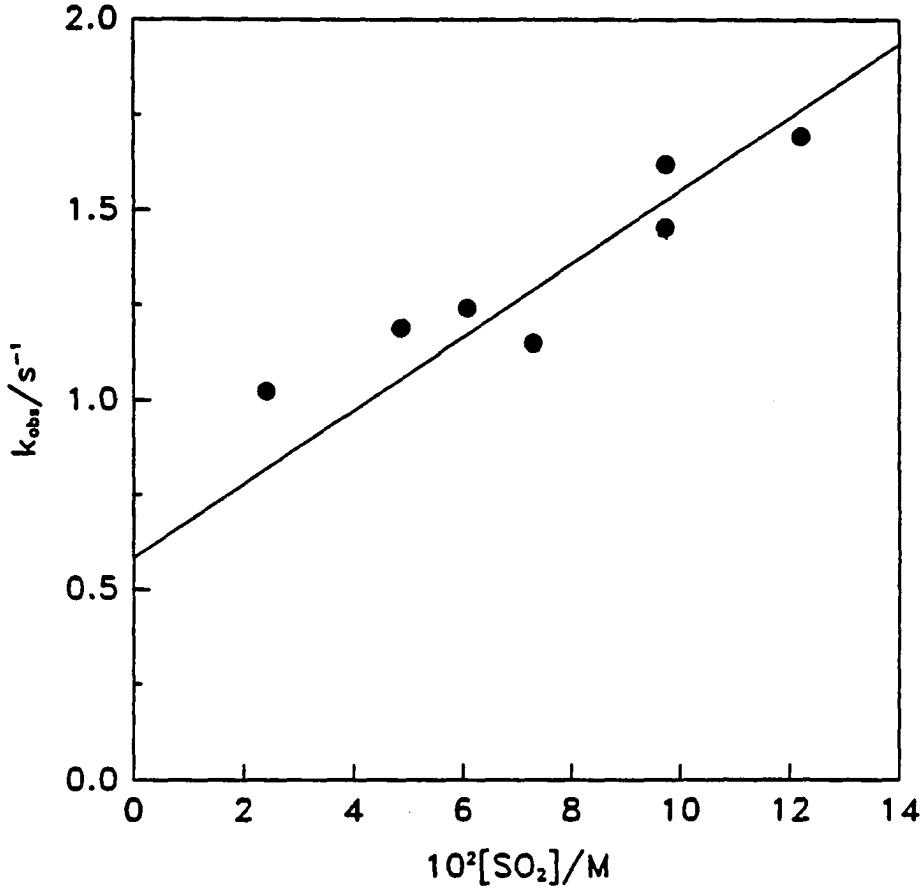

Figure AI-1. Plot of k_{obs} versus $[SO_2]$ for the reaction of SO_2 with $\underline{c}$-$C_5H_9Cr^{2+}$

Table AI-7. Rate Constants for the Reaction between $PhCH_2Cr^{2+}$ and SO_2 at 1.9 ± 0.1 °C in 1.0 M $HClO_4$

$10^3[SO_2]_{av}/M$	$10^4[RCr^{2+}]/M$	$10^2k_{obs}/s^{-1}$ [a]
1.61	1.3	0.266
4.94	1.6	1.57
5.33	6.7	1.22
6.64	1.0	1.92
7.99	6.9	2.19
8.62	1.8	1.91
9.96	1.5	2.24
10.3	1.3	2.40
11.6	1.5	2.62
13.3	1.0	3.68

[a]The second-order rate constant, k_S, derived from a plot of k_{obs} versus $[SO_2]$ (see Figure AI-2) is 2.5 ± 0.2 $M^{-1}s^{-1}$; the intercept, k_H, is 2.7 x 10^{-5} s^{-1}.[18]

Table AI-8. Rate Constants for the Reaction between $PhCH_2Cr^{2+}$ and SO_2 at 11.4 ± 0.2 °C in 1.0 M $HClO_4$ [a]

$10^3[SO_2]_{av}/M$	$10^4[RCr^{2+}]/M$	$10^2k_{obs}/s^{-1}$
3.30	3.5	1.27
5.01	4.0	1.83
8.46	4.5	2.94
12.7	5.7	4.53
15.4	4.0	5.49
17.1	5.7	6.03
21.7	1.4	6.89

[a]The second-order rate constant, k_S, derived from a plot of k_{obs} versus $[SO_2]$ (see Figure AI-2) is (3.46 ± 0.07) $M^{-1}s^{-1}$; the intercept, k_H, is 2.0 x 10^{-4} s^{-1}.[18]

Table AI-9. Rate Constants for the Reaction between $PhCH_2Cr^{2+}$ and SO_2 at 25.0 ± 0.1 °C in 1.0 ± 0.1 M $HClO_4$ [a]

$10^3[SO_2]_{av}$/M	$10^4[RCr^{2+}]$/M	$10^2k_{obs}/s^{-1}$
0.897	3.8	0.84 ± 0.02 [b]
0.938	3.0	0.808
0.900	2.0	0.79 ± 0.05 [c]
1.26	5.5	1.0 ± 0.3 [c]
1.76	4.1	1.3 ± 0.5 [d]
2.14	9.0	1.53
5.67	4.2	3.25
7.01	7.7	3.85
7.16	4.3	4.75
8.65	9.0	4.9 ± 0.2 [c]
9.42	7.6	5.11
10.8	7.2	5.72
12.8	6.7	7.13
14.0	6.2	7.61
15.5	7.8	8.00

[a]The second-order rate constant, k_S, derived from a plot of k_{obs} versus $[SO_2]$ (see Figure AI-2) is (5.2 ± 0.1) $M^{-1}s^{-1}$; the intercept, k_H, is 2.63×10^{-3} $M^{-1}s^{-1}$.[18]

[b]Average of two runs.

[c]Average of four runs.

[d]Average of three runs.

Table AI-10. Rate Constants for the Reaction between $PhCH_2Cr^{2+}$ and SO_2 at 39.9 ± 0.2 °C [a]

$10^3[SO_2]_{av}/M$	$10^4[RCr^{2+}]/M$	$10^2k_{obs}/s^{-1}$	$[H^+]/M$
1.56	1.4	4.54	0.85
2.80	1.5	4.83	0.99
3.19	1.5	5.11	0.85
3.74	2.7	6.75	0.84
4.97	1.0	6.69	1.00
5.66	1.1	6.99	0.85
6.47	1.1	7.11	0.87
7.14	3.2	7.69	0.84
7.25	1.8	9.02	0.85
7.66	8.0	9.20	0.87
8.28	1.6	9.51	1.00
8.87	3.2	9.91	0.84
10.7	1.6	10.9	1.00
11.5	1.2	13.6	0.85
13.3	1.9	12.0	1.00
17.2	1.2	18.9	0.85

[a]The second-order rate constant, k_S, derived from a plot of k_{obs} versus $[SO_2]$ (see Figure AI-2) is 8.0 ± 0.3 $M^{-1}s^{-1}$; the intercept, k_H, is 2.9 x 10^{-3} s^{-1}.[18]

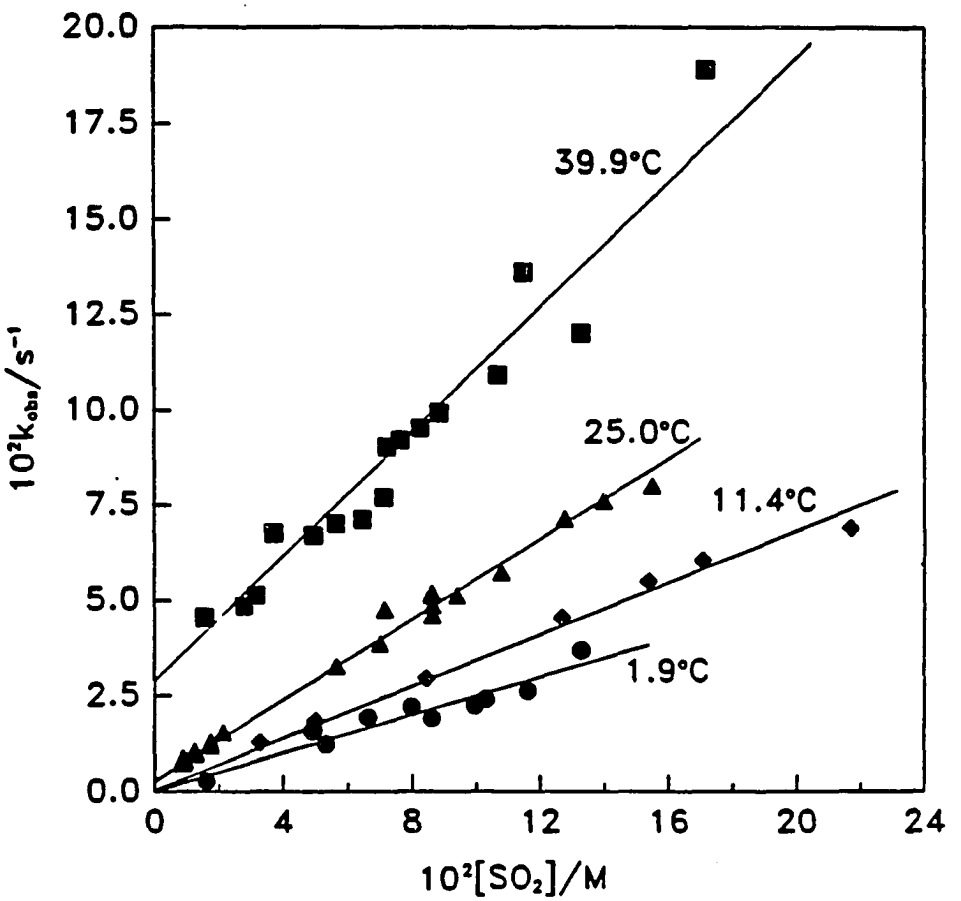

Figure AI-2. Plot of k_{obs} versus $[SO_2]$ for the reaction of SO_2 with $PhCH_2Cr^{2+}$ at 1.9 (●), 11.4 (◆), 25.0 (▲), and 39.9 (■)°C

Table AI-11. Rate Constants for the Reaction of SO_2 with $p\text{-}CH_3OC_6H_4CH_2Cr^{2+}$ at 25.0 ± 0.1 °C in 1.0 M $HClO_4$ [a]

$10^3[SO_2]/M$	$10^2k_{obs}/s^{-1}$
2.33	2.72
2.60	2.67
4.47	4.25
5.44	4.55
5.64	4.89
5.64	4.93
9.85	5.13
11.6	10.0
12.0	9.80
12.0	11.0
12.5	10.9

[a]The second-order rate constant, k_S, derived from a plot of k_{obs} versus $[SO_2]$ (see Figure I-4) is 7.8 ± 0.3 $M^{-1}s^{-1}$; the calculated intercept, k_H, is (7.1 ± 1.4) x 10^{-3} s^{-1}.

Table AI-12. Rate Constants for the Reaction of SO_2 with $p\text{-}CH_3C_6H_4CH_2Cr^{2+}$ at 25.0 ± 0.1 °C in 1.0 M $HClO_4$ [a]

$10^3[SO_2]_{av}$/M	$[H^+]$/M	$10^2k_{obs}/s^{-1}$
2.0	1.09	1.76 ± 0.13 [b]
2.3	0.31	1.98 ± 0.05 [b]
2.3	0.05	1.90 ± 0.08 [b]
6.2	1.09	4.40
6.6	1.09	4.5 ± 0.2 [c]
7.3	0.34	5.4 ± 0.3 [b]

[a]The second-order rate constant, k_S, derived from a plot of k_{obs} versus $[SO_2]$ (see Figure I-4) is 6.7 ± 0.1 $M^{-1}s^{-1}$; the intercept, k_H, is 3.74×10^{-3} s^{-1}.[18]

[b]Average of four runs.

[c]Average of three runs.

Table AI-13. Rate Constants for the Reaction of SO_2 with $p\text{-}BrC_6H_4CH_2Cr^{2+}$ at 25.0 ± 0.1 °C in 1.0 M $HClO_4$ [a]

$10^3[SO_2]_{av}/M$	$10^2k_{obs}/s^{-1}$
2.94	1.06 ± 0.04 [b]
6.00	2.01 ± 0.06 [b]
9.00	2.66 ± 0.13 [c]
12.0	3.32 ± 0.13 [b]
15.0	4.07
17.7	5.06
21.0	5.70

[a]The second-order rate constant, k_S, derived from a plot of k_{obs} versus $[SO_2]$ (see Figure I-4) is (2.81 ± 0.06) $M^{-1}s^{-1}$; the intercept, k_H, is 1.56 x 10^{-3} s^{-1}.[18]

[b]Average of three runs.

[c]Average of two runs.

Table AI-14. Rate Constants for the Reaction of SO_2 with $p\text{-}CF_3C_6H_4CH_2Cr^{2+}$ at 25.0 ± 0.1 °C in 1.0 M $HClO_4$ [a]

$10^3[SO_2]_{av}/M$	$10^2k_{obs}/s^{-1}$ [a]
2.23	4.5 ± 0.9 [b]
4.51	10.1 ± 0.1 [c]
6.90	13.9 ± 0.4 [b]
7.44	14.6 ± 0.7 [c]
9.08	19 ± 1 [b]
12.4	23 ± 1 [b]
14.6	26.7 ± 0.4 [c]
16.9	31.5 ± 0.4 [c]

[a]The second-order rate constant, k_S, derived from a plot of k_{obs} versus $[SO_2]$ (see Figure I-4) is (1.82 ± 0.04) $M^{-1}s^{-1}$; the intercept, k_H, is 7.3×10^{-4} s^{-1}.[4]

[b]Average of four runs.

[c]Average of three runs.

Table AI-15. Rate Constants for the Reaction of SO_2 with $2,4,6\text{-}(CH_3)_3C_6H_2CH_2Cr^{2+}$ at 25.0 ± 0.1 °C in 1.0 M $HClO_4$ [a]

$10^3[SO_2]_{av}$/M	$[H^+]$/M	k_{obs}/s^{-1} [a]
2	0.8	0.215 ± 0.003 [b]
22.0	1.5	0.371 ± 0.007 [b]
22.0	0.8	0.369 ± 0.007 [c]
51.0	1.5	0.47 ± 0.03 [d]
104	0.8	0.744 ± 0.006 [c]

[a]The second-order rate constant, k_S, derived from a plot of k_{obs} versus $[SO_2]$ (see Figure AI-3) is 5.9 ± 0.3 $M^{-1}s^{-1}$; the intercept, k_H, is 0.18 s^{-1}.

[b]Average of two runs.

[c]Average of three runs.

[d]Average of five runs.

Table AI-16. Rate Constants for the Reaction of SO_2 with $(CH_3)_5C_6CH_2Cr^{2+}$ at 25.0 ± 0.1 °C in 1.0 M $HClO_4$ [a]

$10^3[SO_2]_{av}$/M	k_{obs}/s^{-1}
2.84	0.374 ± 0.006
21.7	0.72 ± 0.03

[a]The second-order rate constant, k_S, derived from a plot of k_{obs} versus $[SO_2]$ (see Figure AI-3) is 23 ± 2 $M^{-1}s^{-1}$; the intercept, k_H, is (0.25 ± 0.04) s^{-1}.

[b]Average of three runs.

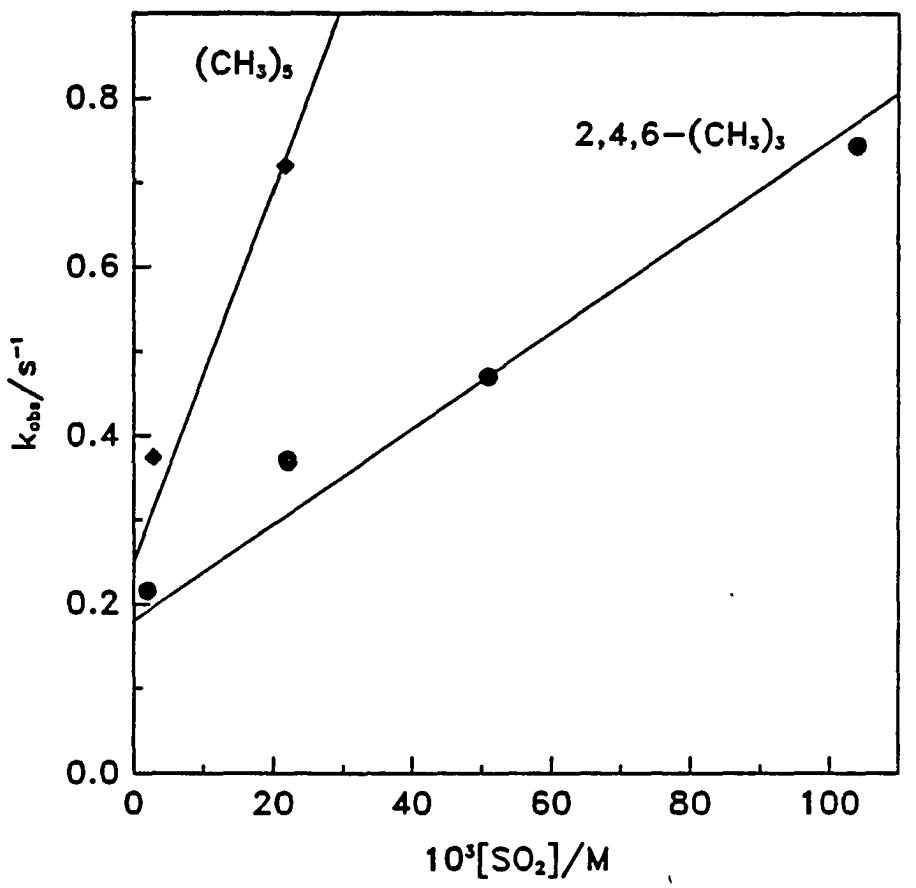

Figure AI-3. Plot of k_{obs} versus $[SO_2]$ for the reaction of SO_2 with $2,4,6\text{-}(CH_3)_3C_6H_2CH_2Cr^{2+}$ (●) and $(CH_3)_5C_6CH_2Cr^{2+}$ (◆)

Table AI-17. Rate Constants for the Reaction of SO_2 with $HOCH_2Cr^{2+}$ at 25.0 ± 0.1 °C in 1.0 ± 0.1 M $HClO_4$ and 4.3 M CH_3OH [a]

$10^3[SO_2]_{av}/M$	$10^3k_{obs}/s^{-1}$
8.77	2.96
17.5	4.58
26.3	6.09
35.0	7.85
43.8	8.41
43.8	8.70
60.2	13.4
70.0	16.1
87.6	19.8

[a]The second-order rate constant, k_S, derived from a plot of k_{obs} versus $[SO_2]$ (see Figure AI-4) is (0.192 ± .006) $M^{-1}s^{-1}$; the intercept, $k_H + k_A$, is 1.13 x 10^{-3} s^{-1}.[1]

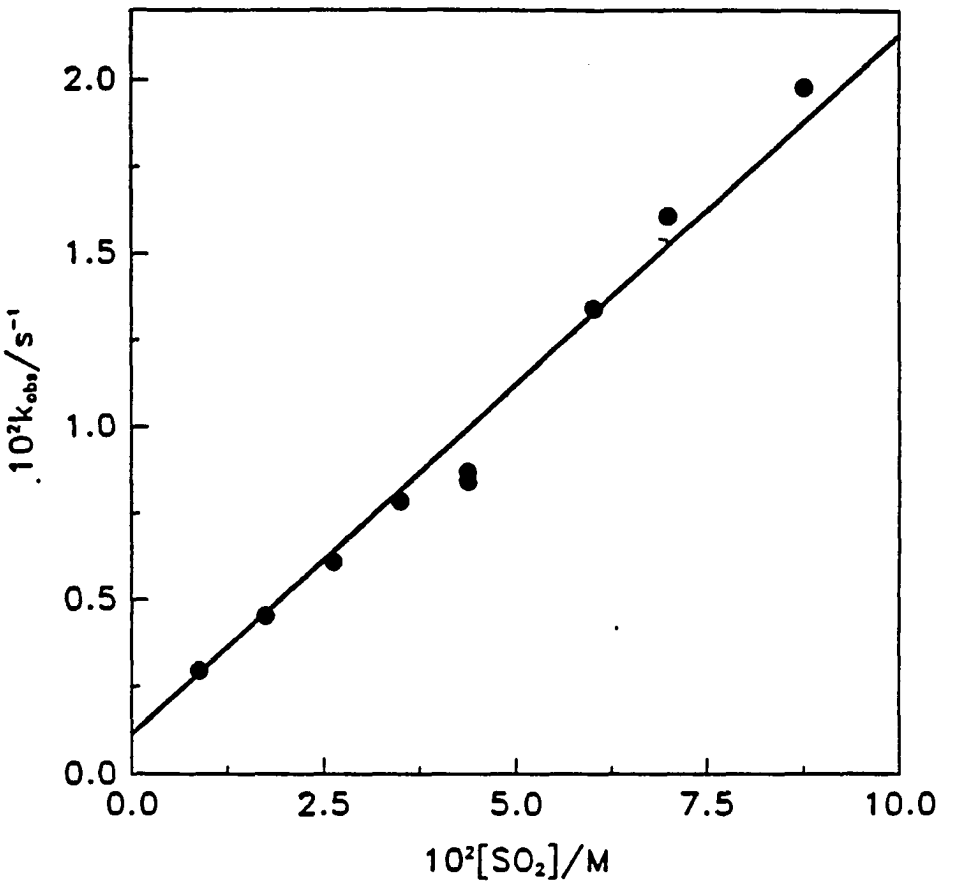

Figure AI-4. Plot of k_{obs} versus $[SO_2]$ for the reaction of SO_2 with $HOCH_2Cr^{2+}$

Table AI-18. Rate Constants for the Reaction of SO_2 with $CH_3OCH_2Cr^{2+}$ at 25.0 ± 0.1 °C in 1.0 M $HClO_4$ [a]

$10^2[SO_2]_{av}/M$	$10^5k_{obs}/s^{-1}$
2.91	4.32
5.83	8.82
7.72	10.0
7.89	9.40
8.73	11.6
8.73	12.3
10.8	15.0

[a]The second-order rate constant, k_S, derived from a plot of k_{obs} versus $[SO_2]$ (see Figure AI-5) is (1.25 ± 0.04) x 10^{-3} $M^{-1}s^{-1}$; the intercept is 0.0 s^{-1}.[1]

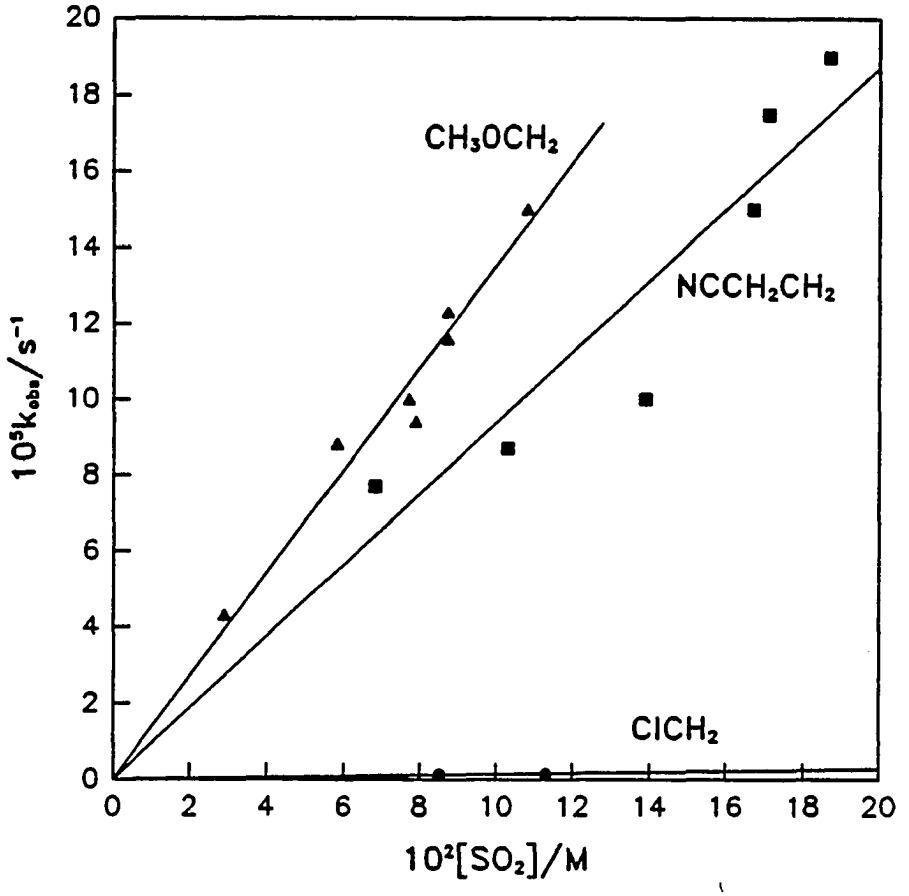

Figure AI-5. Plot of k_{obs} versus $[SO_2]$ for the reaction of SO_2 with $CH_3OCH_2Cr^{2+}$ (▲), $NCCH_2CH_2Cr^{2+}$ (■), and $ClCH_2Cr^{2+}$ (●)

Table AI-19. Rate Constants for the Reaction of SO_2 with $NCCH_2CH_2Cr^{2+}$ at 25.0 ± 0.1 °C in 1.0 M $HClO_4$ [a]

$10^2[SO_2]_{av}$/M	$10^5k_{obs}/s^{-1}$
6.82	7.70
10.3	8.70
13.9	10.0
16.7	15.0
17.1	17.5
18.7	19.0

[a]The second-order rate constant, k_S, derived from a plot of k_{obs} versus $[SO_2]$ (see Figure AI-5) is (7.9 ± 0.6) x 10^{-4} $M^{-1}s^{-1}$; the intercept is 0.0 s^{-1}.[21]

Table AI-20. Rate Constants for the Reaction of SO_2 with $ClCH_2Cr^{2+}$ at 25.0 ± 0.1 °C in 1.0 M $HClO_4$ [a]

$10^2[SO_2]_{av}$/M	$10^6k_{obs}/s^{-1}$
8.51	1.33
11.3	1.48

[a]The second-order rate constant, k_S, derived from a plot of k_{obs} versus $[SO_2]$ (see Figure AI-5) is (8.5 ± 0.3) x 10^{-6} $M^{-1}s^{-1}$; the intercept, k_A, is 5.6 x 10^{-7} s^{-1}.[1]

Table AI-21. Rate Constants for the Reaction of Br_2 with $\underline{n}$-$C_3H_7Cr^{2+}$ at 25.0 ± 0.1 °C in 1.0 M $HClO_4$ [a]

$10^5[Br_2]_{av}$/M	k_{obs}/s^{-1}
5.39	13.9 ± 0.3 [b]
11.2	24 ± 2 [c]
17.4	37 ± 2 [c]
23.0	45.2 ± 0.6 [c]
29.6	57 ± 2 [b]

[a]The second-order rate constant, k_{Br}, derived from a plot of k_{obs} versus $[SO_2]$ (see Figure AI-6) is (1.99 ± 0.03) x 10^5 $M^{-1}s^{-1}$; the intercept, $k_H + k_A$, is 3.6 x 10^{-4} s^{-1}.[1]

[b]Average of four runs.

[c]Average of five runs.

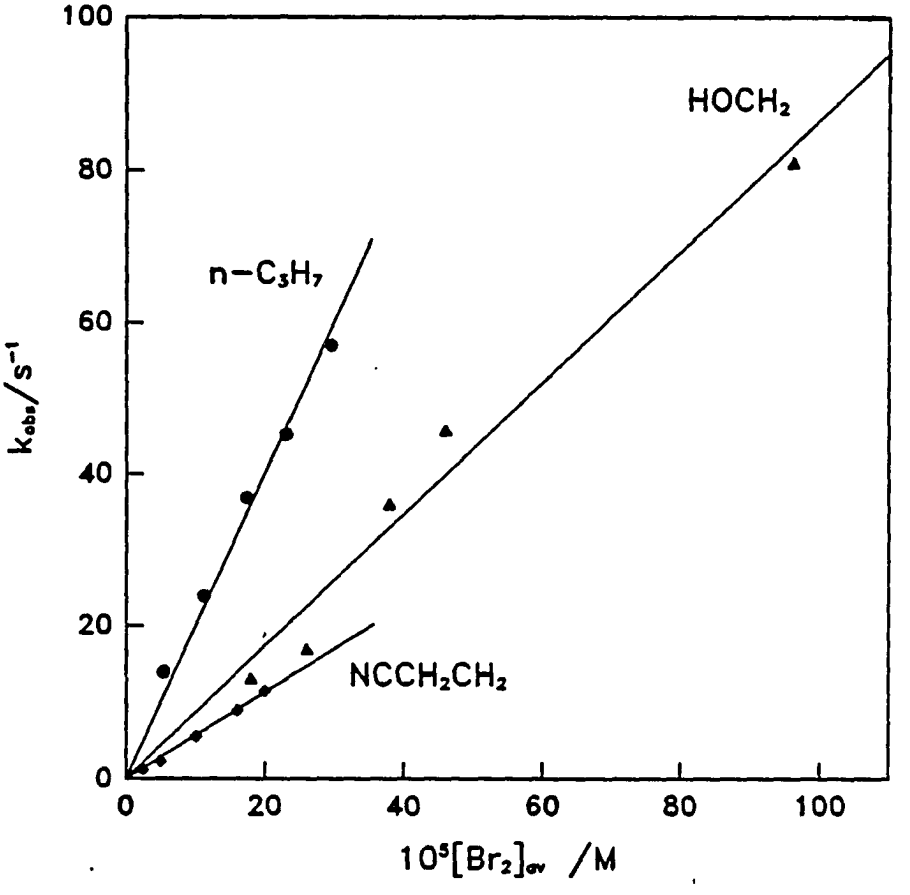

Figure AI-6. Plot of k_{obs} versus $[Br_2]$ for the reaction of bromine with $\underline{n}$-$C_3H_7Cr^{2+}$ (●), $HOCH_2Cr^{2+}$ (▲), and $NCCH_2CH_2Cr^{2+}$ (◆)

Table AI-22. Rate Constants for the Reaction of Br_2 with $HOCH_2Cr^{2+}$ at 25.0 ± 0.1 °C in 1.0 M $HClO_4$ [a]

$10^4[Br_2]_{av}/M$	k_{obs}/s^{-1}
1.8	13.2 ± 0.5 [b]
2.6	17 ± 1 [b]
3.8	36.1 ± 0.5 [b]
4.6	45.8 ± 0.8 [b]
9.6	81 ± 1 [c]

[a]The second-order rate constant, k_S, derived from a plot of k_{obs} versus $[SO_2]$ (see Figure AI-6) is (8.7 ± 0.2) x 10^4 $M^{-1}s^{-1}$; the intercept, $k_H + k_A$, is 1.13 x 10^{-3} s^{-1}.[1]

[b]Average of five runs.

[c]Average of four runs.

Table AI-23. Rate Constants for the Reaction of Br_2 with $NCCH_2CH_2Cr^{2+}$ at 25.0 ± 0.1 °C in 1.0 M $HClO_4$ [a]

$10^5[Br_2]_{av}$/M	k_{obs}/s^{-1}
2.42	1.22 ± 0.04 [b]
4.92	2.33 ± 0.06 [b]
10.0	5.6 ± 0.3 [c]
16.0	9.0 ± 0.3 [d]
20.0	11.5 ± 0.6 [d]

[a]The second-order rate constant, k_S, derived from a plot of k_{obs} versus $[SO_2]$ (see Figure AI-6) is 540 ± 7 $M^{-1}s^{-1}$; the intercept is 0.0 s^{-1}.[1]

[b]Average of four runs.

[c]Average of ten runs.

[d]Average of eight runs.

Table AI-24. Rate Constants for the Reaction of Radical Scavengers with $p\text{-}CH_3OC_6H_4CH_2Cr^{2+}$ at 25.0 ± 0.1 °C in 1.0 M $HClO_4$

Oxidant	10^3[Oxidant]/M	$10^2k_{obs}/s^{-1}$
Fe^{3+}	2.88	1.29
Fe^{3+}	9.29	3.55
Fe^{3+}	25.4	5.97
Fe^{3+}	39.0	8.65
Fe^{3+}	39.0	9.64
O_2	1.0	1.70
O_2	1.0	1.53
Cu^{2+}	50.8	0.788
Cu^{2+}	272	1.08
Cu^{2+}	417	1.20

Table AI-25. Rate Constants for the Reaction of Radical Scavengers with $2,4,6\text{-}(CH_3)_3C_6H_2CH_2Cr^{2+}$ at 25.0 ± 0.1 °C [a]

Oxidant	[Oxidant]/M	$[H^+]$/M	$10^3k_{obs}/s^{-1}$
Cu^{2+}	0.1	0.3	1.68 ± 0.2[b]
$Co(NH_3)_5Cl^{2+}$	0.0085	0.8	1.79 ± 0.5[b]
Fe^{3+}	0.002	1.0	1.77 ± 0.7[c]
Cu^{2+} and O_2	0.1 and 10^{-3}	1.0	1.80 ± 0.2[c]
Cu^{2+}	0.008	1.8	2.04 ± 0.6[c]

[a]The first-order and second-order rate constants, k_H and k_A, derived from a plot of k_{obs} versus $[H^+]$ are 0.156 s^{-1} and 0.025 $M^{-1}s^{-1}$, respectively. $k_H + k_A$ in 1.0 M $HClO_4$ is 0.18 s^{-1}.

[b]Average of two runs.

[c]Average of three runs.

Table AI-26. Rate Constants for the Reaction of Radical Scavengers with $(CH_3)_5C_6CH_2Cr^{2+}$ at 25.0 ± 0.2 °C [a]

Oxidant	10^4[Oxidant]/M	[H^+]/M	$10^1 k_{obs}/s^{-1}$
Cu^{2+}	-[b]	0.55	2.55 ± 0.06[c]
Cu^{2+}	~25	0.55	2.63
Fe^{3+}	-[b]	0.55	2.7 ± 0.3[d]
Fe^{3+}	~20	0.55	2.31
$Co(NH_3)_5Cl^{2+}$	-[b]	0.55	2.00
Fe^{3+}	10	1.0	2.07 ± 0.0[c]
Fe^{3+}	6.0	1.0	2.58 ± 0.04[c]
Fe^{3+}	2.0	1.0	2.24
Cu^{2+}	10	1.0	2.88
Cu^{2+}	104	0.055	2.29 ± 0.02[c]
Cu^{2+}	104	0.115	2.26
Air	2	0.14	3.0 ± 0.2[c]

[a]The average of all of these rate constants yields the rate constant for homolysis, k_H, which is 0.25 ± 0.04 s^{-1}.

[b]Cr^{2+} had been added to these organochromium solutions to retard their decomposition during the course of the day.

[c]Average of two runs.

[d]Average of three runs.

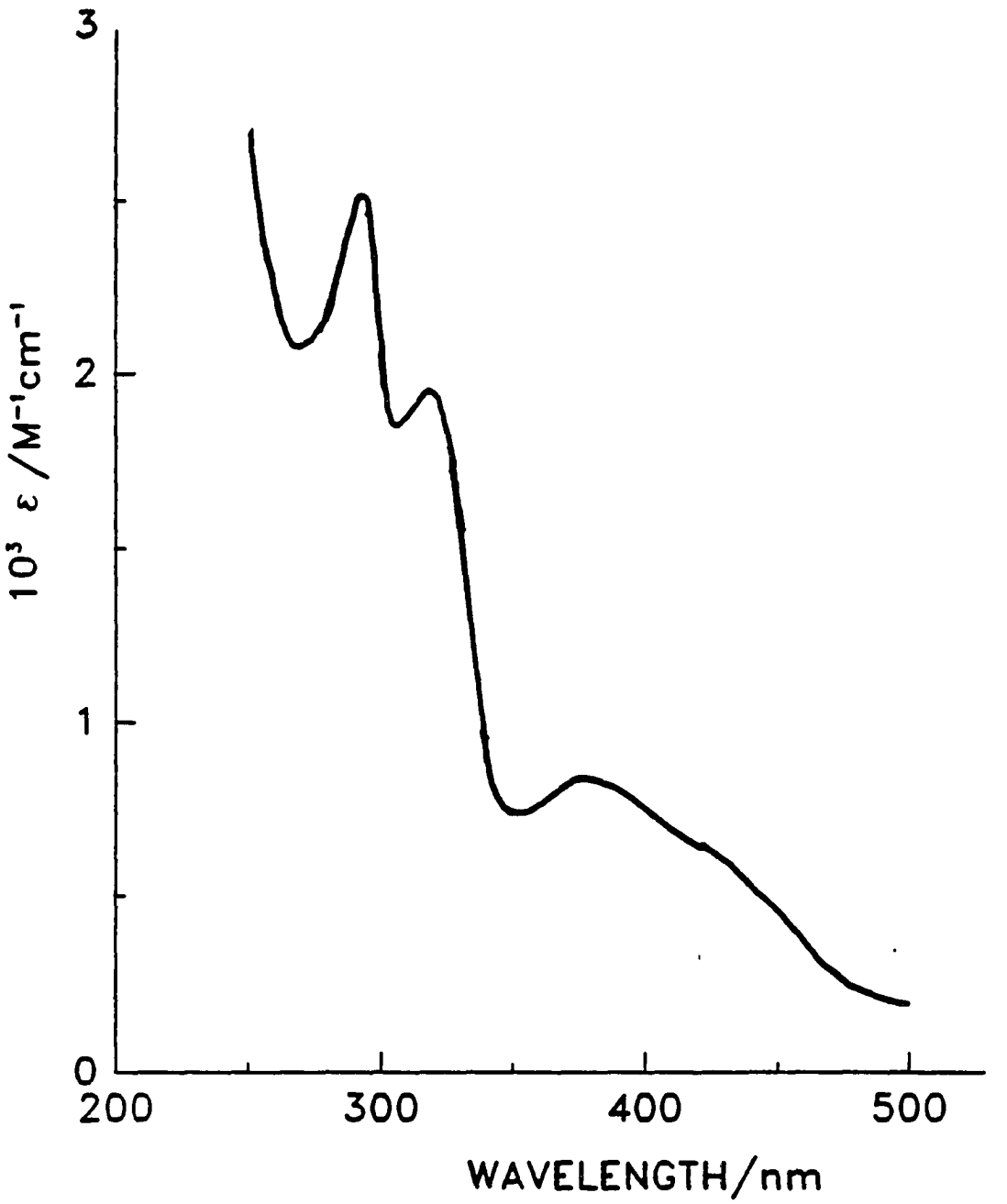

Figure AI-7. The UV-visible spectrum of $(CH_3)_5C_6CH_2Cr^{2+}$ in 0.1 M $HClO_4$

CHAPTER II. REACTIONS OF PHOTOCHEMICALLY GENERATED TRISBIPYRIDINE AND TRISPHENANTHROLINECHROMIUM COMPLEXES. A CALCULATION OF THE SO_2/SO_2^- SELF-EXCHANGE RATE CONSTANT

INTRODUCTION

This chapter endeavors to augment the understanding of outer sphere electron transfer reactions. Electron transfer reactions of transition metal complexes are of importance in biological, catalytic, and solar energy systems. A better understanding of the factors which influence the rates of electron transfer reactions would aid in the design of catalysts and solar energy systems. The transfer of an electron from one compound to another may occur by an inner or outer sphere mechanism. In an inner sphere reaction, an atomic bridge is formed between the two reactants, but outer sphere reactions have no such bridge. Both ground and excited state species may react by electron transfer.

In 1956 Marcus[1] postulated a theory of electron transfer. According to his formulation, the rate constant of an homogeneous electron transfer reaction[2] may be calculated based on the driving force of the reaction and the self-exchange rates of the reactants.[3] Subsequent amplifications of this theory include terms for the size and charge of the reactants and products, temperature, and the ionic strength of the medium. The more recent quantum mechanical[4] and semiclassical[5] theories consider the effects of nuclear tunneling and orbital overlap on the rate constant. Marcus theory has been applied to a myriad of chemical reactions in an attempt to probe its validity. In general, the theory seems applicable to ground and excited state transition metal complexes and small inorganic molecules, such as NO_2^-, ClO_2^-, and N_3^-,[6] and as such provides a method for calculating the self-exchange rate constant of a compound.

The self-exchange rate constant (k_{ex}) of a compound is the rate at

which an electron transfers from a reduced oxidation state of a compound to an oxidized one, for example,

$$D + D^- \xrightarrow[k_{ex}]{} D^- + D \qquad (1)$$

This rate constant may be calculated by using rate constants from cross reactions and expressions from electron transfer theory, or it may be assumed to be approximately equal to the rate constant of the reaction between two similar complexes whose reduction potentials differ only slightly.[7]

The major objective of this work is to determine k_{ex} for the SO_2/SO_2^- couple using electron transfer theories, via the reaction

$$D + SO_2 \longrightarrow D^+ + SO_2^- \qquad (2)$$

It is known that the unpaired electron density on SO_2^- is 75% localized on the sulfur atom,[8] and that upon reduction the OSO angle shrinks from 119.5° to 110°, and the S-O bond lengths increase from 1.43 A° to 1.51 A°,[9] as expected.[10] The HOMO of SO_2 is π, and the LUMO is π^*;[11] additionally, molecular orbital calculations have shown that some contribution from the sulfur d orbitals must be invoked in order to properly correlate experimental and calculated bond lengths and angles.[12]

In order to calculate the SO_2/SO_2^- self-exchange rate constant accurately, one needs the proper values for the reduction potentials of the two reactants and the correct self-exchange rate constant for the other reactant. For the SO_2/SO_2^- couple in aqueous solution there are two reduction potentials available in the literature; E° = -0.262 V,

which is calculated from the ΔG_f° of the reactants and products of the following reaction:[13]

$$SO_2\ (aq) + 1/2\ H_2 \quad \langle\!=\!\rangle \quad SO_2^-\ (aq) + H^+\ (aq) \qquad (3)$$

and $E^\circ = -0.17$ V, which is the experimental result of the cyclic voltammetry of SO_2 in 1.0 M HCl.[14] The experimentally measured reduction potential is pH dependent.

In order for this approach to work, the reaction must be outer sphere, and both k_{ex} and the reduction potential, E°, for D must be known. Preferably, the potential of D will be close to that of the SO_2/SO_2^- couple, as Marcus theory applies most accurately when ΔE is less than 0.4 V.

Many metallic species are known to reduce SO_2 to SO_2^- - for example, Cu metal, Fe(II), Co(II), Cu(I),[15] and Mn(III).[16] In order to avoid reaction of HSO_3^-[17] the reaction must be carried out in a strongly acidic medium, hence D must be stable in acid. For these reasons, the $Cr(NN)_3^{2+}$ series of complexes was chosen:

$$Cr(NN)_3^{2+} + SO_2 \xrightarrow[k_s]{} Cr(NN)_3^{3+} + SO_2^- \qquad (4)$$

The $Cr(NN)_3^{2+}$ complexes are too unstable toward ligand dissosciation and too oxygen sensitive for prior preparation.[18] For this reason, they are made <u>in situ</u> by the reductive quenching of $^*Cr(NN)_3^{3+}$:

$$^*Cr(NN)_3^{3+} + Q \xrightarrow[k_q]{} Cr(NN)_3^{2+} + Q^+ \qquad (5)$$

The photophysics[19] and photochemistry[20] of the series of compounds $Cr(NN)_3^{3+}$,[21] where NN = 2,2'-bipyridine, 1,10-phenanthroline, or their substituted derivatives[22] have been extensively studied.[23] Upon photolysis of the $^4A_2$ ground state of $Cr(NN)_3^{3+}$ with light of wavelength 313 to 464 nm, a $^4T_2$ excited state is formed, which undergoes intersystem crossing to yield the thermally equilibrated $^2T_1$ and ^2E excited states within a matter of nanoseconds.[24] These metal-centered excited states, which are generally referred to as $^*Cr(NN)_3^{3+}$, decay via first-order kinetics,[25] emitting light at 695 nm and 727 nm. Their lifetimes span a range of about 60 to 700 microseconds, although this decay is slightly medium dependent.[20-23,26]

The self-exchange rate constant for the $Cr(NN)_3^{2+/3+}$ series of compounds has been estimated by studying reactions between it and other compounds. The reactions of $Cr(NN)_3^{2+}$ with $Fe(H_2O)_6^{3+}$ cannot be used, as the cross-reaction does not conform to Marcus theory.

Reactions of $Cr(bpy)_3^{2+}$ with $Co(en)_3^{3+}$ and $Co(NH_3)_6^{3+}$ yield values of 1.1×10^9 $M^{-1}s^{-1}$ and $\sim 2 \times 10^8$ $M^{-1}s^{-1}$ for the self-exchange rate constant of $Cr(bpy)_3^{3+/2+}$ respectively; the reaction between $Cr(bpy)_3^{3+}$ and $V^{2+}(aq)$ yields 1.4×10^7 $M^{-1}s^{-1}$.[7] Although the reactions between $Cr(bpy)_3^{2+}$ [27] and $Cr(phen)_3^{2+}$ [28] with $Co(en)_3^{3+}$ [29] and $Co(NH_3)_6^{3+}$ [18] have been studied by several groups, the interpretations of these reactions are dubious, as the reduction potentials for these Co(III) complexes and irreversible and therefore not well-defined. For example, the reported E° for $Co(en)_3^{3+/2+}$ varies from -0.08 V[30] to -0.20 V[31] to -0.24 V[7] depending on the source. Therefore, a reliable k_{ex} cannot be obtained from these data.

The reaction between $Cr(5\text{-Mephen})_3^{3+}$ and $Co(sepulchrate)^{2+}$ yields a self-exchange rate constant of ~1 x 10^9 $M^{-1}s^{-1}$ for $Cr(5\text{-Mephen})_3^{3+/2+}$,[20] whereas the reaction between $Cr(bpy)_3^{2+}$ and $Cr(5,6\text{-Me}_2phen)_3^{3+}$ (in 90% methanol and 0.1 M HCl) yields a self-exchange rate constant of 4 x 10^9 $M^{-1}s^{-1}$ ($(k_{11}k_{22})^{1/2}$) for each $Cr(NN)_3^{3+/2+}$ couple.[32] Roughly speaking, these results indicate a k_{ex} for $Cr(NN)_3^{3+/2+}$ of about (1-4) x 10^9 $M^{-1}s^{-1}$. Based on these constants, 2 x 10^9 $M^{-1}s^{-1}$ is commonly used for the self-exchange rate constant of all of the $Cr(NN)_3^{3+/2+}$ complexes, although it has been noted that phenanthroline complexes often react twice as quickly as bipyridine complexes of the same potential.[20] For this reason, the values k_{ex} = 1 x 10^9 $M^{-1}s^{-1}$ for the bipyridine complexes and 2 x 10^9 $M^{-1}s^{-1}$ for the phenanthroline complexes may be used.

The self-exchange rate constant for the $Cr(NN)_3^{2+}/{}^*Cr(NN)_3^{3+}$ couple calculated from reactions between a series of ${}^*Cr(NN)_3^{3+}$ compounds with a series of $Ru(NN)_3^{2+}$ compounds is 1 x 10^8 $M^{-1}s^{-1}$.[20] However, the authors note that the difference between the self-exchange rate constants of the ${}^*Cr(NN)_3^{3+}/Cr(NN)_3^{2+}$ and $Cr(NN)_3^{3+}/Cr(NN)_3^{2+}$ couples may not be real, but may rather be a reflection of experimental uncertainties. In early work a k_{ex} of 4 x 10^7 was derived from the the quenching of ${}^*Cr(NN)_3^{3+}$ by $Fe(H_2O)_6^{2+}$,[19] but this method is erroneous, as the cross reaction does not conform to Marcus theory.[20]

In order to study the reaction of $Cr(NN)_3^{2+}$ with SO_2, one first needs to form $Cr(NN)_3^{2+}$ from ${}^*Cr(NN)_3^{3+}$, which is done by using a quencher. The quenching, which in this case is facilitated by the long lifetimes of the excited state species, may occur by many mechanisms. Mechanisms which are relevant to transition metal complexes are: electronic energy

transfer (also known as energy transfer), electron transfer, spin-catalyzed deactivation, excimer or exciplex formation, and external heavy atom effect. The most common quenching pathways for $M(NN)_3^{n+}$ transition metal complexes are the energy and electron transfer pathways.[23] The electron transfer mechanism of the $Cr(NN)_3^{n+}$ complexes is outer sphere. For these complexes, electron transfer results in the formation of $Cr(NN)_3^{2+}$, whereas energy transfer produces no $Cr(NN)_3^{2+}$, and the rate constants are independent of the reduction potential of the $Cr(NN)_3^{3+}$.[20,33] O_2, $Co(NH_3)_6^{3+}$, and $Co(en)_3^{3+}$ [34] quench $^*Cr(NN)_3^{3+}$ complexes via energy transfer, whereas I^-, $Ru(NN)_3^{2+}$, $Os(NN)_3^{2+}$, and Fe^{2+} quench via electron transfer.[20,23] For the study of the SO_2 reactions, the quencher must be stable in acid, quench quickly via electron transfer, be unreactive with SO_2, and the products of the quenching must not interfere with the SO_2 reaction. For these reasons, the quencher chosen was $Co([14]aneN_4)^{2+}$.

$$Co([14]aneN_4)^{2+} + {}^*Cr(NN)_3^{3+} \xrightarrow{k_q} Co([14]aneN_4)^{3+} + Cr(NN)_3^{2+} \qquad (6)$$

The quenching of $^*Cr(bpy)_3^{3+}$ by $Co([14]aneN_4)^{2+}$, cursorily and qualitatively noticed by Bakac,[35] has a rate constant k_q of 1.5×10^8 $M^{-1}s^{-1}$ in 0.1 M $HClO_4$,[36] but no further studies have been reported. Consequently, this work also entails the determination of k_q between this series of complexes and $Co([14]aneN_4)^{2+}$. This quenching process happens to be reversible (see equation 7), and consequently the

$$Co([14]aneN_4)^{3+} + Cr(NN)_3^{2+} \xrightarrow{k_{bet}} Co([14]aneN_4)^{2+} + Cr(NN)_3^{3+} \qquad (7)$$

rate constant, k_{bet} for this back-electron transfer process is amenable to determination. Since k_q, k_{bet}, the reduction potential and k_{ex} of $Co([14]aneN_4)^{3+/2+}$ [31] are known, k_{ex} for the $*Cr(NN)_3^{3+}/Cr(NN)_3^{2+}$ and $Cr(NN)_3^{3+}/Cr(NN)_3^{2+}$ couples should be determinable. Correlations of the rate constants for the quenching and back-electron transfer reactions with the driving force of the reaction, as suggested by electron theories, should yield a better understanding of the factors which govern these processes.

Various researchers have attempted to calculate the self-exchange rate constant for the SO_2/SO_2^- couple using the Marcus equation; values obtained range from 10^{-2} $M^{-1}s^{-1}$ to 10^9 $M^{-1}s^{-1}$. Neta, Huie and Harriman[14] found a self-exchange rate constant which varied from 2.8×10^{-2} $M^{-1}s^{-1}$ to 8.2×10^9 $M^{-1}s^{-1}$ for the reactions of radiolytically generated SO_2^- with various metalloporphyrin systems at pH 1 in HCl and $HClO_4$. Mehrotra and Wilkins[37] calculated a self-exchange rate constant of $\sim 10^{-3}$ $M^{-1}s^{-1}$ by measuring reactions of various Co(III) complexes with SO_2^- derived from $S_2O_4^{2-}$ at pH 7; this value was later corrected to 3.4×10^2 $M^{-1}s^{-1}$.[11] Tsukahara and Wilkins[38] studied the reactions of various viologen compounds with SO_2^- derived from dithionite at $\mu = 0.5$ M and pH 8.1; they calculated an SO_2/SO_2^- self-exchange rate constant of 10^8 to 10^9 $M^{-1}s^{-1}$ using an SO_2/SO_2^- reduction potential of -0.26 V. Independent studies of the reaction between SO_2 and methyl viologen radical cation confirmed this result.[14] Bradic and Wilkins,[39] by compiling data for several SO_2^- reactions and comparing them to O_2^- reactions, proposed that the SO_2/SO_2^- self-exchange rate constant is 10^4 times as large as the O_2/O_2^- self-exchange rate constant, for which they used the value 10^3 $M^{-1}s^{-1}$.

Balahura and Johnson[40] obtained values for the SO_2/SO_2^- self-exchange rate constant which ranged from 2×10^2 to 6×10^4 $M^{-1}s^{-1}$ for reactions of SO_2^- (derived from $S_2O_4^{2-}$) with several Co(III), Fe(III), and Ru(III) complexes in aqueous solution at pH 8.1.

In summary, four families of rate constants will be considered. The families of rate constants are obtained by changing the substituents on the chromium complexes, which causes a concomitant change in the reduction potentials of both the ground and excited state species, which should affect the rate of the electron transfer reactions. The kinetic data generated will be discussed in terms of the electron transfer theories.

The four specific reactions to be studied are: the decay of $^*Cr(NN)_3^{3+}$ in 1.0 M H_2SO_4, the quenching of $^*Cr(NN)_3^{3+}$ by $Co([14]aneN_4)^{2+}$, the back-electron transfer reaction of $Cr(NN)_3^{2+}$ with $Co([14]aneN_4)^{3+}$, and the reaction of $Cr(NN)_3^{2+}$ with SO_2. The self-exchange rate constant for the SO_2/SO_2^- couple will be derived from the reaction of SO_2 with $Cr(NN)_3^{2+}$ using Marcus theory. Since both the self-exchange rate constant and standard reduction potential for $Co([14]aneN_4)^{3+/2+}$ are known,[32] the self-exchange rate constants for the $^*Cr(NN)_3^{3+/2+}$ and $Cr(NN)_3^{3+/2+}$ couples may also be checked, assuming that these reactions lie within the assumptions of Marcus theory.

RESULTS

Decay of $^*Cr(NN)_3^{3+}$ complexes

The rates of decay of the $^*Cr(NN)_3^{3+}$ complexes at infinite dilution, monitored in 1.0 M H_2SO_4 at the 727 nm emission wavelength, are generally close to the literature values (see Table II-1). The decay traces followed first-order kinetics only when the concentration of $Cr(NN)_3^{3+}$ was less than 10^{-4} M; at higher concentrations (up to 10^{-3} M) deviations were observed. It was also found that the lifetimes (τ, where $\tau = 1/k_{decay}$) of the $^*Cr(NN)_3^{3+}$ complexes depend upon the concentration of the ground state species.

$$^*Cr(NN)_3^{3+} \xrightarrow[\tau_o]{} Cr(NN)_3^{3+} + h\nu \qquad (8)$$

$$^*Cr(NN)_3^{3+} + Cr(NN)_3^{3+} \xrightarrow[2k_g]{} 2\ Cr(NN)_3^{3+} \qquad (9)$$

$$1/\tau = 1/\tau_o + {}^2k_g\,[Cr(NN)_3^{3+}] \qquad (10)$$

A plot of k_{obs} versus $[Cr(NN)_3^{3+}]$ yields a straight line of slope ^2k_g and intercept $1/\tau_o$ (see Figure II-1). For the $Cr(phen)_3^{3+}$ and $Cr(5\text{-}Clphen)_3^{3+}$ complexes it was found that the plots of k_{obs} versus $[Cr(NN)_3^{3+}]$ are linear[25] only for concentration ranges of less than 10^{-4} M[41] (see Figures II-1, AII-1, AII-2), hence the ^2k_g values reported (Table II-1) are for concentration ranges of less than 10^{-4} M.[42]

The τ values provide the background on which all of the other measurements are made.

Table II-1. Summary of lifetime data for the decay of $^*Cr(NN)_3^{3+}$ in 1.0 M H_2SO_4

Compound	τ_o [a] /μs	τ_o lit[b] /μs	$10^{-7}\ ^2k_g$ [a] /$M^{-1}s^{-1}$	$10^{-7}\ ^2k_g$ lit[c] /$M^{-1}s^{-1}$
$^*Cr(5\text{-Clphen})_3^{3+}$	141 ± 1	180	6.76 ± 0.05	1.7
$^*Cr(bpy)_3^{3+}$	71 ± 2	76[d]	0[d]	0.13[e]
$^*Cr(phen)_3^{3+}$	304 ± 8	325	2.92 ± 0.03	0.3[e], 0.23[f]
$^*Cr(5\text{-Mephen})_3^{3+}$	414 ± 3	380	3.9 ± 0.1	0.5
$^*Cr(5,6\text{-Me}_2\text{phen})_3^{3+}$	548 ± 5		1.04 ± 0.02	0.75[g]
$^*Cr(4,4'\text{-Me}_2\text{bpy})_3^{3+}$	210 ± 2	210	0.71 ± 0.06	0.2
$^*Cr(4,7\text{-Me}_2\text{phen})_3^{3+}$	683 ± 13	642	2.0 ± 0.1	1.0[g]

[a] In 1.0 M H_2SO_4. $[Cr(NN)_3^{3+}] < 1 \times 10^{-4}$ M.

[b] In 1 M H_2SO_4. Brunschwig and Sutin.[20]

[c] Serpone et al.[21] $[Cr(NN)_3^{3+}] < 12 \times 10^{-4}$ M, in 1 M HCl unless otherwise indicated.

[d] Jamieson et al.[25]

[e] In 5 M HCl.

[f] Sriram et al.[26]

[g] In 4% V/V CH_3CN.

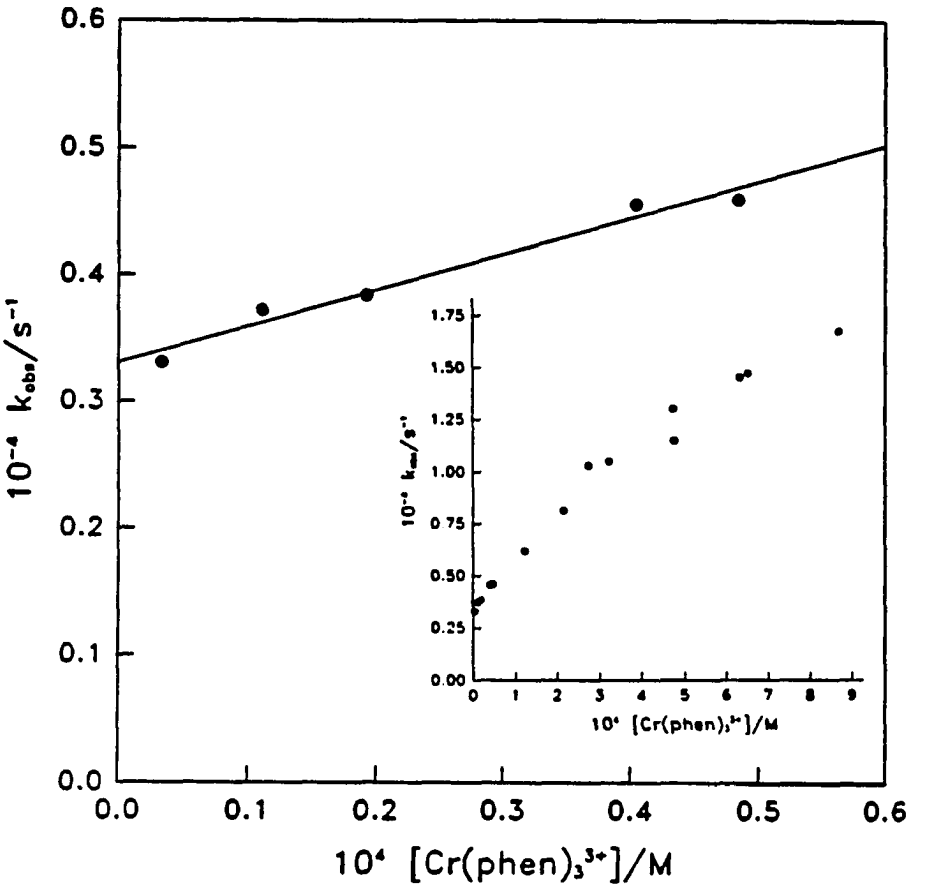

Figure II-1. Plot of k_{obs} versus [Cr(phen)$_3^{3+}$] for the decay of *Cr(phen)$_3^{3+}$ in 1.0 M H_2SO_4. The inset shows the curvature which becomes apparent when the concentration of the ground state chromium complex exceeds 1 x 10^{-4} M

Quenching of $^*Cr(NN)_3^{3+}$ complexes by $Co([14]aneN_4)^{2+}$

The addition of $Co([14]aneN_4)^{2+}$ to solutions of $Cr(NN)_3^{3+}$ increases the rate of decay of the $^*Cr(NN)_3^{3+}$ as observed at the emission wavelength (see Figure II-2); all of these traces follow first-order kinetics. For the emission experiments, a plot of k_{obs} versus $[Co([14]aneN_4)^{2+}]$ yields a straight line of slope k_q and an intercept which is due to contributions from the emission (τ_o), ground state quenching, and quenching by $Cr(NN)_3^{2+}$ (see Figure II-3). The reactions occurring are:

$$^*Cr(NN)_3^{3+} \xrightarrow{\tau_o} Cr(NN)_3^{3+} \tag{11}$$

$$^*Cr(NN)_3^{3+} + Cr(NN)_3^{3+} \xrightarrow{2k_g} Cr(NN)_3^{3+} + Cr(NN)_3^{3+} \tag{12}$$

$$^*Cr(NN)_3^{3+} + Co([14]aneN_4)^{2+} \xrightarrow{k_q} Cr(NN)_3^{2+} + Co([14]aneN_4)^{3+} \tag{13}$$

$$^*Cr(NN)_3^{3+} + Cr(NN)_3^{2+} \xrightarrow{k_{Cr}} Cr(NN)_3^{2+}\ Cr(NN)_3^{3+} \tag{14}$$

$$k_{obs} = k_o + {}^2k_g[Cr(NN)_3^{3+}] + k_q[Co([14]aneN_4)^{2+}] + k_{Cr}[Cr(NN)_3^{2+}] \tag{15}$$

The overall contribution of equation 14 to the k_{obs} in the quenching experiments is small in spite of the fact that k_{Cr} is ~ 5 x 10^9 $M^{-1}s^{-1}$.[43] The $Cr(NN)_3^{2+}$ present is formed by the quenching process in equation 13, and its concentration is not constant. However, the reactions were performed under conditions such that the concentration of $Cr(NN)_3^{3+}$ is

always less than 4 micromolar. Consequently, the total contribution from this pathway, $k_{Cr}[Cr(NN)_3^{2+}]$, is always less than 2 x 10^4 s^{-1}. Since it is so small, it does not cause the observed kinetic traces to deviate from first-order kinetics. The contributions to k_{obs} from the decay of the excited state (k_o) and ground state quenching $^2k_g[Cr(NN)_3^{3+}]$ are about 10^4 s^{-1} and 10^3 s^{-1} respectively. Figure II-3 clearly shows that these three contributions are dwarfed by $k_q[Co([14]aneN_4)^{2+}]$, as the intercept is small compared to k_{obs}.

When monitored at a wavelength corresponding to a $Cr(bpy)_3^{2+}$ absorbance, the quenching of $^*Cr(bpy)_3^{3+}$ by $Co([14]aneN_4)^{2+}$ was observed to form $Cr(bpy)_3^{2+}$ at the same rate as the $^*Cr(bpy)_3^{3+}$ decay. The $[Cr(bpy)_3^{2+}]$ is found from these experiments. The $[^*Cr(bpy)_3^{3+}]$ is found by flashing a solution which is equimolar in acid and $Cr(bpy)_3^{3+}$ but contains no $Co([14]aneN_4)^{2+}$ quencher, monitoring an absorbance wavelength, and using the known extinction coefficients. From these experiments, the yield of $Cr(bpy)_3^{2+}$ was found to be ~100%. Similar results were obtained for the 5-Clphen complex. The second-order rate constant of the reaction is independent of $[Cr(NN)_3^{3+}]$ and $[H^+]$.

Reaction of $Cr(NN)_3^{2+}$ complexes with $Co([14]aneN_4)^{3+}$

When observed at an appropriate absorbance wavelength, the $Cr(NN)_3^{2+}$ formed in the quenching experiments was seen to go away (see the sample experiments in Figure II-4). This disappearance of $Cr(NN)_3^{2+}$ was assigned to a reaction with the $Co([14]aneN_4)^{3+}$ produced by the quenching. This reaction, known as back-electron transfer, was further studied by adding independently synthesized $Co([14]aneN_4)^{3+}$ to the

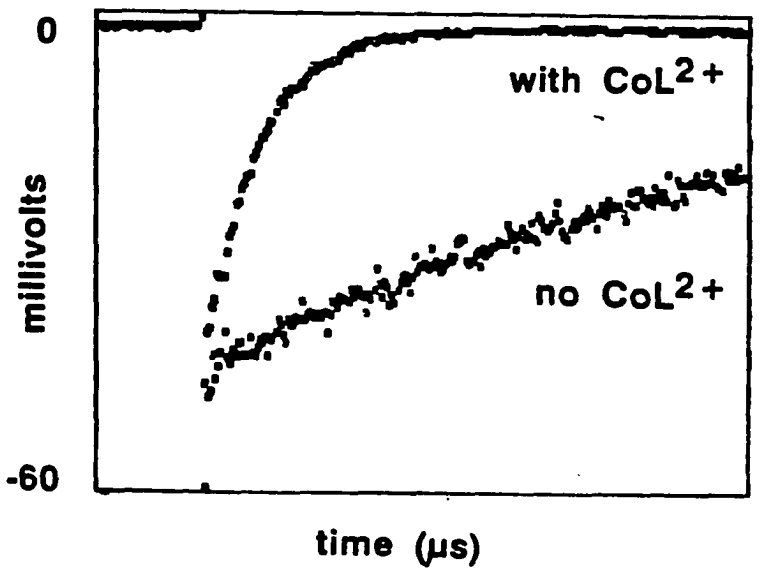

Figure II-2. Sample experiment for the quenching of $^{*}Cr(4,4'\text{-}Me_2bpy)_3^{3+}$ by $Co([14]aneN_4)^{2+}$ at 727 nm. Data points were taken at 1 microsecond intervals; the total time represented is 250 microseconds

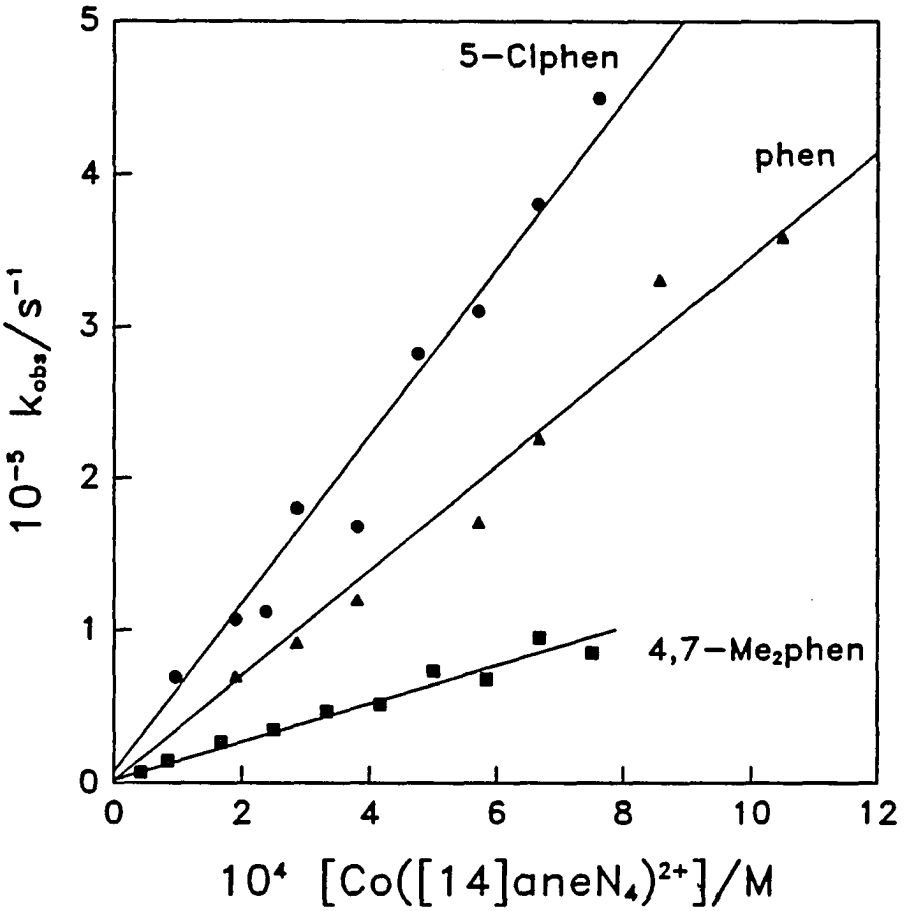

Figure II-3. Plot of k_{obs} versus $[Co([14]aneN_4)^{2+}]$ for the quenching of $^*Cr(5\text{-Clphen})_3^{3+}$ (●), $^*Cr(phen)_3^{3+}$ (▲), and $^*Cr(4,7\text{-Me}_2phen)_3^{3+}$ (■) in 1.0 M H_2SO_4

reaction mixture before the photolysis. One possible competing reaction is the quenching of $^{*}Cr(NN)_3^{3+}$ by $Co([14]aneN_4)^{3+}$ instead of $Co([14]aneN_4)^{2+}$; but the k_q expected for this reaction is only about 10^6 $M^{-1}s^{-1}$,[34] and since less than millimolar concentrations of $Co([14]aneN_4)^{3+}$ were used, this contribution will be negligible compared to the $Co([14]aneN_4)^{2+}$ quenching. All traces obtained followed first-order kinetics. The overall scheme expected is:

$$^{*}Cr(NN)_3^{3+} \xrightarrow[k_o]{} Cr(NN)_3^{3+} \qquad (16)$$

$$^{*}Cr(NN)_3^{3+} + Cr(NN)_3^{3+} \xrightarrow[2k_g]{} 2\ Cr(NN)_3^{3+} \qquad (17)$$

$$^{*}Cr(NN)_3^{3+} + Co([14]aneN_4)^{2+} \xrightarrow[k_q]{} Cr(NN)_3^{2+} + Co([14]aneN_4)^{3+} \qquad (18)$$

$$Cr(NN)_3^{2+} + Co([14]aneN_4)^{3+} \xrightarrow[k_{bet}]{} Cr(NN)_3^{3+} + Co([14]aneN_4)^{2+} \qquad (19)$$

From this scheme, one would expect a plot of k_{obs} versus the total concentration of $Co([14]aneN_4)^{3+}$ to yield a straight line of zero intercept, but in reality one observes a straight line that has an intercept (see Figure II-5). The intercept increases as the $E^{3+/2+}$

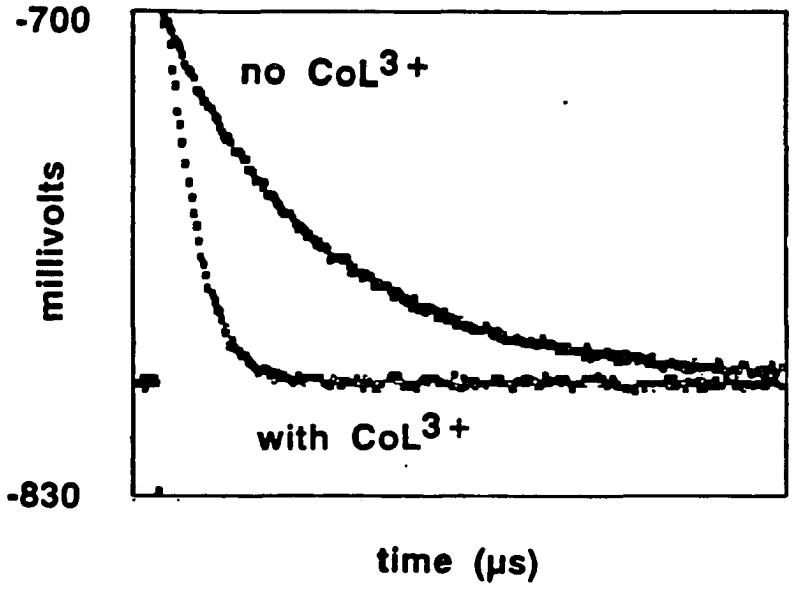

Figure II-4. A sample absorption trace for the back-electron transfer reaction between $Cr(5\text{-Mephen})_3^{2+}$ and $Co([14]aneN_4)^{3+}$ at 440 nm. Data points were taken at 1 microsecond intervals, and the total time represented is 250 microseconds

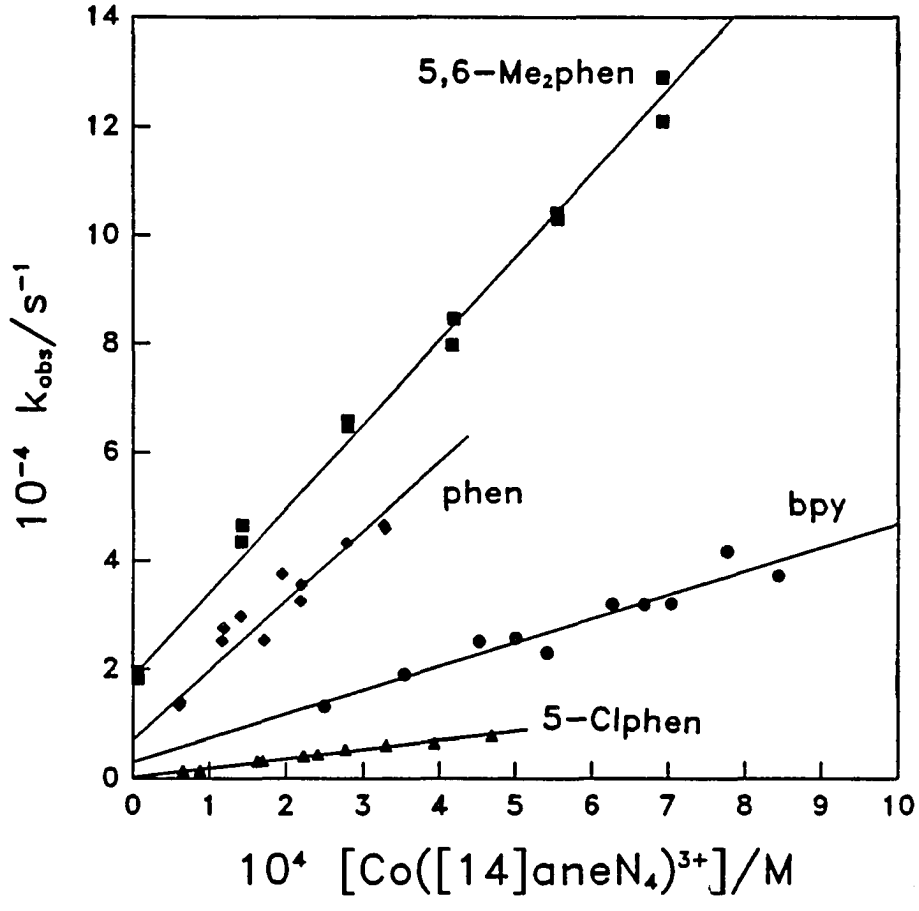

Figure II-5. A plot of k_{obs} versus [Co([14]aneN$_4$)$^{3+}$] for the back-electron transfer reaction between Cr(NN)$_3^{2+}$ and Co([14]aneN$_4$)$^{3+}$ for Cr(5,6-Me$_2$phen)$_3^{2+}$ (■), Cr(phen)$_3^{2+}$ (◆), Cr(bpy)$_3^{2+}$ (●), and Cr(5-Clphen)$_3^{2+}$ (▲)

Table II-2. Summary of Quenching and Back-Electron Transfer Rate Constants for the Reaction between $^*Cr(NN)_3^{3+}$ and $Co([14]aneN_4)^{2+}$

Compound	$E^{3+*/2+}$ [a] /V	$10^{-8}k_q$ [b] /$M^{-1}s^{-1}$	$E^{3+/2+}$ [c] /V	$10^{-7}k_{bet}$ [b] /$M^{-1}s^{-1}$
$Cr(5\text{-}Clphen)_3^{3+}$	1.53	5.2 ± 0.2	-0.17	1.70 ± 0.08
$Cr(bpy)_3^{3+}$	1.44	1.8 ± 0.2[d]	-0.26	4.4 ± 0.4
$Cr(phen)_3^{3+}$	1.42	3.3 ± 0.2	-0.28	13 ± 1
$Cr(5,6\text{-}Me_2phen)_3^{3+}$	1.40	2.55 ± 0.07	-0.29	15.8 ± 0.4
$Cr(5\text{-}Mephen)_3^{3+}$	1.39	4.04 ± 0.09	-0.30	10.5 ± 0.4
$Cr(4,4'\text{-}Me_2bpy)_3^{3+}$	1.25	0.7 ± 0.2	-0.45	~70[e]
$Cr(4,7\text{-}Me_2phen)_3^{3+}$	1.23	1.28 ± 0.05	-0.45	~70[e]

[a]Potentials calculated from emission wavelength.[20,23]

[b]In 1.0 M H_2SO_4.

[c]Potentials measured in LiCl, versus NHE.[20]

[d]In 0.1 M $LiClO_4$ this value is 1.5 x 10^8 $M^{-1}s^{-1}$.[36]

[e]Estimated from fits to second-order kinetics of traces from quenching experiments monitored by absorption at 485 or 560 nm.

potential decreases; the origin of this intercept is unknown.

The back-electron transfer and quenching rate constants are listed in Table II-2. The back-electron transfer rate constant values span a much larger range than the quenching rate constant values do. For the 5,6-Me_2phen complex, the k_q is only barely twice the k_{bet}. For the 4,4'-bpy and 4,7-Me_2phen complexes, calculations indicate that k_{bet} should be faster than k_q (see Tables AII-25 and AII-26). Since the back-electron transfer reaction for these complexes is so fast, the k_{bet} were derived from second-order kinetic analyses of reactions in which the only Co(III) present was formed by the quenching. The second-order rate constant of the reaction is independent of the wavelength of observation, $[Co([14]aneN_4)^{2+}]$, $[H^+]$, and $[Cr(NN)_3^{3+}]$.

Reaction of $Cr(NN)_3^{2+}$ complexes with SO_2

The addition of SO_2 to a mixture of $Cr(NN)_3^{3+}$ and $Co([14]aneN_4)^{2+}$ and then flashing resulted in an increase in the rate at which the $Cr(NN)_3^{2+}$ absorbance decayed. The reaction sequence is:

$$^*Cr(NN)_3^{3+} + Co([14]aneN_4)^{2+} \xrightarrow[k_q]{} Cr(NN)_3^{2+} + Co([14]aneN_4)^{3+} \qquad (20)$$

$$Cr(NN)_3^{2+} + SO_2 \xrightarrow[k_s]{} Cr(NN)_3^{3+} + SO_2^- \qquad (21)$$

$$Cr(NN)_3^{2+} + Co([14]aneN_4)^{3+} \xrightarrow[k_{bet}]{} Cr(NN)_3^{3+} + Co([14]aneN_4)^{2+} \qquad (22)$$

All of the kinetic traces were first-order. For the determination of k_s, these reactions were performed under conditions in which $[SO_2] > [Co([14]aneN_4)^{3+}]$, and therefore reaction 21 dominated over reaction 22. A plot of k_{obs} versus $[SO_2]$ yielded a straight line of slope k_s and an

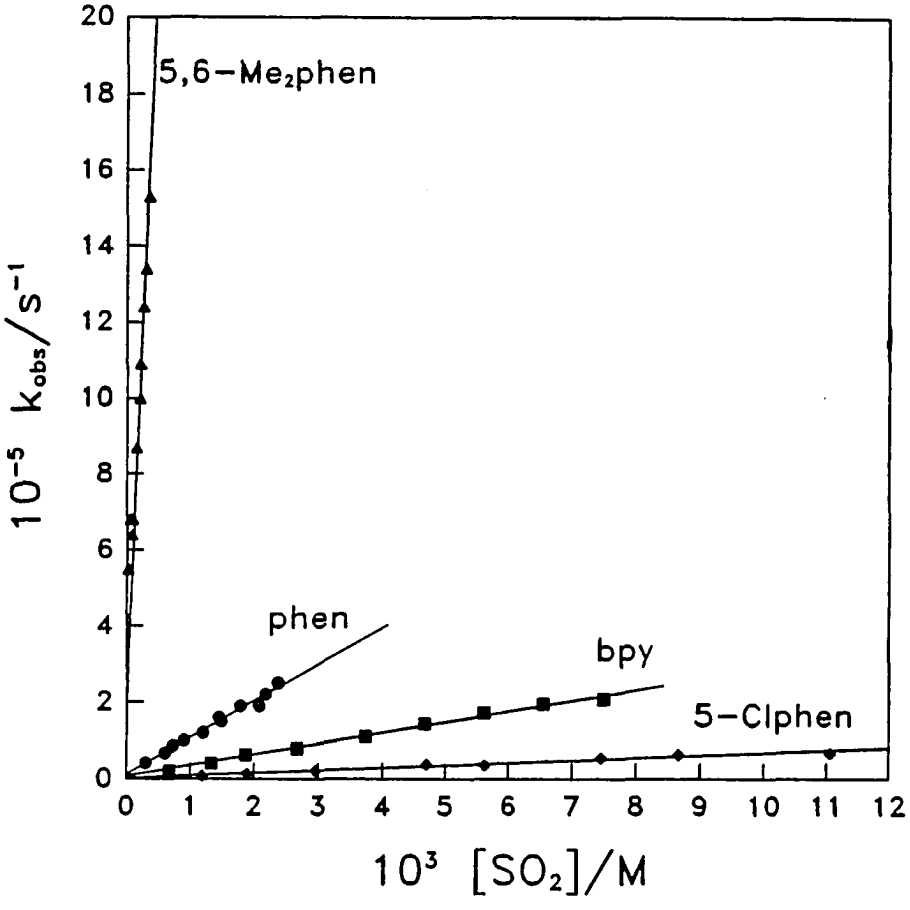

Figure II-6. Plot of k_{obs} versus [SO_2] for the reaction between $Cr(NN)_3^{2+}$ and SO_2 in 1.0 M H_2SO_4. Shown are the plots for $Cr(5,6\text{-}Me_2phen)_3^{2+}$ (▲), $Cr(phen)_3^{2+}$ (●), $Cr(bpy)_3^{2+}$ (■), and $Cr(5\text{-}Clphen)_3^{2+}$ (◆)

intercept corresponding to $k_{bet}[Co([14]aneN_4)^{3+}]$. The second-order rate constant of the reaction is independent of wavelength of observation, $[Co([14]aneN_4)^{2+}]$, and $[Cr(NN)_3^{3+}]$ (see Figure II-6, Tables AII-19 to AII-24). The rate constant for the reaction of $Cr(bpy)_3^{2+}$ with SO_2 in perchloric acid (0.5 M < $[HClO_4]$ < 1.0 M) was found to be 3.39×10^7 $M^{-1}s^{-1}$, which is not significantly different from the rate constant of 2.97×10^7 $M^{-1}s^{-1}$ in 1.0 M H_2SO_4. It was not possible to obtain reproducible results for the $Cr(4,4'\text{-}Me_2bpy)_3^{2+}$ or $Cr(4,7\text{-}Me_2phen)_3^{2+}$ compounds as their k_{bet} are so fast that they preclude the measurement of additional reactions. The rate constants k_s are listed in Table II-3, which also shows that the ratio k_{bet}/k_s decreases with decreasing $E^{3+/2+}$ potential.

Since both SO_2 and $Co([14]aneN_4)^{3+}$ react with $Cr(NN)_3^{2+}$, but do not react with each other, it was thought that each reaction should proceed in spite of the presence of the other reactant. However, experiments in which both SO_2 and $Co([14]aneN_4)^{3+}$ were allowed to react with $Cr(bpy)_3^{2+}$ simultaneously yielded somewhat perplexing results. When $[Co([14]aneN_4)^{3+}] = 8.7 \times 10^{-5}$ M and $[SO_2]$ was varied from 2 to 20 mM, the observed rate constant for each reaction was the sum of the two individual reactions (equation 23), and by varying $[SO_2]$, the same k_s was obtained as in reactions with no added $Co([14]aneN_4)^{3+}$.

$$k_{obs} = k_s[SO_2] + k_{bet}[Co([14]aneN_4)^{3+}] \qquad (23)$$

If, on the other hand, $[SO_2]$ was fixed at 2.24 mM, and the $[Co([14]aneN_4)^{3+}]$ was varied from (3 to 20) $\times 10^{-4}$ M, no dependence on $[Co([14]aneN_4)^{3+}]$ was observed - that is, $k_{obs} = k_s[SO_2]$, but the solution turned bright green in color. This could be due to a reaction

between the SO_2^- (formed from the $Cr(NN)_3^{2+}$) and the $Co([14]aneN_4)^{3+}$ which was present. Presumably, the green color was seen in the latter experiments because there was more $Co([14]aneN_4)^{3+}$ present. Because these results are anomalous, they were not used.

Table II-3. Rate Constants for the Reaction of $Cr(NN)_3^{2+}$ with SO_2

Compound	$10^{-7}k_s$ /$M^{-1}s^{-1}$	k_{bet}/k_s
$Cr(5\text{-}Clphen)_3^{2+}$	0.683 ± 0.004	2.5
$Cr(bpy)_3^{2+}$	2.97 ± 0.07[a]	1.5
$Cr(phen)_3^{2+}$	9.5 ± 0.2	1.4
$Cr(5,6\text{-}Me_2phen)_3^{2+}$	28 ± 2	0.56
$Cr(5\text{-}Mephen)_3^{2+}$	17 ± 1	0.62

[a]In 1.0 M $HClO_4$, $k_s = (3.39 \pm 0.04) \times 10^7$ $M^{-1}s^{-1}$.

DISCUSSION

Decay of $^*Cr(NN)_3^{3+}$ complexes

As each compound has its own rate of decay at infinite dilution, this provides a convenient method for characterizing them. The lifetimes of the complexes at infinite dilution (τ_o) which were measured in this work are in good agreement with the literature values (see Table II-1). The dependence of the rate of decay of the $^*Cr(NN)_3^{3+}$ complexes on the concentration of ground state $Cr(NN)_3^{3+}$ complexes was observed. This phenomenon, which is known as ground state quenching, has previously been observed in HCl (1 M and 5M),[41] 1 M NaCl,[44] and in other media.[22,25] The explanation for the phenomenon is as follows: the anion forms an ion pair with the ground state $Cr(NN)_3^{3+}$ (or $^*Cr(NN)_3^{3+}$), this ion pair in turn forms a three-membered ion pair with the excited state $^*Cr(NN)_3^{3+}$ (or $Cr(NN)_3^{3+}$). This three-membered species decays faster than the isolated $^*Cr(NN)_3^{3+}$ does. When lifetime studies are conducted on $[Cr(NN)_3^{3+}](ClO_4)_3$ which has been dissolved in water no ground state quenching is seen.[25] Whereas the τ_o obtained in this work are close to the literature values, the ^2k_g deviate by as much as a factor of 10, and, unlike the τ_o, are not reproducible from batch to batch (see Table II-2). For example, the $Cr(phen)_3^{3+}$ complex used in this study had a ^2k_g value of 2×10^7 $M^{-1}s^{-1}$ in both 1 M H_2SO_4 and HCl; the same complex from a different preparation[45] exhibited a ^2k_g of 3×10^7 $M^{-1}s^{-1}$ in 1 M HCl.[46] The reasons for such variations are unknown, which is not surprising, since the ground state quenching phemomenon itself is ill understood. The numerical knowledge of τ_o and ^2k_g for each compound is important, as

they are the background on which all the other rate constants are measured. On the other hand, no need to study the phemonenon itself was perceived, as they are a rather small correction in the intercept.

Electron transfer theories

In this section, various theories of electron transfer will be presented, and then an attempt will be made to rationalize the rate constants obtained for the various $Cr(NN)_3^{n+}$ electron transfer reactions in terms of these theories.

There are three main theories of electron transfer: classical, semiclassical, and quantum mechanical. Whereas one might expect the quantum mechanical theory to be the most accurate of the three, the developers of the semi-classical model[5] have shown that it gives results which approximate those of the quantum mechanical model. An additional advantage of the semiclassical model is that it uses parameters that are often available from experimental data, whereas the quantum mechanical model needs calculated data. Marcus theory of electron transfer, which is used with great frequency, is a classical theory, and it considers electron transfer to be a function of k_{ex} and K_{12}; corrections to it may be made for work terms, ionic strength, and the size and charge of the reactants. The semiclassical method treats the solvent classically and the inner sphere quantum mechanically. This approach allows one to take into account electron tunneling and nonadiabaticity, which cannot be expressed explicitly in the classical models.

Since Marcus theory is the simplest, initial attempts to rationalize the rate constants will be made using it. If it fails, more complex

treatments will be applied.

Marcus theory

Marcus theory seeks to predict the rate of a reaction based on the driving force of the reaction and the self-exchange rate constants of the reactants. Some of the assumptions of Marcus Theory are:[7]

-within the activated complex, the probability of electron transfer is unity (that is, the reaction is adiabatic)

-the electron-tranfer reagents may be treated as if they were spherical and structureless

-the motions of the inner coordination shells are harmonic.

The simple form of the theory may be written:[47]

$$k_{12} = (k_{11}k_{22}K_{12}f)^{1/2} \qquad \log f = (\log K_{12})^2/(4\log (k_{11}k_{22}/Z^2)) \qquad (24)$$

$$\log k_{11} = (-\log (k_{22}^2K_{12}/(Z^2k_{12}^2)) \pm (4\log (K_{12}Z/k_{12})\log(Z/k_{12}))^{1/2})/2 \qquad (25)$$

Z = collision frequency, $\sim 10^{11}$ $M^{-1}s^{-1}$ $\qquad K_{12} = \Delta E/0.0591\ n$

This may be rearranged to yield:[20]

$$\log k_{12} = 0.50 \log k_{11}k_{22} + 0.50(1 + \alpha) \log K_{12} \qquad (26)$$

$$\alpha = (\log K_{12}) / (4 \log (k_{11}k_{22}/Z^2)) \qquad (27)$$

The plot of $\log(k_{12})$ versus $\log(K_{12})$ (or ΔE) is a curve, but over a small range of ΔE it approximates a straight line.[4] In the electrostatics-corrected form, the work required to bring charged reactants together is

considered. This form may be written:[6,48]

$$k_{12} = (k_{11}k_{22}K_{12}f_{12})^{1/2}W_{12} \tag{28}$$

$$k_{11} = (\frac{k_{12}}{W_{12}})^2(\frac{1}{k_{22}K_{12}f_{12}}) \tag{29}$$

$$\ln f_{12} = \frac{[\ln K_{12} + (w_{12} - w_{21})/RT]^2}{4[\ln (k_{11}k_{22}/A_{11}A_{22}) + (w_{11} + w_{22})/RT]} \tag{30}$$

$$W_{12} = \exp [\frac{-(w_{12} + w_{21} - w_{11} - w_{22})}{2RT}] \tag{31}$$

$$A = N(\frac{8RT}{\pi(m_1m_2/m_1 + m_2)})^{1/2}\pi\sigma^2 \quad \text{(collision rate, } \sim 10^{11}M^{-1}s^{-1}) \tag{32}$$
$$(\sigma = (r_1 + r_2) \text{ in meters, } m_i \text{ in kilograms})$$

$$w_{ij} = \frac{\alpha Z_iZ_j}{\sigma(1 + \beta\sigma(\mu^{1/2}))} \tag{33}$$

$$\alpha = \frac{e^2 N}{4\pi\varepsilon_o D} = 1.75 \times 10^{-6} \text{ J mol}^{-1}\text{m} \tag{34}$$

$$\beta = \frac{8\pi N^2e^2}{1000\ D_sRT} = 3.285 \times 10^9\ \text{m}^{-1}\text{L}^{1/2}\text{mol}^{-1/2} \tag{35}$$

r = radius of the reactant

N = Avogadro's number

μ = ionic strength of the medium

Z_i = charge on atoms

ε_o = permittivity of free space, $8.85 \times 10^{12}\ C^2N^{-1}m^{-2}$

D = dielectric constant, 78.85

e = charge of an electron, 1.60×10^{-19} C

The latter form has adjustments for temperature, ionic strength of the medium of the reaction, and the size and charge of the reactants and products. If Marcus theory is applicable to any given series of reactions, then the same self-exchange rate constant for one reactant should be obtained from any series of related complexes studied. The back-electron transfer, SO_2, and quenching reactions will be discussed in terms of Marcus theory.

Reaction of $Cr(NN)_3^{2+}$ complexes with $Co([14]aneN_4)^{3+}$: the back-electron transfer reaction

The $Cr(NN)_3^{2+}$ reacts with $Co([14]aneN_4)^{3+}$ to form $Cr(NN)_3^{3+}$ and $Co([14]aneN_4)^{2+}$. The plot of $\log_{10}(k_{bet})$ versus $\log_{10}(K_{12})$ gives a slope of 0.4 ± 0.1 and an intercept of 3 ± 1 (see Figure II-7); the values calculated from equations 26 and 27, using k_{11} = 2 x 10^9 $M^{-1}s^{-1}$; k_{22} = 8 x 10^{-4} $M^{-1}s^{-1}$, ΔE = 0.70 V are 0.41 and 3.1 respectively. Since ΔE is small (0.59 to 0.72 V) the instantaneous slope and the intercept calculated for one point in this range are applicable to the entire range. The excellent agreement between the observed and calculated values implies that the self-exchange rate constants used were approximately correct, and that the $\Delta E°$ were sufficiently low that Marcus theory was applicable. From these results, a refined k_{ex} for the individual $Cr(NN)_3^{3+/2+}$ couples may be calculated by using equations 28 to 35; the results are shown in Table II-4. These k_{ex} are in good general agreement with the literature values, although they do vary by a factor of about 9, which is somewhat larger than expected from the literature. These k_{ex} may be used in subsequent calculations.

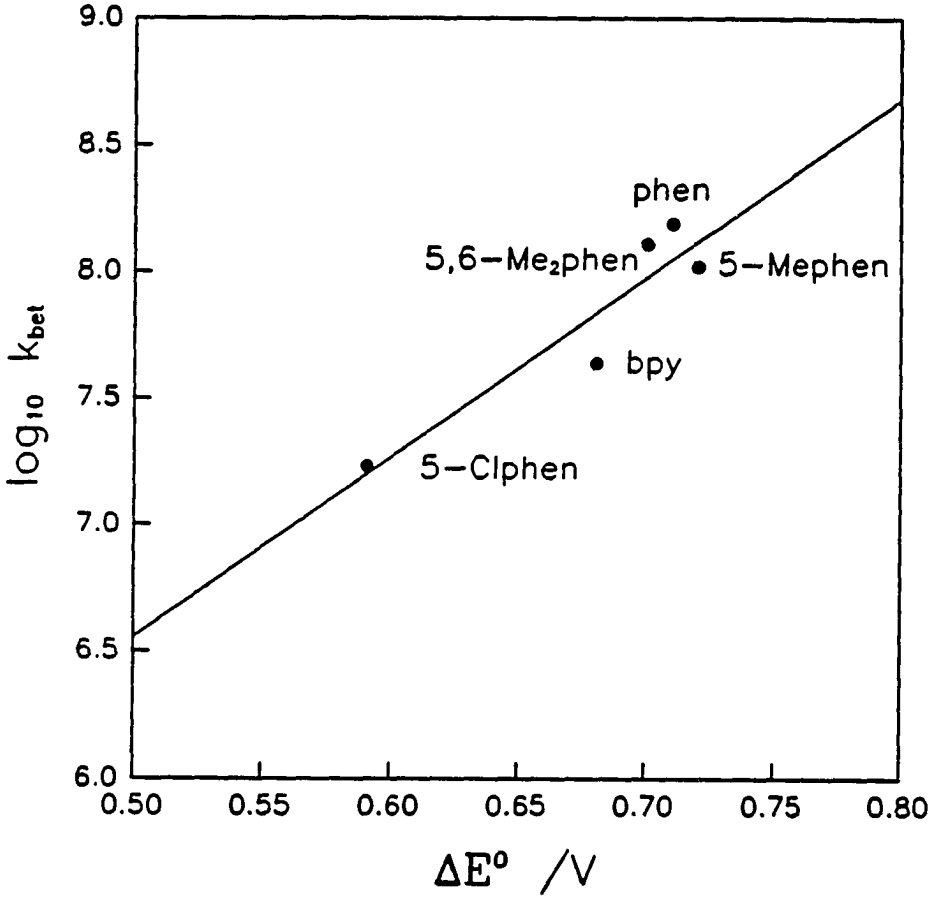

Figure II-7. A plot of $\log_{10}(k_{bet})$ versus ΔE° for the reaction between $Cr(NN)_3^{2+}$ and $Co([14]aneN_4)^{3+}$

Table II-4. Calculated Self-Exchange Rate Constants for $Cr(NN)_3^{3+/2+}$ Complexes from Back-Electron Transfer Reaction Data [a]

$Cr(NN)_3^{n+}$ Complex	$10^{-9}k_{ex}/M^{-1}s^{-1}$	k_{rel} [b]	$10^{-9}k_{lit}/M^{-1}s^{-1}$
5-Clphen	1.2	1.6	-
bpy	0.76	1.0	1.1[7],4[27]
phen	5.7	7.5	-
5,6-Me_2phen	6.9	9.1	4[27]
5-Mephen	1.9	2.5	1[20]

[a]Electrostatics-corrected values, from equations 28 to 35. $k_{ex}(Co[14]aneN_4)^{2+/3+}$ = 8 x 10^{-4} $M^{-1}s^{-1}$; $r(Co[14]aneN_4)^{2+}$) = 4.4 A°, $r((Co[14]aneN_4)^{3+})$ = 4.0 A°, Estimated values;[30,49] $r(Cr(NN)_3^{n+})$ = 6.8 A°.[50]

[b]$k_{rel} = k_{ex}(NN)/k_{ex}(bpy)$.

Reaction of $Cr(NN)_3^{3+}$ complexes with SO_2

The plots of $\log_{10}(k_s)$ versus ΔE^o are linear (see Figure II-8). A plot of $\log_{10}(k_s)$ versus $\log_{10}(K_{12})$ gives a slope of 0.5 ± 0.3 and an intercept of 7.1 ± 0.6. The k_{ex} for the SO_2/SO_2^- couple calculated from the intercept (using equation 26) is (7.9 ± 0.7) x 10^4 $M^{-1}s^{-1}$. The k_{ex} for the SO_2/SO_2^- couple may also be calculated from each $Cr(NN)_3^{n+}$ complex by using both the literature values for k_{ex} for $Cr(NN)_3^{3+}/Cr(NN)_3^{2+}$ and the k_{ex} calculated from the back-electron transfer data. The results are presented in Table II-5. It is clear that using the individual k_{ex} for the $Cr(NN)_3^{n+}$ complexes yields more

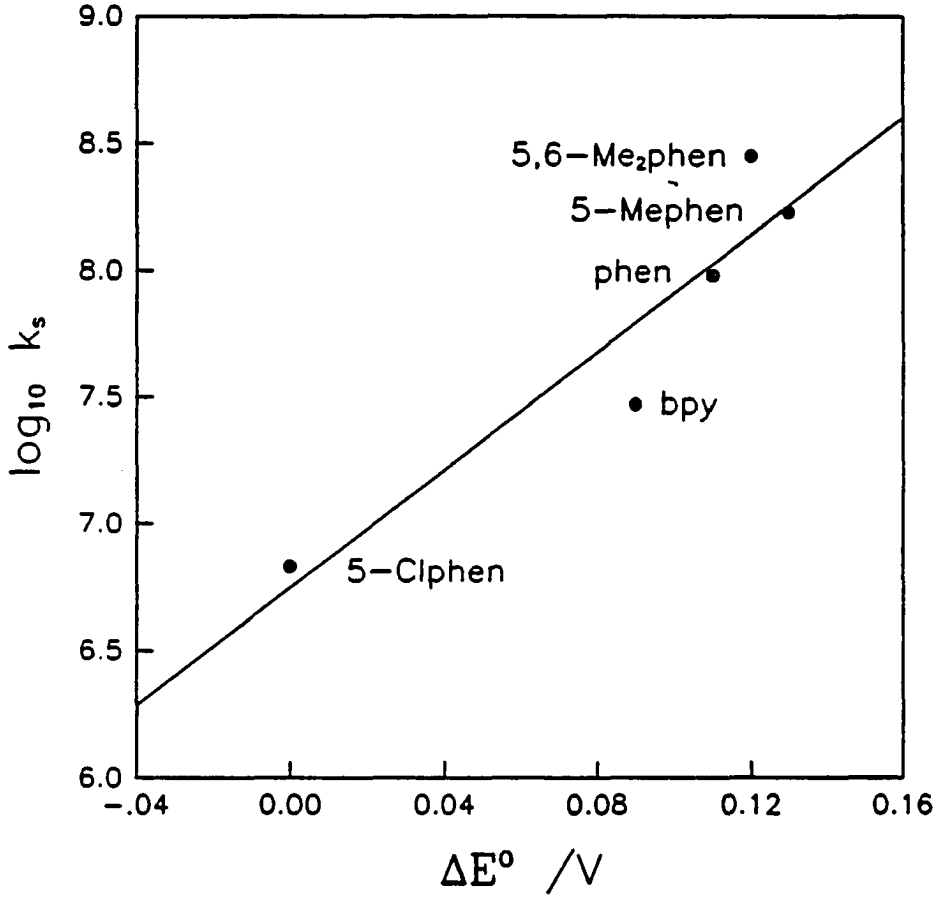

Figure II-8. Plot of $\log_{10}(k_s)$ versus ΔE° for the reaction of SO_2 with various $Cr(NN)_3^{2+}$ complexes

Table II-5. Calculated Self-exchange Rate Constants (k_{ex}) for the SO_2/SO_2^- couple in 1.0 M H_2SO_4 [a]

Compound	$10^{-4}k_{ex}$ [b] /$M^{-1}s^{-1}$	$10^{-4}k_{ex}$ [c] /$M^{-1}s^{-1}$
$Cr(5\text{-}Clphen)_3^{2+}$	0.78	1.3
$Cr(bpy)_3^{2+}$	1.08	1.4
$Cr(phen)_3^{2+}$	2.8	1.0
$Cr(5,6\text{-}Me_2phen)_3^{2+}$	18	5.3
$Cr(5\text{-}Mephen)_3^{2+}$	4.7	5.0
Average	5 ± 6	3 ± 2

[a]Electrostatics-corrected rate constants. Parameters used: $E(SO_2/SO_2^-)$ = -0.17 V versus NHE;[14] $r(SO_2^{0/-})$ = 2.83 A°;[13] $r(Cr(NN)_3^{3+/2+})$ = 6.8 A°.[50]

[b]k_{22} = 2 x 10^9 $M^{-1}s^{-1}$ for the phenanthroline compounds, 1 x 10^9 $M^{-1}s^{-1}$ for the bipyridine compounds.[20]

[c]k_{ex} for SO_2/SO_2^- calculated using the individual k_{ex} for the chromium complexes derived from back-electron transfer data, as presented in Table II-4.

self-consistent results, giving k_{ex} for SO_2/SO_2^- = (3 ± 2) x 10^4 $M^{-1}s^{-1}$.

The self-exchange rate constants for the SO_2/SO_2^- reaction derived here are quite constant. This is in contrast to the range of 10^{-2} to 10^9 $M^{-1}s^{-1}$ obtained when SO_2^- is used as the reductant (see Table II-6). The self-consistency of the k_{ex} obtained when SO_2 reacts with $Cr(NN)_3^{2+}$ parallels the situation in the literature in which reactions of O_2 with $Cr(NN)_3^{2+}$ yield a self-consistent k_{ex} for the O_2/O_2^- reaction.[51] By contrast, the reductions of various compounds by O_2^- give a range of 10^{-7} to 10^7 for the same k_{ex}.[30] The reasons for this are not clear.

Fate of the SO_2^-

There are two possible reactions by which the very reactive SO_2^- may be removed from the reaction solutions:

$$SO_2^- + [Co([14]aneN_4)(OH_2)_2]^{3+} \xrightarrow[k_{cos}]{} SO_2 + [Co([14]aneN_4)(OH_2)_2]^{2+} \quad (36)$$

$$k_{cos} \sim 10^4 \ M^{-1}s^{-1}$$

$$2\ SO_2^- \quad \underset{k_r}{\overset{k_f}{\rightleftharpoons}} \quad S_2O_4^{2-} \quad (37)$$

$$K = 7.14 \times 10^8 \ M^{-1}; \quad k_r = 2.5 \ s^{-1}; \quad k_f = 1.8 \times 10^9 \ s^{-1}$$

The rate constant k_{cos} is unknown, but it may be estimated from literature data. At pH 8.1 in 1.0 M $LiClO_4$, $[Co([14]aneN_4)(NH_3)_2]^{3+}$ is reduced by SO_2^- with a rate constant of 918 ± 130 $M^{-1}s^{-1}$; the rate constant for the analogous reduction of $[Co([14]aneN_4)(Cl)_2]^+$ is (6.25 ± 0.01) x 10^5 $M^{-1}s^{-1}$.[40] Comparisons of the SO_2^- reductions of $Co(EDTA)Cl^{2-}$ and $Co(EDTA)^-$ show that the chloride is reduced ~200 times faster than

Table II-6. Summary of Literature SO_2/SO_2^- Self-exchange Rate Constants from Reactions of SO_2^- with Various Species

Compound	ΔE/V	$k_{12}/M^{-1}s^{-1}$	$k_{ex}/M^{-1}s^{-1}$	Conditions	Ref.
EPQ^{2+}	0.01	1.4×10^8	1.3×10^8 [a]	I=0.5 M $NaSO_4$,	
DQ^{2+}	-0.09	6.4×10^7	1.8×10^9 [a]	0.1 M $C(NH_2)(CH_2OH)_3$,	
MV^{2+}	-0.19	9.0×10^6	5.3×10^9 [a]	pH=8.1	38
$Mn^{III}TMPyP^{3-}$	0.31	4.9×10^8	2.7×10^9	0.1 M HCl or $HClO_4$	
$Fe^{III}TMPyP^{5+}$	0.45	3.4×10^9	9.3×10^7		
$Co^{III}TMPyP^{5+}$	0.71	2×10^8	4.7×10^5		14
$Co(EDTA)^-$	0.64	1×10^3	10^3	pH=7, I=0.4 M,	
$Fe(EDTA)^-$	0.38	$<2 \times 10^6$	5×10^2	$C(NH_2)(CH_2OH)$.	37,40
$Co(sep)^{3+}$	-0.038	7.1×10^1	3.6×10^2	I=1, pH=8.1	
$Co(NH_3)_6^{3+}$	0.32[b]	1.17×10^2	5.5×10^4	NaCl, $LiClO_4$, or	
$Co(bpy)_3^{3+}$	0.63	2.1×10^7	1.9×10^4	$NaClO_4$	
$Fe(CN)_6^{3+}$	0.67	1.2×10^8	5×10^3		
$Fe(CN)_5py^{2+}$	0.81	1.2×10^8	3.3×10^2		
$Ru(NH_3)_5im^{2+}$	0.37	1.1×10^8	8×10^3		40

[a]The k_{ex} was calculated in this work, using E° for SO_2/SO_2^- = 0.26 V.

[b]$Co^{3+/2+}$ potential not well-determined, therefore the k_{ex} for SO_2/SO_2^- is dubious.

the aquo species; for Co(III)MEDTA complexes, the bromide is reduced about 400 times faster than the aquo species.[37] For the sake of argument, 10^4 $M^{-1}s^{-1}$ seems a reasonable estimate for k_{cos} for $[Co([14]aneN_4)(H_2O)_2]^{3+}$.

The rate constants in equation 37 are for pH 6.5;[52] in acidic solution the dithionite formed will decompose, eventually yielding elemental sulfur and various sulfite species.[53] Based on the relative rates and concentrations of the various reactants, the dimerization of dithionite should predominate over reactions with $Co([14]aneN_4)^{3+}$ and $Cr(NN)_3^{3+}$, and $Co([14]aneN_4)^{3+}$ will build up in the solution.

Quenching of $^*Cr(NN)_3^{3+}$ complexes by $Co([14]aneN_4)^{2+}$

The quenching of $^*Cr(III)$ complexes by various cobalt(III) complexes has been reported,[34] but the quenching by $Co([14]aneN_4)^{2+}$ has not been published.[35,36] For the $Cr(bpy)_3^{3+}$ and $Cr(5\text{-}Clphen)_3^{3+}$ compounds, the formation of about 100% $Cr(NN)_3^{2+}$ indicates that the reaction goes completely via electron transfer.

Competing reactions in this study are the quenching of $^*Cr(NN)_3^{3+}$ by both the ground state $Cr(NN)_3^{3+}$ and the $Cr(NN)_3^{2+}$ produced. It is these reactions which cause the small intercept in the plot of k_{obs} versus $[Co([14]aneN_4)^{2+}]$. The second-order rate constants for these quenching reactions are ~10^7 $M^{-1}s^{-1}$ (Table II-1) and 5 x 10^9 $M^{-1}s^{-1}$ respectively;[43] their contributions are minimized by adjusting the experimental conditions.

For each $Cr(NN)_3^{3+}$ complex, the observed k_q is within a factor of 5 of the rate constant calculated using Marcus theory (equation 24) (see

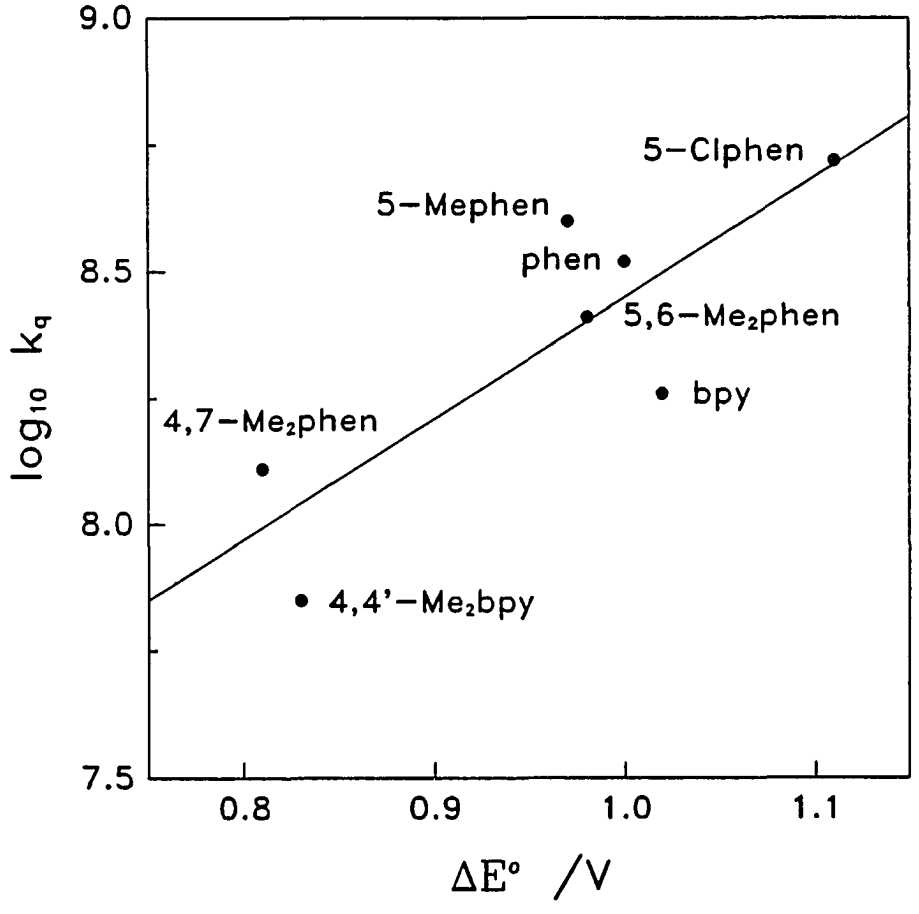

Figure II-9. A plot of $\log_{10}(k_q)$ versus ΔE° for the quenching of $^*Cr(NN)_3^{3+}$ by $Co([14]aneN_4)^{2+}$

Table AII-25). However, the overall variation of k_q with $\Delta E°$, which should be a factor of 20, is only a factor of 8. A plot of $\log(k_q)$ versus $\log(K_{12})$ (equation 26) for this reaction gives a slope of 0.15 ± 0.04 and an intercept of 6.0 ± 0.7 (see Figure II-9). The line in Figure II-9 has a lot of scatter, the slope is shallower and the intercept higher than the values calculated from Marcus theory, which are ~0.38 and ~2.45 respectively, based on equations 26 and 27, using $\log(K_{12}) = 17$, $k_{11} = 1 \times 10^8$ $M^{-1}s^{-1}$,[20] and $k_{22} = 8 \pm 3 \times 10^{-4}$ $M^{-1}s^{-1}$.[31]

Since Marcus theory has failed to account for the kinetic data for the reaction between $^*Cr(NN)_3^{3+}$ and $Co([14]aneN_4)^{2+}$, more complicated theories may be used. Possible reasons for the failure of Marcus theory are: 1) nuclear tunneling, 2) nonadiabaticity, 3) different values of k_{ex} for each of the $^*Cr(NN)_3^{3+}$ complexes, and 4) simultaneous participation of an energy transfer process.

Nuclear tunneling and nonadiabaticity may be evaluated by using the semiclassical theory which was developed by Brunschwig, Logan, Newton, and Sutin in 1980.[5] The general expression is:

$$k_{sc} = \kappa_{el} \Gamma_n k_{Cl} \sim k_{qm} \qquad (38)$$

Γ_n = thermally averaged nuclear tunneling factor

κ_{el} = thermally averaged electronic transmission coefficient

Marcus theory calculations yield the term k_{Cl}; if the observed rate constant for a given reaction is lower than the calculated, the presence of nonadiabaticity is assumed; if faster, tunneling is assumed. The semiclassical theory shows how nonadiabaticity and tunneling may cancel.

The nuclear tunneling factor, Γ_n, may be calculated.[54] Sample values of Γ_n are given in Table II-7. Generally, Γ_n values of

less than 10 are not considered significant, and therefore, for this quenching reaction, nuclear tunneling may be ignored. $Co([14]aneN_4)^{3+/2+}$ is assumed to have a Γ_n similar to the other $Co^{3+/2+}$ couples.

Table II-7. Sample Nuclear Tunneling Factors

Couple	Γ_n	Reference/Comment
SO_2/SO_2^-	2.8	Stanbury and Lednicky[13]
$Co(NH_3)_6^{3+/2+}$	7.0	Sutin[4]
$Co(bpy)_3^{3+/2+}$	5.0	Marcus and Sutin[55]
$Cr(bpy)_3^{3+/2+}$	~1	$\Delta d = 0$;[20]
$Cr(bpy)_3^{*3+/2+}$	~1	$\Delta d = 0$; add a nonbonding electron
$Cr(bpy)_3^{*3+/3+}$	1.0	$\Delta d = 0$; excited state is a t_{2g} spin flip[22,23]

Nonadiabaticity may also be evaluated numerically. If κ_{el}, the probability of electron transfer, is less than unity, then the system is termed nonadiabatic.[5] The nonadiabaticity of a cross reaction, $(\kappa_{el})_{12}$, may be calculated from the following semiclassical expression, which assumes that nuclear tunneling effects cancel:[4]

$$k_{12} = (\kappa_{el})_{12}\left[\frac{k_{11}k_{22}K_{12}f_{12}}{(\kappa_{el})_{11}(\kappa_{el})_{22}}\right]^{1/2} W_{12} \tag{39}$$

$$\ln f_{12} = \frac{[\ln K_{12} + (w_{12} - w_{21})/RT]^2}{4\{\ln[k_{11}k_{22}/A_{11}A_{22}(\kappa_{el})_{11}(\kappa_{el})_{22}] + (w_{11} + w_{22})/RT\}} \tag{40}$$

Note that when $(\kappa_{el})_{11} = (\kappa_{el})_{22} = (\kappa_{el})_{12} = 1$, this simplifies to the Marcus cross-relation equation. If the reaction is not too exothermic (hence $f_{12} \sim 1$), and the ratio of the electronic factors is ~1, then the observed rate constant for the cross reaction may not exhibit any nonadiabaticity, even though $(\kappa_{el})_{12} << 1$.

A plot of $\log(k_{12})$ versus $\log(K_{12})$ yields a curve of instantaneous slope α,[4]

$$\alpha = \frac{1}{2}\left[1 + \frac{2 \ln f_{12}}{\ln K_{12} + (w_{12} - w_{21})/RT}\right] \qquad (41)$$

from which $\ln f_{12}$ may be found, and using equation 40, the product $(\kappa_{el})_{11}(\kappa_{el})_{22}$ may be extracted. Using $(\kappa_{el})_{11}(\kappa_{el})_{22}$ in equation 39 in conjunction with the experimental rate constant, k_{12}, yields $(\kappa_{el})_{12}$.[4] For these quenching reactions, $5 \times 10^{-8} < (\kappa_{el})_{11}(\kappa_{el})_{22} < 2 \times 10^{-4}$, and $1 \times 10^{-3} < (\kappa_{el})_{12} < 2 \times 10^{-2}$. κ_{el} for $Cr(NN)_3^{n+}$ is generally assumed to be 1,[5] and κ_{el} for the quencher is expected to be $\sim 10^{-3\pm1}$ based on reactions between a series of <u>trans</u>-$Co(N_4)(OH_2)_2^{3+/2+}$ complexes.[49] The product of the electronic transmission coeffients measured in this work is not only lower than would be expected based on the known $(\kappa_{el})_{11}$ and $(\kappa_{el})_{22}$, but also varies by a factor of 10^4. In comparison, $(\kappa_{el})_{12}$, although not constant, only varies by a factor of 20. One might suggest that the variation of $(\kappa_{el})_{12}$ obtained from this series implies that the different $^*Cr(NN)_3^{3+/2+}$ complexes couple to the cobalt complex differently, but if this were the case one would expect to see evidence for this in the back-electron transfer reaction also.

On the other hand, reactions of $Co(bpy)_3^{2+}$ and $Co(phen)_3^{2+}$ with a

series of ruthenium amine complexes are very nearly adiabatic ($(\kappa_{el})_{12}$ ~ 0.1).[56] Calculations of κ_{el} for the $Co(NH_3)_6^{3+/2+}$ self-exchange reaction yield a value of ~ 10^{-3}, but experimental data indicate κ_{el} ~ 0.1. A similar situation exists for $Co(bpy)_3^{3+/2+}$, $Co(en)_3^{3+/2+}$, and $Co(sep)_3^{3+/2+}$.[5] Theoretically, one would expect spin forbidden reactions (that is, $\Delta S \neq 0$, S = spin quantum number), such as this electron transfer quenching reaction and the $Co([14]aneN_4)^{3+/2+}$ self-exchange reaction to be nonadiabatic, but in reality, spin multiplicity restrictions do not seem to influence the rate of a reaction much.[55] Therefore, nonadiabaticity or spin multiplicity restrictions are probably not the causes for the lack of correlation of this quenching reaction with Marcus theory.

A third postulate is that each $*Cr(NN)_3^{3+/2+}$ couple has a self-exchange rate constant that is slightly different from the value of 1×10^8 $M^{-1}s^{-1}$ that was used. This is not unreasonable, as slightly different k_{ex} were found for the $Cr(NN)_3^{3+/2+}$ couples from the back-electron transfer reaction. In order to get the results observed by adjusting the k_{ex}, the k_{ex} would have to be lowered for the 5-Clphen and raised for the 4,7-Me_2phen; this trend is in agreement with that observed in Table II-4. However, if this were the case, one would still expect a rough agreement with Marcus theory, as was seen for the back-electron transfer reaction. Therefore, different k_{ex} for each $*Cr(NN)_3^{3+/2+}$ couple will not account for the scatter and shallowness observed in Figure II-9.

A shallow dependence of k_q on $\Delta E°$ often suggests an energy transfer mechanism, although electron transfer products which form at the same

rate as the $^*Cr(NN)_3^{3+}$ decay are clearly seen in this case. Mechanisms which combine energy and electron transfer may be suggested and compared to the electron transfer mechanism.

Scheme I. (Energy Transfer followed by Electron Transfer)

$$^*Cr(NN)_3^{3+} + Co([14]aneN_4)^{2+} \xrightarrow[k_{en}]{} Cr(NN)_3^{3+} + {}^*Co([14]aneN_4)^{2+} \quad (42)$$

$$^*Co([14]aneN_4)^{2+} + Cr(NN)_3^{3+} \xrightarrow[k_{el}]{} Cr(NN)_3^{2+} + Co([14]aneN_4)^{3+} \quad (43)$$

Scheme II. (Simultaneous Energy and Electron Transfer)

$$^*Cr(NN)_3^{3+} + Co([14]aneN_4)^{2+} \xrightarrow[k_{enel}]{} Cr(NN)_3^{2+} + {}^*Co([14]aneN_4)^{3+} \quad (44)$$

^2E $\quad$ "$^4T_{1g}$" $\quad$ $^3T_1$ $\quad$ "$^3T_{1g}$" $\quad$ $\Delta S=0$

$$^*Co([14]aneN_4)^{3+} \xrightarrow[k_{deact}]{} Co([14]aneN_4)^{3+} \quad (45)$$

"$^3T_{1g}$" $\quad$ "$^1A_{1g}$"

Scheme III. (Electron Transfer)

$$^*Cr(NN)_3^{3+} + Co([14]aneN_4)^{2+} \xrightarrow[k_q]{} Cr(NN)_3^{2+} + Co([14]aneN_4)^{3+} \quad (46)$$

^2E $\quad$ "$^4T_{1g}$" $\quad$ $^3T_1$ $\quad$ "$^1A_{1g}$" $\quad$ $\Delta S=1$

If Scheme I is occurs, then k_{el} will have to be greater than 10^9 $M^{-1}s^{-1}$, as k_q is about 10^8 $M^{-1}s^{-1}$. Since no $^*Co([14]aneN_4)^{2+}$ emission is seen, this species must have a short lifetime, and therefore its decay will occur more quickly than the bimolecular reaction in equation 43. Therefore, Scheme I may be ruled out.

Scheme II is a simultaneous energy/electron transfer. The combination would yield a shallow dependence of k_q on $\Delta E°$, and 100%

$Cr(NN)_3^{2+}$ per $^*Cr(NN)_3^{3+}$. The occurrence of reaction 45 independently will not affect the reactions and kinetics of the $^*Cr(NN)_3^{3+}$ species. In comparison to Scheme III, which depicts electron transfer from the $Co([14]aneN_4)^{2+}$ to the $^*Cr(NN)_3^{3+}$, Scheme II also includes energy transfer from the $^*Cr(NN)_3^{3+}$ to form $Co([14]aneN_4)^{3+}$. As it happens, Scheme III is spin forbidden, but Scheme II is spin allowed. Scheme III was ruled out because the observed rate constants do not correlate with electron transfer theories, and therefore it is postulated that Scheme II is the one which really occurs.

Summary

The $Cr(NN)_3^{2+}$ complexes react with both SO_2 and $Co([14]aneN_4)^{3+}$ via electron transfer mechanisms which may easily be rationalized by Marcus theory. They show no evidence of any nuclear tunneling or adiabaticity.

The quenching of $^*Cr(NN)_3^{3+}$ by $Co([14]aneN_4)^{2+}$ does not correlate with Marcus theory; of the possible reasons for deviation, a combination energy/electron transfer mechanism seems to be the most plausible at the present time.

EXPERIMENTAL

Materials

The $[Cr(NN)_3](ClO_4)_3$ compounds were prepared based on literature methods.[20] $Cr(H_2O)_6^{2+}$ was made by the electrochemical reduction of $[Cr(H_2O)_6](ClO_4)_3$ in 0.1 M $HClO_4$. This was added to an air-free mixture of a one-and-a-half to two-fold excess of the ligand in 0.01 M $HClO_4$ and stirred for one hour. Saturated bromine water was added to oxidize the $Cr(NN)_3^{2+}$ to the yellow $Cr(NN)_3^{3+}$, and this was stirred for 20 minutes in the fume hood to help remove the excess bromine. The yellow precipitate was dissolved in water (pH ~ 6), and extracted four times with chloroform. Saturated $NaClO_4$ solution was added to the aqueous layer, and the solution was chilled in the refrigerator overnight. The resulting precipitate was filtered in dim light, washed with a small amount of cold water, diethyl ether, and then air dried. The complexes were stored in air in the dark. The ligands were all obtained from G. F. Smith and Co., and were used as received. The complexes were identified on the basis of their UV-visible spectra[22,24,57] and τ_o values.[20,22,24]

The $Co([14]aneN_4)(OH_2)_2^{2+}$ was made in aqueous solution by mixing equimolar amounts of air-free $Co(ClO_4)_2$ (G. F. Smith and Co.) and $[14]aneN_4$ (Strem Chemicals Inc.) in water, as per the literature.[58] The mixture was stirred under an argon atmosphere until the blue precipitate turned into an orange solution, at which time acid was added (the resultant solution was about 0.033 M in H_2SO_4). The mixture was kept for up to 90 minutes in ice, under an argon atmosphere, in the dark. It was

characterized by its UV-visible spectrum (ε(465 nm) = 22 $M^{-1}cm^{-1}$; minimum at 435 nm).

$[Co([14]aneN_4)(OH_2)_2](ClO_4)_3$ was made according to the literature.[58] Equimolar amounts of $CoCl_2.6H_2O$ and $[14]aneN_4$ in methanol were mixed, and then bubbled with oxygen for one hour. After the addition of concentrated HCl and further bubbling with O_2 for one hour, green crystals of $[Co([14]aneN_4)Cl_2]Cl_3$ were obtained.[59] It was found necessary to purify the compound before use by running a solution of it through Dowex 1-X8, 50-100 mesh resin in the hydroxide form, which produces a red solution of $[Co([14]aneN_4)(OH)_2]ClO_4$, and then obtaining the $[Co([14]aneN_4)(OH_2)_2](ClO_4)_3$ as dark green crystals by the addition of concentrated $HClO_4$ to the red solution. The compound was identified by its UV-visible spectrum, (ε(560 nm) = 28 $M^{-1}cm^{-1}$; ε(430 nm) ~46 $M^{-1}cm^{-1}$). The complex was stored in the refrigerator as crystals in the mother liquor.

Anhydrous sulfur dioxide gas (Matheson) was bubbled into a solution of 1.0 M H_2SO_4. The concentration of SO_2 was calculated using ε(276 nm) = 388 $M^{-1}cm^{-1}$;[60] the $[SO_2]$ obtained using this value was verified by iodometric analysis techniques.

The H_2SO_4 (Captree Chemical Corp.) solutions were all made using Millipore-purified water.

Photochemical experiments

The laser system used has been previously described.[61] The dye used in these experiments was LD 423 (Exciton, 2 x 10^{-4} M in methanol), which emits light at 423 nm (the range is 415-447 nm). An electronic shutter

which was coupled to the firing switch of the laser prevented the analyzing beam (needed only for the absorbance experiments) from photolyzing the solutions before the experiments were performed.

All solutions used in these experiments were deaerated with oxygen-removing R3-11 catalyst (Chemalog) scrubbed argon before use. Experiments are in 1.0 M H_2SO_4 unless otherwise noted. Reactions which used $Co([14]aneN_4)^{2+}$ were studied with at least two different batches of this reagent in all cases. For most of the experiments, the rate constants reported are the average of two runs from flashes of different areas of the same solution. For the back-electron transfer reactions, the $[Cr(NN)_3^{2+}]$ formed in the flash varied; hence the $[Co([14]aneN_4)^{3+}]$ varied, and therefore duplicate flashes of the same cell are recorded as two separate rate constants.

The kinetics for the decay of the $^*Cr(NN)_3^{3+}$ were collected using the emission band at 727 nm. The $[Cr(NN)_3^{3+}]$, which was usually 10^{-6} to 10^{-3} M, was determined by UV-visible spectrophotometry for each experiment.

The kinetic data for the quenching experiments were collected at 727 nm, but the formation of $Cr(NN)_3^{2+}$ was verified by looking at the absorbance at 560 nm (bpy) or 445 nm (all compounds). The ratio of $Cr(NN)_3^{2+}$ produced can be compared to the amount of $^*Cr(NN)_3^{3+}$ formed, which was found by flashing a solution of $^*Cr(bpy)_3^{3+}$, monitoring at an absorbance wavelength, and using a known extinction coefficient to find its concentration. The quenching is about 100% efficient for the bpy complex, but these numbers have relatively high (~20%) errors associated with them, as the methods for calculating them have experimental errors of about 20% (see Table II-8 and references therein). The 5-Clphen

complex gives the same results.[62] The individual cells for these experiments were prepared by adding the $Co([14]aneN_4)^{2+}$ to the cell last, pressurizing the cell with argon, and then sealing the septum with rubber cement. The data were accumulated immediately. The concentrations of $Cr(NN)_3^{3+}$ and $Co([14]aneN_4)^{2+}$ were calculated from the concentrations of

Table II-8. Extinction Coefficients of $^*Cr(bpy)_3^{3+}$ and $Cr(bpy)_3^{2+}$ Species

$^*Cr(bpy)_3^{3+}$ [λ/nm, (ε)/$M^{-1}cm^{-1}$]	References
590 (300), 445 (3000), 390 (7000)	Maestri et al.[24]
560 (~500), 480 (~2300) 460 (~2800)	Ferraudi and Endicott[32]
590 (400), 560 (400), 470 (2400), 440 (4600), 390 (8200)	Bakac et al.[43]
600 (200), 390 (3100)	Ohno and Kato[63]

$Cr(bpy)_3^{2+}$ [λ/nm, (ε)/$M^{-1}cm^{-1}$]	References
560 (4786)	Ferraudi and Endicott[32]
562.5 (4340), 467 (3950)	Candlin et al.[64]
565 (3700), 475 (4100)	Lawrance and Sangster[65]
560 (4600), 470 (4000)	Serpone et al.[22]

the stock solutions. In a typical experiment, the $Cr(NN)_3^{3+}$ and $Co([14]aneN_4)^{2+}$ have absorbances of about 0.015 and 0.008 absorbance units at the excitation wavelength of 423 nm,respectively. It is assumed that the $Co([14]aneN_4)^{2+}$ does not absorb this light to form any excited states. To avoid interference from quenching by the ground state and the $Cr(NN)_3^{2+}$ species formed in the reaction, the $[Cr(NN)_3^{3+}]$ was less than 5 x 10^{-5} M in all cases, and the laser power was adjusted such that only 2-5 μM $Cr(NN)_3^{2+}$ was formed. In a worst case scenario, these contributions would add about 2.8 x 10^4 s^{-1} to the observed rate constant.

The solutions for the back-electron transfer experiments were prepared by mixing the $Cr(NN)_3^{3+}$, $Co([14]aneN_4)^{3+}$, H_2SO_4, and adding the $Co([14]aneN_4)^{2+}$ lastly, as above. Typical absorbances at the excitation wavelength of 423 nm are $Cr(NN)_3^{3+}$, 0.061; $Co([14]aneN_4)^{2+}$, 0.016; and $Co([14]aneN_4)^{3+}$; 0.022 absorbance units. The $[Co([14]aneN_4)^{3+}]$ was calculated from the concentration of the stock solution, which was kept on ice and in the dark for a period not exceeding 3 hours. The kinetic data were collected at one or two wavelengths corresponding to $Cr(NN)_3^{2+}$ absorbances for the compound under study. In most experiments, the absorbance due to the $Cr(NN)_3^{3+}$ was at least three times greater than that due to the $Co([14]aneN_4)^{3+}$.

In the SO_2 experiments, microliter quantities of SO_2 were added just before flashing to a cell prepared as in the quenching experiments. The kinetic data were collected as for the back-electron transfer experiments.

The exact composition used for the individual experiments is given in

Tables AII-19 - AII-24. Note that much more quencher is used for the back-electron transfer and SO_2 experiments than for the quenching experiments. This is to ensure that all of the quenching to form $Cr(NN)_3^{2+}$ is complete before the decay of the $Cr(NN)_3^{2+}$ begins. In each experiment, the first 15 ± 5% of the decay was not analyzed, as there was superposition of quenching and decay, which would cause deviations from good first-order kinetics.

The data were analyzed using a least squares program on an Apple IIe computer.

GENERAL SUMMARY

Two types of reactions of SO_2 with chromium species in acidic aqueous solution were studied. In one instance, the SO_2 was found to react with pentaaquoorganochromium(III) complexes via an electrophilic mechanism, eventually yielding both insertion and decomposition products. This reaction is analogous to other electrophilic reactions of these RCr^{2+} complexes. In the other case, the SO_2 reacted with $Cr(NN)_3^{2+}$ via an electron transfer mechanism to produce SO_2^-. From this study, the self-exchange rate constant for the SO_2/SO_2^- couple was calculated. Information about the reactivity of $Cr(NN)_3^{n+}$ complexes was also obtained. The rate constants for the quenching of $^*Cr(NN)_3^{3+}$ by $Co([14]aneN_4)^{2+}$ were measured, but although electron transfer products were found, the rate constants did not correlate with any of the electron transfer theories. The back-electron transfer reaction between $Cr(NN)_3^{2+}$ and $Co([14]aneN_4)^{3+}$ was studied, from which the k_{ex} for each $Cr(NN)_3^{3+/2+}$ couple was obtained.

REFERENCES

1. Marcus, R. A. J. Chem. Phys., 1956, 22 966.

2. Marcus, R. A. Can. J. Chem., 1959, 37, 155-163.

3. Marcus, R. A. J. Phys. Chem., 1963, 67, 853-857.

4. Sutin, N. Prog. Inorg. Chem., 1983, 30, 441.

5. Brunschwig, B. S.; Logan, J.; Newton, M. D.; Sutin, N. J. Am. Chem. Soc., 1980, 102, 5798-5809.

6. a) Ram. M. S.; Stanbury, D. M. J. Phys. Chem., 1986, 90, 3691-3696. b) Wilmarth, W. K.; Stanbury, D. M.; Byrd, J. E.; Po, H. N.; Chua, C.-P. Coord. Chem. Rev., 1983, 51, 155-179.

7. Chou, M., Creutz, C., Sutin, N. J. Am. Chem. Soc., 1977, 99, 5615-5623.

8. Ozawa, T.; Kwan, T. Polyhedron, 1983, 2, 1019-1023.

9. Bencivenni, L.; Teghil, R.; Pelino, M. Inorg. Chim. Acta, 1986, 121, 207-212.

10. Walsh, A. D. J. Chem. Soc., 1953, 2266.

11. a) Implied by Heicklen, J.; Kelly, N.; Partymiller, K. Rev. Chem. Intermed., 1980, 3, 315-404. and b) from a qualitative correlation with the molecular orbital diagrams of ozone, Jorgensen, W. L.; Salem, L. The Organic Chemist's Book of Molecular Orbitals, Academic Press: New York, 1973, 151-152.

12. Hillier, I. H.; Saunders, V. R. Mol. Phys., 1971, 22, 193-201.

13. Stanbury, D. M.; Lednicky, L. A. J. Am. Chem. Soc., 1984, 106, 2847-2853.

14. Neta, P.; Huie, R. E.; Harriman, A. J. Phys. Chem., 1987, 91, 1606-1611

15. Gill, J. B.; Goodall, D. C.; Harrison, W. D. J. Chem. Soc. Dalton, 1987, 2995-2997.

16. Siskos, P. A.; Peterson, N. C.; Huie, R. E. Inorg. Chem., 1984, 23, 1134-1137.

17. pK_a SO_2/HSO_3^- = 1.86. Huss, A.; Eckert, C. A. J. Phys. Chem., 1977, 81, 2268.

18. Zwickel, A. M.; Taube, H. Diss. Faraday Soc., 1960, 29, 42.

19. Serpone, N.; Jamieson, M. A.; Henry, M. S.; Hoffman, M. Z.; Bolletta, F.; Maestri, M. J. Am. Chem. Soc., 1979, 101, 2907-2916.

20. Brunschwig, B.; Sutin, N. J. Am. Chem. Soc., 1978, 100, 7568-7577.

21. Serpone, N.; Jamieson, M. A.; Sriram, R.; Hoffman, M. Z. Inorg. Chem., 1981, 20, 3983-3988.

22. Serpone, N.; Jamieson, M. A.; Emmi, S. S.; Fuochi, P. G.; Mulazzani, Q. G.; Hoffman, M. Z. J. Am. Chem. Soc., 1981, 103, 1091-1098.

23. Jamieson, M. A.; Serpone, N.; Hoffman, M. Z. Coord. Chem. Rev., 1981, 39, 121-179.

24. Maestri, M.; Bolletta, F.; Moggi, L.; Balzani, V.; Henry, M. S.; Hoffman, M. Z. J. Am. Chem. Soc., 1978, 100, 2694-2701.

25. Jamieson, M. A.; Serpone, N.; Hoffman, M. Z.; Bolletta, F. Inorg. Chim. Acta, 1983, 72, 247-252.

26. Sriram, R.; Hoffman, M. Z.; Jamieson, M. A.; Serpone, N. J. Am. Chem. Soc., 1980, 102, 1754-1756.

27. Ulstrup, J. Trans. Faraday Soc., 1971, 67, 2645-2651.

28. Narusawa, Y.; Kimura, M.; Nakano, K. Bull. Chem. Soc. Japan, 1974, 47, 2017-2025.

29. Beattie, J. K.; Binstead, R. A.; Broccardo, M. Inorg. Chem., 1978, 17, 1822-1826.

30. McDowell, M. S.; Bakac, A.; Espenson, J. H. Inorg. Chem., 1984, 23, 2232-2236.

31. Endicott, J. F.; Kumar, K.; Ramasami, T.; Rotzinger, F. P.; Prog. Inorg. Chem., 1983, 30, 151.

32. Ferraudi, G. J.; Endicott, J. F. Inorg. Chim. Acta, 1979, 37, 219-223.

33. Ballardini, R.; Varani, G.; Indelli, M. T.; Scandola, F.; Balzani, V. J. Am. Chem. Soc., 1977, 100, 7219-7223.

34. Gandolfi, M. T.; Maestri, M.; Sandrini, D.; Balzani, V. Inorg. Chem., 1983, 22, 3435-3439.

35. Bakac, A. Ames Laboratory, Ames, Iowa, 50011. Personal Communication, 1987.

36. Lee, S. Department of Chemistry and Ames Laboratory, Iowa State University, Ames, Iowa, 50011. Personal Communication, 1988.

37. Mehrotra, R. N.; Wilkins, R. G. Inorg. Chem., 1980, 19, 2177-2178.

38. Tsukahara, K.; Wilkins, R. G. J. Am. Chem. Soc., 1985, 107, 2632-2635.

39. Bradic, Z.; Wilkins, R. G. J. Am. Chem. Soc., 1984, 106, 2236-2239.

40. Balahura, R. J.; Johnson, M. D. Inorg. Chem., 1987, 26, 3860-3863.

41. This sort of occurrence was not mentioned in the literature; for five points in a 10^{-5} M to 10^{-3} M range in Na_2SO_4 and NaBr a straight line was obtained.

42. Only the $Cr(phen)_3^{3+}$ and $Cr(5\text{-}Clphen)_3^{3+}$ complexes were studied to concentrations as high as 10^{-3} M; the others were only examined at concentration ranges below 10^{-4} M.

43. Bakac, A; Zahir, K.; Espenson, J. H. Inorg. Chem., 1988, 27, 315-318.

44. Bolletta, F.; Maestri, M.; Moggi, L.; Jamieson, M. A.; Serpone, N.; Henry, M. S.; Hoffman, M. Z. Inorg. Chem., 1983, 22, 2502-2509.

45. Compound made by Zahir, K. Ames Laboratory, Ames, Iowa, 50011.

46. Huston, P. Ames Laboratory and Department of Chemistry, Ames, Iowa. Personal communication, 1988.

47. Stanbury, D. M.; Wilmarth, W. K.; Khalat, S.; Po, H. N.; Byrd, J. E. Inorg. Chem., 1980, 19, 2715-22.

48. a) Furholz, U; Haim, A. Inorg. Chem., 1985, 24, 3091-3095. b) Stanbury, D. M.; Gaswick, D.; Brown, G. M.; Taube, H. Inorg. Chem., 1983, 22, 1975.

49. Endicott, J. F.; Durham, B; Glick, M. D.; Anderson, T. J.; Kuszaj, J. M.; Schmonsees, W. G.; Balakrishnan, K. P. J. Am. Chem. Soc., 1981, 103, 1431-1440.

50. This radius is assumed to be about the same size as its Ru(III) and Co(III) analogues. a) Brown, G. M.; Sutin, N. J. Am. Chem. Soc., 1979, 101, 883. b) Cummins, D.; Gray, H. B. J. Am. Chem. Soc., 1977, 99, 5158.

51. Zahir, K.; Bakac, A.; Espenson, J. H. J. Am. Chem. Soc., 1988, 110, 0000.

52. Creutz, C.; Sutin, N. Inorg. Chem., 1974, 13, 2041-2043.

53. Cotton, A. L.; Wilkinson, G. Advanced Inorganic Chemistry, Wiley-Interscience: New York, 1980, Fourth Edition, 535.

54. Γ_n is given by

$$\Gamma_n = \exp\{-\frac{E_{in}}{h\nu_{in}}[\tanh(\frac{h\nu_{in}}{4kT}) - (\frac{h\nu_{in}}{4kT})]\} \quad (47)$$

ν_{in} is the breathing frequency of the complex

$$E_{in} = 3(f_2 + f_3)(d_2^o - d_3^o)^2 \quad (48)$$

$$f_i = 4\pi\bar{\nu}_i^2 c^2 \mu \qquad \mu \text{ is the reduced mass} \quad (49)$$

d_i = equilibrium M-L distance for oxidation state i

Based on the expression for Γ_n, when there is no change in bond length upon oxidation or reduction, (that is, $\Delta d = 0$), then $E_{in}/h\nu_{in} = 0$, therefore $\Gamma_n = e^0 = 1.0$. In other words, if there is no change in bond length upon oxidation or reduction, there is no nuclear tunneling. From a classical viewpoint, if $\Delta d = 0$ for a self-exchange reaction, then the products and reactants have identical potential energy curves, and therefore there is no energy barrier for the electrons to tunnel through.

55. Marcus, R. A.; Sutin, N. Biochim. Biophys. Acta, 1985, 811, 265-322.

56. Furholz, U.; Haim, A. J. Phys. Chem., 1986, 90, 3686-3690.

57. Konig, E.; Herzog, S. J. Inorg. Nucl. Chem., 1970, 32, 585-599.

58. Heckman, R. A., Ph.D. Thesis, Iowa State University, 1978.

59. Poon, C. K.; Tobe, M. L. J. Chem. Soc. (A), 1968, 1549-1555.

60. Seo, E. T.; Sawyer, D. T. J. Electroanal. Chem., 1964, 7, 184.

61. Connolly, P. Ph.D. Thesis, Iowa State University, 1985.

62. The extinction coefficients for $*Cr(5\text{-Clphen})_3^{3+}$ are $\varepsilon(490\text{ nm}) = 4800\ M^{-1}cm^{-1}$; $\varepsilon(480) = 4200\ M^{-1}cm^{-1}$; $\varepsilon(440) = 3850\ M^{-1}cm^{-1}$. Carl Steffan, Ames Laboratory and Department of Chemistry, Ames, Iowa, 50011. Personal communication, 1988.

63. Ohno, T.; Kato, S. Bull. Chem. Soc. Japan., 1984, 57, 1528-1533.

64. Candlin, J. P.; Halpern, J.; Trimm, D. L. J. Am. Chem. Soc., 1964, 86, 1019-1022.

65. Lawrance, G. A.; Sangster, D. F. J. Chem. Soc. Dalton, 1987, 1425.

APPENDIX II. KINETIC DATA FOR REACTIONS OF POLYPYRIDINECHROMIUM COMPLEXES

Table AII-1. Rate Constants for the Decay of *$Cr(5\text{-}Clphen)_3^{3+}$ in 1.0 M H_2SO_4

$10^4[Cr(5\text{-}Clphen)_3^{3+}]/M$	$10^{-4}k_{obs}/s^{-1}$
0.0318	0.741
0.0558	0.742
0.150	0.779
0.344	0.987
0.885	1.29
1.11	1.59
1.38	1.91
1.42	2.00
1.42	1.80
1.51	2.00
2.05	2.59
2.22	2.64
2.22	2.19
2.49	2.52
2.58	2.55
2.85	2.42
3.15	2.63
3.61	2.57
3.65	3.00
4.24	3.25
5.87	3.63
6.73	3.98

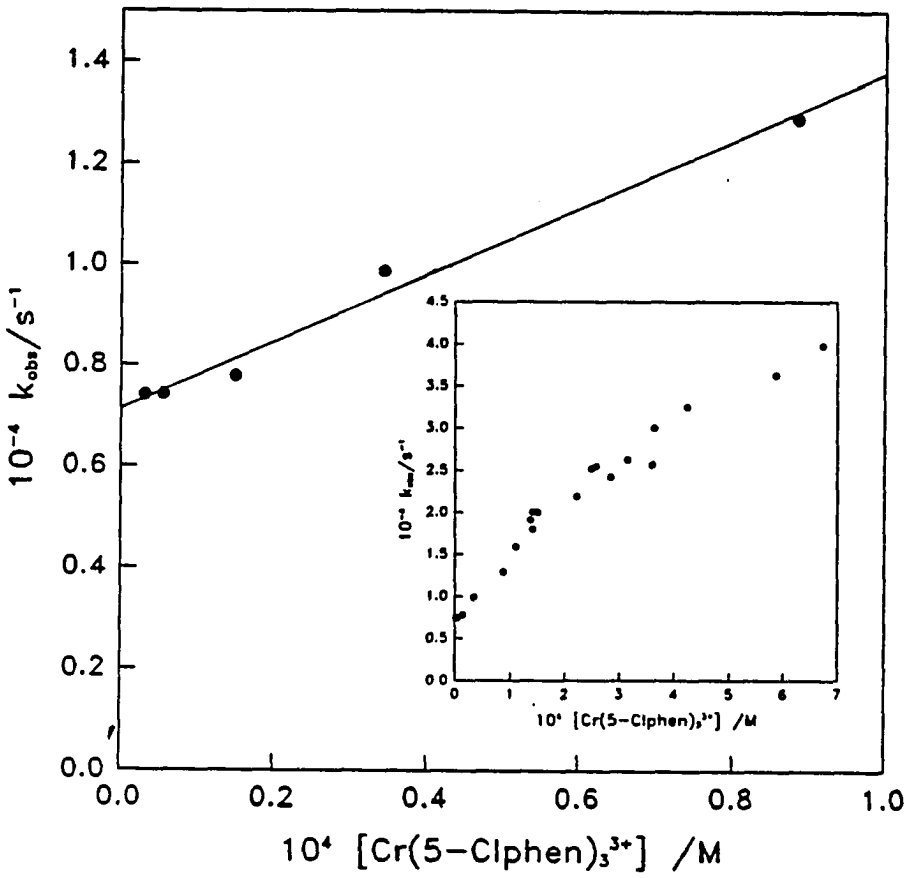

Figure AII-1. Plot of k_{obs} versus [Cr(5-Clphen)$_3^{3+}$] for the decay of *Cr(5-Clphen)$_3^{3+}$ in 1.0 M H_2SO_4. The inset shows the curvature which becomes apparent when the concentration of the ground state chromium complex exceeds 1 x 10^{-4} M

Table AII-2. Rate Constants for the Decay of $^*Cr(phen)_3^{3+}$ in 1.0 M H_2SO_4

$10^4[Cr(phen)_3^{3+}]/M$	$10^{-4}k_{obs}/s^{-1}$
0.0337	0.331
0.111	0.372
0.193	0.384
0.405	0.456
0.484	0.460
1.23	0.619
2.17	0.814
2.77	1.03
3.25	1.05
4.76	1.30
4.78	1.15
6.34	1.45
6.53	1.47
8.72	1.67

Table AII-3. Rate Constants for the Decay of $^*Cr(5\text{-Mephen})_3^{3+}$ in 1.0 M H_2SO_4

$10^5[Cr(5\text{-Mephen})_3^{3+}]/M$	$10^{-3}k_{obs}/s^{-1}$
0.651	2.63
0.796	2.77
1.16	2.85
1.55	2.91
5.52	4.61
7.36	5.22

Table AII-4. Rate Constants for the Decay of $^*Cr(4,4'Me_2bpy)_3^{3+}$ in 1.0 M H_2SO_4

$10^5[Cr(4,4'Me_2bpy)_3^{3+}]/M$	$10^{-3}k_{obs}/s^{-1}$
1.05	4.806
1.61	4.944
3.13	4.958
5.96	5.181
11.2	5.562

Table AII-5. Rate Constants for the Decay of $^{*}Cr(5,6\text{-}Me_2phen)_3^{3+}$ in 1.0 M H_2SO_4 [a]

$10^6[Cr(5,6\text{-}Me_2phen)_3^{3+}]/M$	$10^{-3}k_{obs}/s^{-1}$
0.777	1.88 [b]
0.819	1.95
1.55	1.99
2.97	2.14
3.81	2.18
4.42	2.29
10.3	2.91 [c]
10.3	2.95
10.6	2.92
10.6	2.93 [d]

[a] λ = 735 nm unless otherwise noted. This wavelength was found to be more intense than 727 or 722 nm. All rate constants are the average of two runs, unless otherwise noted.

[b] Average of four runs.

[c] λ = 727 nm.

[d] λ = 722 nm.

Table AII-6. Rate Constants for the Decay of $^{*}Cr(4,7\text{-}Me_2phen)_3^{3+}$ in 1.0 M H_2SO_4

$10^5[Cr(4,7\text{-}Me_2phen)_3^{3+}]/M$	$10^{-3}k_{obs}/s^{-1}$
0.11	1.44
0.239	1.53
0.322	1.57
0.598	1.57
1.18	1.78
3.64	2.1
6.8	2.93
15.5	4.22

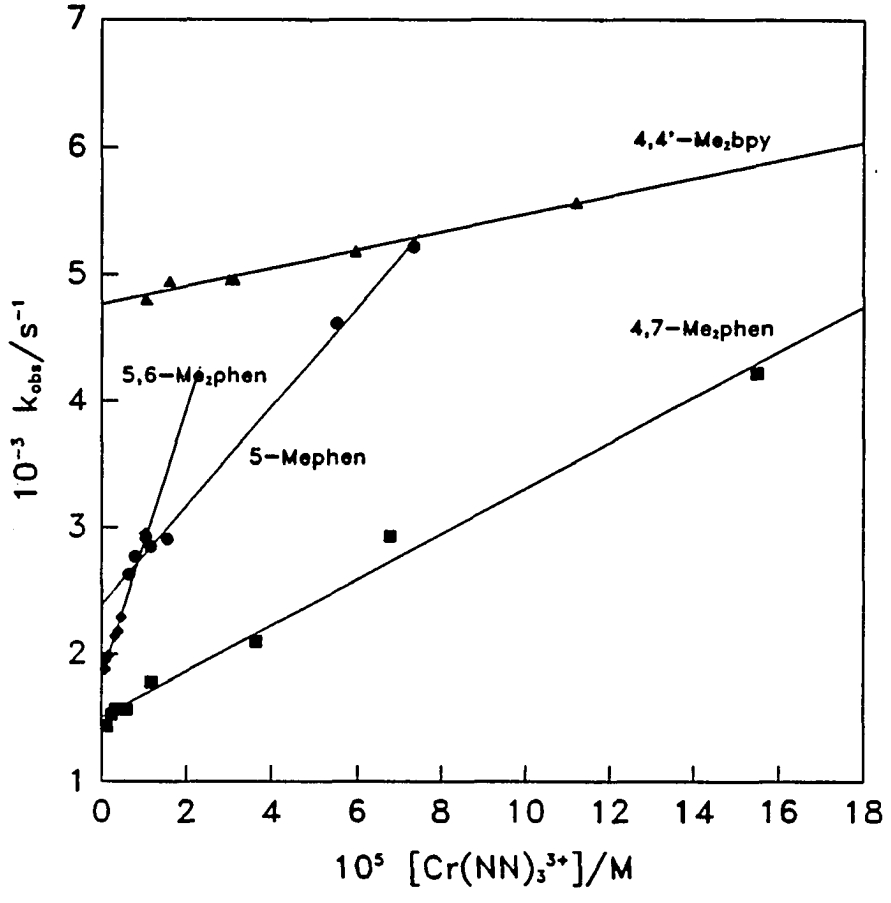

Figure AII-2. Plot of k_{obs} versus $[Cr(NN)_3^{3+}]$ for the decay of $^*Cr(NN)_3^{3+}$ in 1.0 M H_2SO_4. Shown are the plots for 5-Mephen (●), 4,4'Me_2bpy (▲), 4,7-Me_2phen (■), and 5,6-Me_2phen (◆)

Table AII-7. Rate Constants for the Quenching of $^*Cr(5\text{-Clphen})_3^{3+}$ by $Co([14]aneN_4)^{2+}$ in 1.0 M H_2SO_4 [a]

$10^5[Cr(5\text{-Clphen})_3^{3+}]$	$10^4[Co([14]aneN_4)^{2+}]$	$10^{-5}k_{obs}/s^{-1}$
2.10	0.0	0.076
2.10	0.952	0.69
2.10	1.90	1.07
2.81	2.38	1.12
2.10	2.86	1.8
2.10	3.81	1.68
2.10	4.76	2.82
2.10	5.71	3.10
2.10	6.66	3.8
2.10	7.62	4.5

[a]The second-order rate constant, k_q, derived from a plot of k_{obs} versus $[SO_2]$ (see Figure II-3) is $(5.2 \pm 0.2) \times 10^8$ $M^{-1}s^{-1}$, and the intercept is $(7 \pm 1) \times 10^3$ s^{-1}.

Table AII-8. Rate Constants for the Quenching of $^*Cr(bpy)_3^{3+}$ by $Co([14]aneN_4)^{2+}$ in 1.0 M H_2SO_4 [a]

$10^5[Cr(bpy)_3^{3+}]/M$	$10^4[Co([14]aneN_4)^{2+}]/M$	$10^{-4}k_{obs}/s^{-1}$
2.05	1.90	5.22
2.05	3.17	6.24
2.05	3.33	9.19
1.54	4.76	8.27
2.05	6.67	12.1
1.54	8.10	15.4
2.56	9.52	20.6
2.05	11.1	25.4

[a]The second-order rate constant, k_q, derived from a plot of k_{obs} versus $[SO_2]$ (see Figure II-3) is $(1.8 \pm 0.2) \times 10^8$ $M^{-1}s^{-1}$, and the intercept is $(1 \pm 1) \times 10^4$ s^{-1}.

Table AII-9. Rate Constants for the Quenching of $^{*}Cr(phen)_3^{3+}$ by $Co([14]aneN_4)^{2+}$ in 1.0 M H_2SO_4 [a]

$10^5[Cr(phen)_3^{3+}]/M$	$10^4[Co([14]aneN_4)^{2+}]/M$	$10^{-5}k_{obs}/s^{-1}$
1.45	1.90	0.695
1.81	2.86	0.916
1.45	3.81	1.20
1.45	5.71	1.71
1.81	6.67	2.26
1.45	8.57	3.31
1.81	10.5	3.59

[a]The second-order rate constant, k_q, derived from a plot of k_{obs} versus $[SO_2]$ (see Figure II-3) is $(3.3 \pm 0.2) \times 10^8$ $M^{-1}s^{-1}$, and the intercept is $(1 \pm 9) \times 10^4$ s^{-1}.

Table AII-10. Rate Constants for the Quenching of $^*Cr(5,6\text{-}Me_2phen)_3^{3+}$ by $Co([14]aneN_4)^{2+}$ in H_2SO_4 [a]

$10^5[Cr(5,6\text{-}Me_2phen)_3^{3+}]$ /M	$[H_2SO_4]$ /M	$10^4[Co([14]aneN_4)^{2+}]$ /M	$10^{-4}k_{obs}$ /s^{-1}
2.3	1.00	0.483	1.30
2.4	1.00	0.769	2.04
2.5	1.04	1.60	3.81
4.6	1.00	2.47	7.1
2.4	1.00	3.08	8.9
2.4	1.46	3.85	9.6
2.4	1.00	4.61	12.4
2.4	1.00	6.15	16.3
4.6	1.00	7.40	20.98
2.3	1.00	12.5	34.7

[a]All rate constants are the average of two runs. The kinetics were monitored at 735 nm. The second-order rate constant, k_q, derived from a plot of k_{obs} versus $[SO_2]$ (see Figure II-3) is $(2.55 \pm 0.04) \times 10^8$ $M^{-1}s^{-1}$, the intercept was set at 2.155×10^4 s^{-1}.

Table AII-11. Rate Constants for the Quenching of $^*Cr(5\text{-Mephen})_3^{3+}$ by $Co([14]aneN_4)^{2+}$ in 1.0 M H_2SO_4 [a]

$10^4[Co([14]aneN_4)^{2+}]/M$	$10^{-5}k_{obs}/s^{-1}$
0.476	0.265
0.95	0.513
1.90	0.866
2.38	1.02
3.81	1.65
4.76	2.01
7.14	2.90
9.15	3.71

[a] $[Cr(5\text{-Mephen})_3^{3+}] = 4.87 \times 10^{-5}$ M. The second-order rate constant, k_q, derived from a plot of k_{obs} versus $[SO_2]$ (see Figure AII-3) is $(4.04 \pm 0.09) \times 10^8$ $M^{-1}s^{-1}$, and the intercept is $(8 \pm 1) \times 10^3$ s^{-1}.

Table AII-12. Rate Constants for the Quenching of $^*Cr(4,4'Me_2bpy)_3^{3+}$ by $Co([14]aneN_4)^{2+}$ in 1.0 M H_2SO_4 [a]

$10^5[Cr(4,4'Me_2bpy)_3^{3+}]/M$	$10^4[Co([14]aneN_4)^{2+}]/M$	$10^{-4}k_{obs}/s^{-1}$
3.6	0.595	1.01
1.0	0.833	1.19
1.0	0.833	1.14
3.0	1.19	1.81
0.69	1.67	1.6
1.0	1.67	1.73
3.0	2.38	2.29
4.0	2.38	1.69
3.6	2.38	2.20
1.0	2.50	2.56
3.6	2.98	2.81
0.69	3.33	2.6
1.0	3.33	3.14
3.0	3.57	3.94
1.0	4.17	4.1
3.6	4.76	4.04
4.0	4.76	2.96

[a]The second-order rate constant, k_q, derived from a plot of k_{obs} versus $[SO_2]$ (see Figure AII-4) is $(0.7 \pm 0.2) \times 10^8$ $M^{-1}s^{-1}$; the intercept was set at 4.765×10^3 s^{-1}.

Table AII-12. Continued

10^5[Cr(4,4'Me_2bpy)$_3^{3+}$]/M	10^4[Co([14]aneN_4)$^{2+}$]/M	$10^{-4}k_{obs}/s^{-1}$
0.69	5.00	3.6
1.0	5.00	4.28
1.0	5.83	5.0
3.0	5.95	5.77
0.69	6.67	5.6
1.0	6.67	5.78
3.6	7.14	5.82
4.0	7.14	4.61
3.6	8.33	6.51
1.0	8.33	7.06
1.0	9.17	7.96
3.0	9.52	9.29
4.0	11.9	7.41

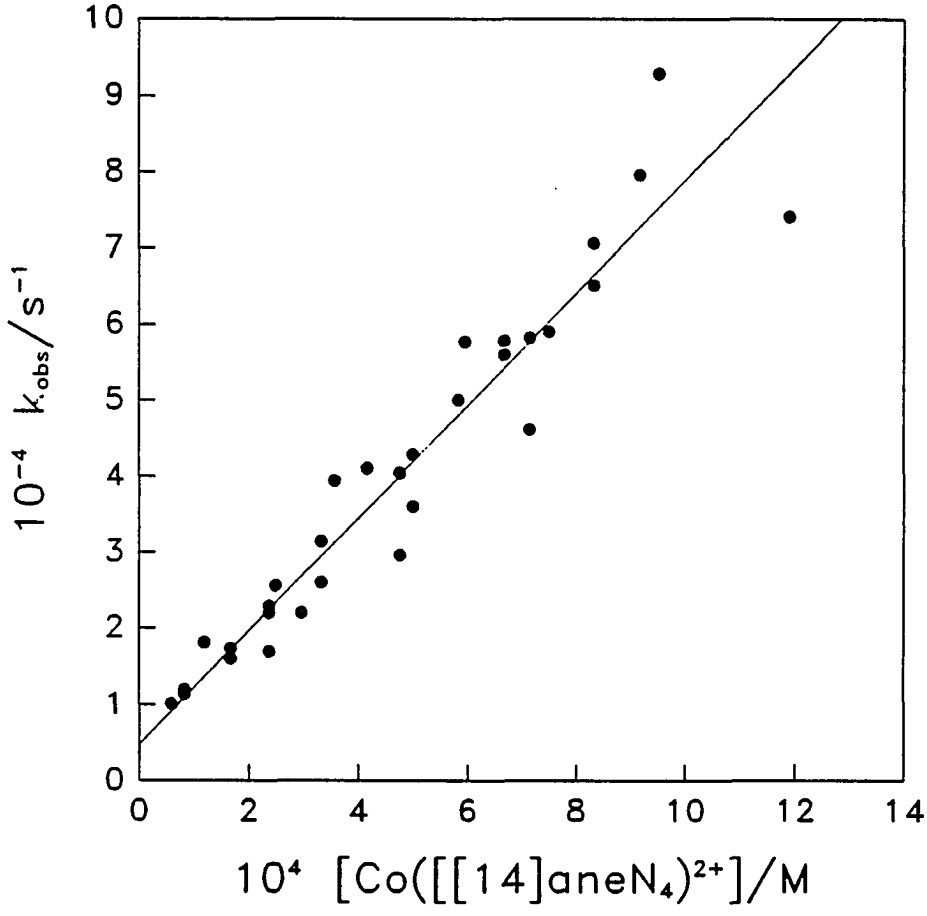

Figure AII-4. A plot of k_{obs} versus [Co([14]aneN$_4$)$^{2+}$] for the quenching of *Cr(4,4'Me$_2$bpy)$_3^{3+}$ in 1.0 M H_2SO_4

Table AII-13. Rate Constants for the Quenching of $^*Cr(4,7\text{-}Me_2phen)_3^{3+}$ by $Co([14]aneN_4)^{2+}$ in 1.0 M H_2SO_4 [a]

$10^5[Cr(4,7\text{-}Me_2phen)_3^{3+}]/M$	$10^4[Co([14]aneN_4)^{2+}]/M$	$10^{-4}k_{obs}/s^{-1}$
3.15	0.417	0.70
2.84	0.833	1.46
2.84	1.67	2.68
2.84	2.50	3.5
2.84	3.33	4.7
3.15	4.17	5.16
2.84	5.00	7.31
3.15	5.83	6.8
2.84	6.67	9.5
3.15	7.50	8.5

[a]The second-order rate constant, k_q, derived from a plot of k_{obs} versus $[SO_2]$ (see Figure II-3) is $(1.28 \pm 0.05) \times 10^8$ $M^{-1}s^{-1}$; the intercept was set at 2.06×10^3 s^{-1}.

Table AII-14. Rate Constants for the Back-Electron Transfer Reaction between $Cr(5\text{-Clphen})_3^{2+}$ and $Co([14]aneN_4)^{3+}$ in 1.0 M H_2SO_4 [a]

$10^4[Cr(5\text{-Clphen})_3^{3+}]$ /M	$10^5[Cr(5\text{-Clphen})_3^{2+}]$ /M	$10^4[Co([14]aneN_4)^{3+}]_{av}$ /M	$10^{-3}k_{obs}$ /s^{-1}
1.01	2.43	0.657	1.41
1.36	2.25	0.878	1.51
1.36	2.04	1.63	3.20
1.01	1.83	1.70	3.24
1.01	1.83	2.23	4.06
1.36	2.12	2.41	4.42
1.01	1.89	2.77	5.30
1.01	1.87	3.30	5.36
1.36	1.95	3.16	6.02
1.36	2.29	3.94	6.43
1.36	2.03	4.69	7.91

[a] $[Co([14]aneN_4)^{2+}] = 9.52 \times 10^{-4}$ M; all experiments done at $\lambda = 480$ nm; all points are the average of two runs. The second-order rate constant, k_{bet}, derived from a plot of k_{obs} versus $[Co([14]aneN_4)^{3+}]$ (see Figure II-5) is $(1.70 \pm 0.08) \times 10^7$ $M^{-1}s^{-1}$ with an intercept of (200 ± 100) s^{-1}.

Table AII-15. Rate Constants for the Back-Electron Transfer Reaction between $Cr(bpy)_3^{2+}$ and $Co([14]aneN_4)^{3+}$ in 1.0 M H_2SO_4 [a]

$10^5[Cr(NN)_3^{2+}]$ /M	$10^5[Cr(NN)_3^{3+}]$ /M	$10^3[CoL^{2+}]$ /M	$10^4[CoL^{3+}]_{av}$ /M	$10^{-4}\ k_{obs}$ /s^{-1}
1.23	11.1	4.35	2.49	1.31
~0.8	10.6	2.92	3.54	1.90
1.04	10.2	4.00	4.53	2.51
1.4	18.4	1.96	5.01	2.57
~0.8	9.84	2.69	5.42	2.30
1.02	9.47	3.70	6.27	3.19
~1.4	17.0	1.82	6.69	3.19
~0.8	9.13	2.50	7.04	3.21
~1.0	8.82	3.45	7.77	4.17
0.77	8.52	2.33	8.44	3.72

[a]The second-order rate constant, k_{bet}, derived from a plot of k_{obs} versus $[Co([14]aneN_4)^{3+}]$ (see Figure II-5) is $(4.4 \pm 0.4) \times 10^7\ M^{-1}s^{-1}$ with an intercept of $(3 \pm 2) \times 10^3\ s^{-1}$.

Table AII-16. Rate Constants for the Back-Electron Transfer Reaction between $Cr(phen)_3^{2+}$ and $Co([14]aneN_4)^{3+}$ in 1.0 M H_2SO_4 [a]

$10^4[Cr(phen)^{3+}]$ /M	$10^5[Cr(phen)_3^{2+}]$ /M	$10^4[Co([14]aneN_4)^{3+}]_{av}$ /M	$10^{-4}k_{obs}$ /s^{-1}
0.98	1.33	0.602	1.33
0.98	1.56	0.614	1.39
1.31	1.97	1.17	2.52
1.31	2.37	1.19	2.75
1.31	1.35	1.41	2.97
0.98	1.10	1.72	2.53 [b]
1.31	1.41	1.95	3.75
0.98	0.964	2.19	3.25 [b]
0.98	1.21	2.20	3.55 [b]
1.31	2.02	2.78	4.32
0.98	1.16	3.27	4.66
0.98	1.61	3.29	4.59

[a] $[Co([14]aneN_4)^{2+}] = 9.52 \times 10^{-4}$ M; experiments done at $\lambda = 470$ nm unless otherwise indicated. The second-order rate constant, k_{bet}, derived from a plot of k_{obs} versus $[Co([14]aneN_4)^{3+}]$ (see Figure II-5) is $(13 \pm 1) \times 10^7$ $M^{-1}s^{-1}$ with an intercept of $(7 \pm 2) \times 10^3$ s^{-1}.

[b] $\lambda = 700$ nm.

Table AII-17. Rate Constants for the Back-Electron Transfer Reaction between $Cr(5,6\text{-}Me_2phen)_3^{2+}$ and $Co([14]aneN_4)^{3+}$ in 1.0 M H_2SO_4 [a]

$10^5[Cr(5,6\text{-}Me_2phen)_3^{2+}]$ /M	$10^4[Co([14]aneN_4)^{3+}]_{av}$ /M	$10^{-4}k_{obs}$ /s^{-1}
1.12	0.056	1.82
1.08	0.054	1.95
0.967	1.42	4.35
1.01	1.43	4.65
0.909	2.80	6.47
0.916	2.80	6.57
1.44	4.20	8.45
0.967	4.17	7.97
0.898	5.54	10.4
0.961	5.55	10.3
0.909	6.93	12.1
0.967	6.93	12.9

[a]Experiments performed at 485 nm; $[Co([14]aneN_4)^{2+}] = 1.04 \times 10^{-3}$ M; $[Cr(5,6\text{-}Me_2phen)_3^{3+}] = 1.04 \times 10^{-4}$ M. The second-order rate constant, k_{bet}, derived from a plot of k_{obs} versus $[Co([14]aneN_4)^{3+}]$ (see Figure II-5) is $(15.8 \pm 0.4) \times 10^7$ $M^{-1}s^{-1}$ with an intercept of $(1.85 \pm 0.07) \times 10^4$ s^{-1}.

Table AII-18. Rate Constants for the Back-Electron Transfer Reaction of $Cr(5\text{-Mephen})_3^{2+}$ with $Co([14]aneN_4)^{3+}$ in 1.0 M H_2SO_4 [a]

$10^5[Cr(5\text{-Mephen})_3^{2+}]/M$	$10^4[Co([14]aneN_4)^{3+}]_{av}/M$	$10^{-4}k_{obs}/s^{-1}$
2.32	0.116	1.74
2.27	0.113	1.45
2.19	1.49	3.77
2.19	1.49	3.77
2.48	2.87	4.88
2.48	2.87	4.80
2.21	3.55	5.07
2.38	3.56	5.33
2.32	4.24	6.14
2.36	4.24	6.12
2.10	4.91	6.88
2.32	5.61	7.28
2.18	5.61	7.55
2.11	6.29	7.60
2.03	6.29	7.71
2.30	6.99	8.46
2.30	6.99	8.29

[a]Experiments performed at 485 nm; $[Co([14]aneN_4)^{2+}] = 8.75 \times 10^{-4}$ M; $[Cr(5\text{-Mephen})_3^{3+}] = 8.55 \times 10^{-5}$ M.

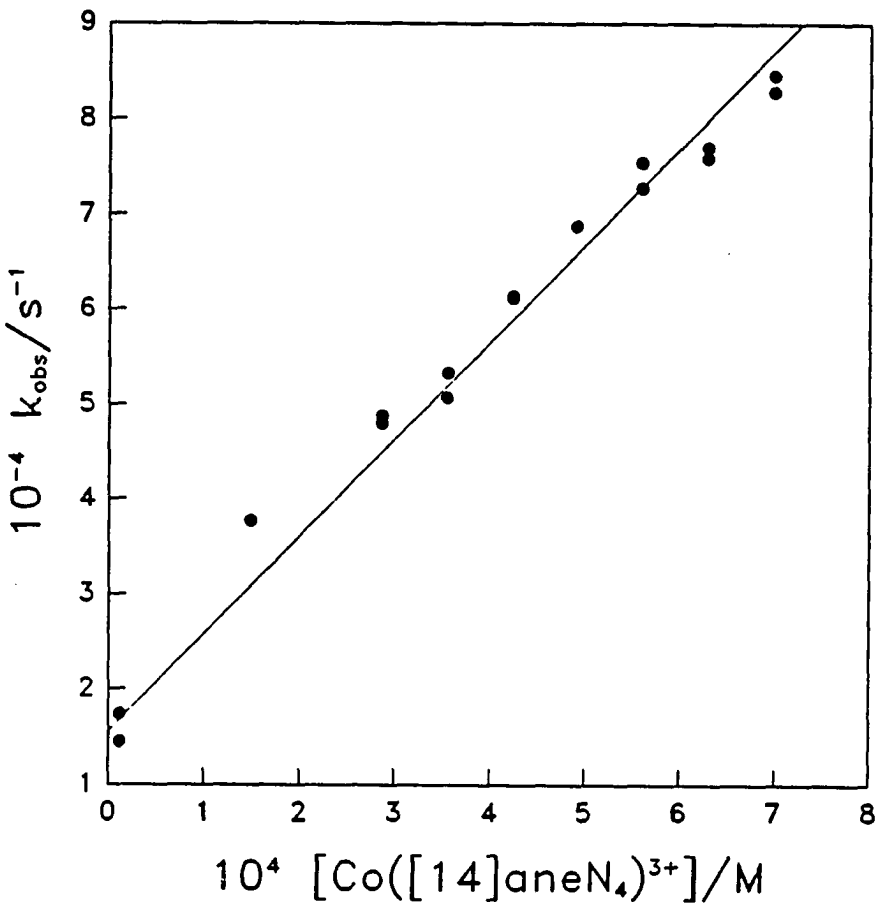

Figure AII-5. A plot of k_{obs} versus [Co([14]aneN$_4$)$^{3+}$] for the back-electron transfer reaction between Co([14]aneN$_4$)$^{3+}$ and Cr(5-Mephen)$_3^{2+}$. From a non-linear least squares regression analysis of the data, slope = (10.5 ± 0.4) x 10^7 $M^{-1}s^{-1}$; intercept = (1.56 ± 0.09) x 10^4 s^{-1}

Table AII-19. Rate Constants for the Reaction of SO_2 with $Cr(5\text{-}Clphen)_3^{2+}$ in 1.0 M H_2SO_4 [a]

$10^3[SO_2]/M$	$10^{-5}k_{obs}/s^{-1}$
1.19	0.0913
1.89	0.144
2.96	0.222
4.71	0.385
5.62	0.363
7.45	0.562
8.67	0.640
11.06	0.683

[a] $[Cr(5\text{-}Clphen)_3^{3+}] = 1.73 \times 10^{-4}$ M; $[Co([14]aneN_4)^{2+}] = 5 \times 10^{-3}$ M; all rate constants are the average of two kinetic traces. The second-order rate constant, k_s, derived from a plot of k_{obs} versus $[SO_2]$ (see Figure II-6) is $(0.683 \pm 0.004) \times 10^7$ $M^{-1}s^{-1}$, and the intercept is $(1 \pm 1) \times 10^3$ s^{-1}.

Table AII-20. Rate Constants for the Reaction of SO_2 with $Cr(bpy)_3^{2+}$ in $HClO_4$

$10^4[Cr(bpy)_3^{3+}]$ /M	$10^3[Co([14]aneN_4)^{2+}]$ /M	$[HClO_4]$ /M	$10^3[SO_2]$ /M	$10^{-5}k_{obs}$ /s^{-1}
2.4	2.8	0.72	0.60	0.32
2.4	2.8	0.49	0.89	0.38
2.4	2.0	0.92	1.5	0.75
2.4	2.8	0.72	1.78	0.82
1.3	2.8	0.95	2.4	1.2
2.4	3.3	0.92	2.6	1.36
1.3	2.8	0.95	3.0	1.5
2.4	2.0	0.92	4.0	1.6
2.4	2.8	0.95	5.0	2.0
2.4	3.3	0.92	5.9	2.0
2.4	2.8	0.50	6.0	1.9
2.4	2.8	0.95	7.0	2.5
2.4	3.3	0.92	7.8	2.6
4.8	2.8	0.96	8.67	3.8
2.4	2.8	1.0	8.94	3.5
2.4	2.8	0.95	9.0	2.8
2.4	3.3	0.92	10.0	2.8

[a]The second-order rate constant, k_s, derived from a plot of k_{obs} versus $[SO_2]$ (see Figure AII-6) is $(3.39 \pm 0.02) \times 10^7$ $M^{-1}s^{-1}$, and the intercept is $(1.4 \pm 0.4) \times 10^4$ s^{-1}.

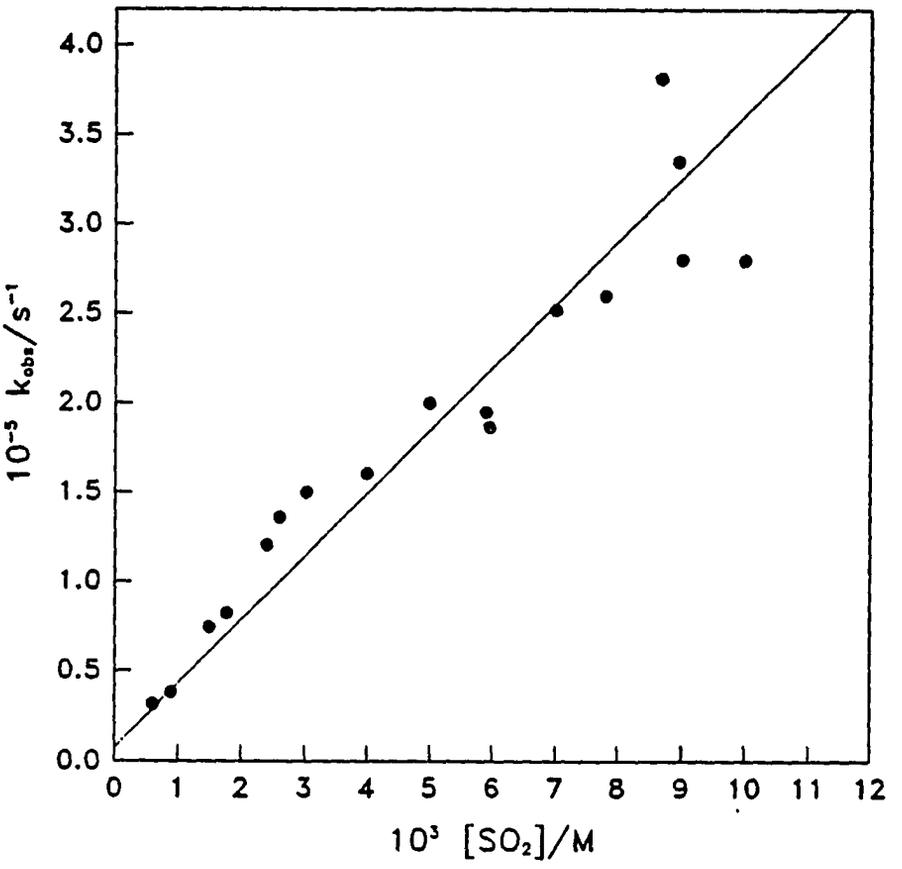

Figure AII-6. Plot of k_{obs} versus $[SO_2]$ for the reaction between $Cr(bpy)_3^{2+}$ and SO_2 in $HClO_4$

Table AII-21. Rate Constants for the Reaction of SO_2 with $Cr(bpy)_3^{2+}$ in 1.0 M H_2SO_4 [a]

$10^3[Co([14]aneN_4)^{2+}]/M$	$10^3[SO_2]/M$	$10^{-4}k_{obs}/s^{-1}$
3.17	0.669	2.11
3.17	1.33	4.08
4.76	1.87	6.35
3.17	2.67	8.02
4.76	3.74	11.1
4.76	4.68	14.4
4.76	5.61	17.3
4.76	6.55	19.6
4.76	7.49	20.9

[a] $[Cr(bpy)_3^{3+}] = 6.16 \times 10^{-5}$ M. The second-order rate constant, k_s, derived from a plot of k_{obs} versus $[SO_2]$ (see Figure II-6) is $(2.97 \pm 0.07) \times 10^7$ $M^{-1}s^{-1}$, and the intercept is $(2 \pm 1) \times 10^4$ s^{-1}.

Table AII-22. Rate Constants for the Reaction of SO_2 with $Cr(phen)_3^{2+}$ in 1.0 M H_2SO_4 [a]

$10^3[Co([14]aneN_4)^{2+}]/M$	$10^3[SO_2]/M$	$10^{-5}k_{obs}/s^{-1}$
2.5	0.303	0.42
2.5	0.605	0.68
5.0	0.725	0.86
2.5	0.900	1.0
5.0	1.20	1.2
5.0	1.45	1.6
5.0	1.49	1.5
2.5	1.79	1.9
5.0	2.08	1.9
4.0	2.18	2.2
5.0	2.37	2.5

[a] $[Cr(phen)_3^{3+}] = 1.65 \times 10^{-4}$ M. The second-order rate constant, k_s, derived from a plot of k_{obs} versus $[SO_2]$ (see Figure II-6) is $(9.5 \pm 0.2) \times 10^7$ $M^{-1}s^{-1}$; the intercept was set at 1.2×10^4 s^{-1}.

Table AII-23. Rate Constants for the Reaction of SO_2 with $Cr(5\text{-Mephen})_3^{2+}$ in 1 M H_2SO_4 [a]

$10^4[Cr(5\text{-Mephen})_3^{3+}]$ /M	$10^3[Co([14]aneN_4)^{2+}]$ /M	$10^4[SO_2]$ /M	$10^{-4}k_{obs}$ /s^{-1}
1.7	1.19	0.89	3.91
1.5	1.19	1.04	4.31
3.7	1.43	1.53	4.52
1.7	1.19	1.78	4.86
1.7	0.952	2.09	7.21
1.5	1.19	3.13	10.9
1.7	1.19	3.56	8.8
3.7	1.43	3.83	9.0
1.4	1.43	4.17	13.6
1.7	0.952	5.21	13.0
1.7	1.19	5.34	13.0
1.4	1.43	6.26	18.4
1.7	1.19	7.12	15.7
3.7	1.43	7.67	13.7
1.4	1.19	7.74	14.1
3.7	1.43	9.20	16.1
1.7	1.19	10.7	23.5
3.7	1.43	11.5	17.7

[a]The second-order rate constant, k_s, derived from a plot of k_{obs} versus $[SO_2]$ (see Figure AII-7) is $(17 \pm 1) \times 10^7$ $M^{-1}s^{-1}$, and the intercept is $(2.5 \pm 0.5) \times 10^4$ s^{-1}.

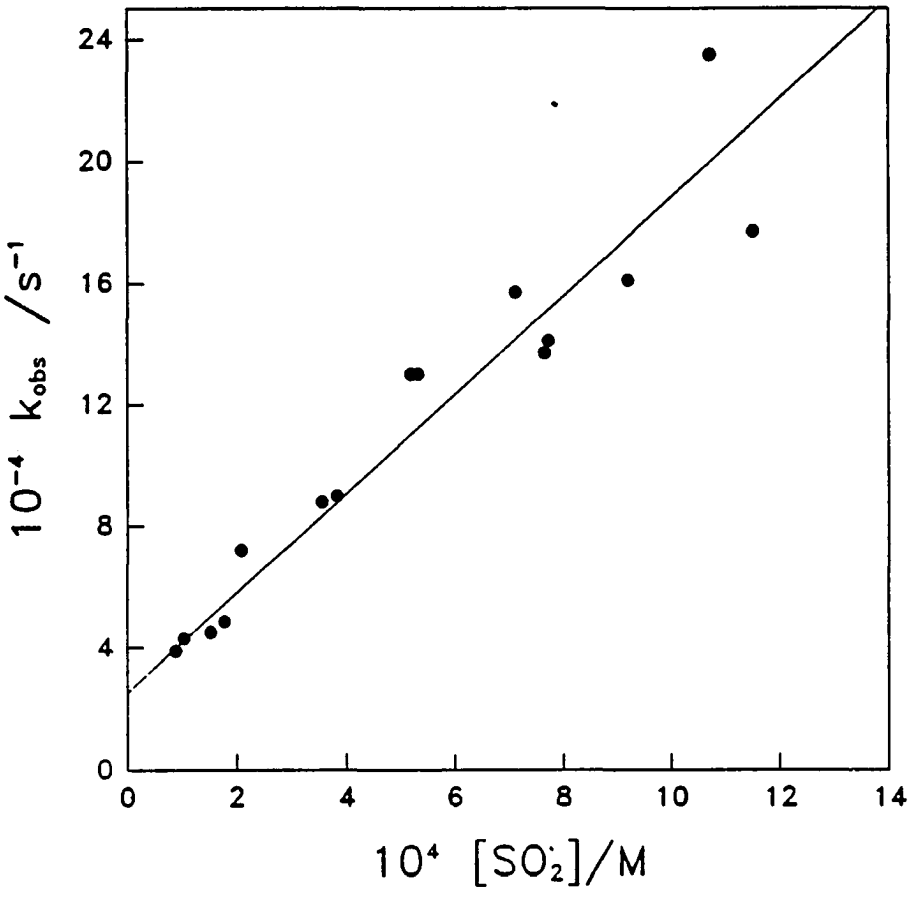

Figure AII-7. Plot of k_{obs} versus [SO_2] for the reaction between SO_2 and $Cr(5\text{-Mephen})_3^{2+}$ in 1.0 M H_2SO_4

Table AII-24. Rate Constants for the Reaction of SO_2 with $Cr(5,6\text{-}Me_2phen)_3^{2+}$ in 1.0 M H_2SO_4 [a]

$10^4[Cr(5,6\text{-}Me_2phen)_3^{3+}]$ /M	$10^3[Co([14]aneN_4)^{2+}]$ /M	$10^4[SO_2]$ /M	$10^{-4}k_{obs}$ /s^{-1}
1.1	1.00	0.178	5.5
1.1	1.00	0.53	6.8
2.2	1.43	0.76	6.4
1.1	1.00	0.89	6.8
2.2	1.43	1.53	8.7
1.1	0.857	2.14	10.9
2.2	1.43	2.03	10.0
1.1	1.00	2.64	12.4
1.1	0.857	3.03	13.4
1.1	1.00	3.56	15.3

[a]The second-order rate constant, k_s, derived from a plot of k_{obs} versus $[SO_2]$ (see Figure II-6) is $(28 \pm 2) \times 10^7$ $M^{-1}s^{-1}$, and the intercept is $(1.8 \pm 0.2) \times 10^3$ s^{-1}.

Table AII-25. Calculation of k_q from Marcus Theory [a]

$Cr(NN)_3^{3+}$	ΔE /V	$10^8 k_{calc}$ /$M^{-1}s^{-1}$	$10^8 k_{obs}$ /$M^{-1}s^{-1}$	k_{calc}/k_{obs}
5-Clphen	1.109	18	5.2	3.5
bpy	1.019	7.9	1.8	4.4
phen	0.999	6.5	3.3	2.0
5,6-Me_2phen	0.979	5.3	2.55	2.1
5-Mephen	0.969	4.8	4.04	1.2
4,4'-Me_2bpy	0.829	1.1	0.7	1.6
4,7-Me_2phen	0.809	0.84	1.28	0.86

[a]Calculated using equation 24, with $k_{ex}(^*Cr(NN)_3^{3+}/Cr(NN)_3^{2+}) = 1 \times 10^8$ $M^{-1}s^{-1}$ and $k_{ex}(Co([14]aneN_4)^{3+/2+}) = 8 \times 10^{-4}$ $M^{-1}s^{-1}$.

Table AII-26. Calculation of k_{bet} from Marcus Theory [a]

$Cr(NN)_3^{3+}$	ΔE /V	$10^7 k_{calc}$ /$M^{-1}s^{-1}$	$10^7 k_{obs}$ /$M^{-1}s^{-1}$	k_{calc}/k_{obs}
5-Clphen	0.591	2.0	1.7	1.2
bpy	0.681	6.5	4.4	1.5
phen	0.701	8.3	13	0.64
5,6-Me_2phen	0.711	9.4	15.8	0.59
5-Mephen	0.721	11	10.5	1.05
4,4'-Me_2bpy	0.671	56	~70	~0.8
4,7-Me_2phen	0.671	56	~70	~0.8

[a]Calculated using equation 24, with $k_{ex}(Cr(NN)_3^{3+/2+}) = 2 \times 10^9$ $M^{-1}s^{-1}$ and $k_{ex}(Co([14]aneN_4)^{3+/2+}) = 8 \times 10^{-4}$ $M^{-1}s^{-1}$.